

GLUCOSYLCERAMIDE MAINTAINS INFLUENZA INFECTION THROUGH REGULATION OF CELLULAR ENDOCYTOSIS

A DISSERTATION

*Presented to the faculty of the School of Medicine in
partial fulfillment of the requirements for the
degree of*

Doctor of Philosophy

by KELLY CHRISTOPHER DREWS

April 2019



©Copyright by
Kelly Christopher Drews
All Rights Reserved
April 2019

APPROVAL SHEET

*This dissertation is in partial fulfillment of the requirements for the degree of
Doctor of Philosophy in Experimental Pathology*

Kelly Christopher Drews
Author

This dissertation has been read and approved by the examining committee:

Mark Kester, Ph.D.
Dissertation Advisor
Department of Pharmacology

Janet Cross, Ph.D.
Committee Chair
Department of Pathology

Judith White, Ph.D.
Committee Member
Department of Cell Biology

Thomas Braciale, Ph.D.
Committee Member
Department of Pathology

James Casanova, Ph.D.
Committee Member
Department of Cell Biology

Accepted by the School of Medicine:

David S. Wilkes, M.D.
Dean
School of Medicine

Dedication

This work is dedicated to my loving wife, Camille. When I first arrived at UVA in 2014 I knew that the project I was about to undertake would be hard, and I hoped that I'd make friends that would provide comfort in trying times. However, I never dreamed I'd find someone as gifted, caring, and generous as you. You literally saved me years of work with your scientific brilliance but more importantly you gave me someone to talk to whenever an experiment failed (which happened far more often than I'd ever imagined possible). You transformed simple coffee meetings into the highlights of my week, and you provided the inspiration for everything I sought to achieve. Every single step I've taken in my life, both my accomplishments and my mistakes, has led me here and led me to you. I'm eternally thankful I was lucky enough to meet you and nothing in this entire world makes me as proud as knowing that I get to experience this lifelong journey with you.

Acknowledgments

This thesis would have been impossible if not for the support and guidance of my two amazing mentors, Judy White and Mark Kester. Judy, you are the epitome of what I wanted to be when I imagined becoming a scientist – deliberate, respected, curious, and supportive. Whenever I presented my data you walked the fine line of providing thorough and informative criticism while instilling confidence in the unproven ideas and skills of a first year graduate student. Your door was always open and you trusted me enough to make my own mistakes. Most importantly you taught me how to learn from my failures and become a more comprehensive scientist – despite my tendency to rush through things as quickly as possible. Your impact will be felt not only through the incredible science you performed, but also by the untold number of students and trainees you’ve guided throughout your career. I wish you nothing but happiness and I am eternally grateful I was able to work with you before you took a well-deserved retirement.

Mark, I still remember the first time I presented my project idea to you. I was probably 3 or 4 months into my time at UVA and you were just starting up your lab here. I was incredibly nervous to pitch a brand new idea that had nothing to do with any of your past research, but after I finished you lit up and said “that sounds great! Let’s do it.” That confidence in me helped me to grow as both a person and a scientist, and is something that will carry over throughout the rest of my life. You are an incredibly generous mentor, never taking issue with the numerous side projects or internships I sought to fulfill while I was a student. You taught me how to navigate the fog of interpersonal and professional relationships, helping me develop skills beyond the bench that I believe will ultimately provide the most long-lasting and impactful benefits as I continue my career. You showed me that the best scientists must have skills beyond the bench and for that I am incredibly thankful.

I must thank my committee members, as they were an incredible source of encouragement while at the same time nurturing my development through tough, but fair, critiques. Dr. Tom Braciale – you were always available to chat about flu questions and your ability to cut through to the heart of an issue saved me countless months of frustration. My entire project got a turbo-charged boost when you offered to let me use some of the GFP-flu you had been making in your lab. Dr. Jim Casanova – I must admit I probably took up enough time and effort from your lab members (especially Ryan D’Souza) to have qualified as a part-time student of yours. Your expertise on endosome trafficking was incredibly helpful as I tried to narrow down my mechanism. Dr. Janet Cross – Thank you for being my committee chair, but more importantly thank you for being a mentor and friend throughout my time at UVA. Your door was always open and it’s obvious how much you care about the students in the BIMS program. Whenever I’m asked about the pressures and departmental headaches that come with being a

graduate student I find I cannot relate, as your guidance and openness make the Pathology program at UVA a wonderful place to be.

I would not be in a position to write this thesis without the support of the friends I've made during my time at UVA. It would be impossible to fully thank everyone who had an impact on my life, but I wanted to recognize a few people. Jeremy Shaw, we came in to the Kester lab together and since day one you've been one of the hardest working people I've ever met. You're a wonderful example of someone who puts others first and I know that wherever you go in life you'll undoubtedly transform the lives of all those around you for the better. Pedro Pinheiro, I respect your opinions and knowledge as a scientist more than you'll ever know – I have no doubt that whatever you want to do with your career you'll achieve it. I'm thankful to consider you one of my closest friends and I sincerely believe that without you my time at UVA would have been far less rewarding, far less happy, and far less fulfilling. Logan Patterson, ever since we met at Virginia Tech you've been someone who wasn't afraid to be honest with what you believe, and sharing jokes, movie thoughts, and being able to have open conversations on all manner of topics was an incredible stress relief from the daily grind of being a graduate student. I didn't realize how valuable having that sort of relationship was and I feel very lucky that I've counted you as a friend for the past six years. Finally I must thank Tori Osinski for her soccer captaining, student leadership, and infectious happy attitude and Ali Harris – for her wonderful sense of humor and ability to withstand my jokes.

Most importantly, I have to thank my family for all of their support and guidance over the past 27 years of my life. Mom and Dad – you both pushed me to excel and taught me that hard work pays off in the end. You managed to strike a perfect balance of being there when I needed you and yet teaching me how to become an independent person able to overcome obstacles on my own. You were there for every baseball game, every trumpet concert, and every graduation. I could not ask for better parents and I hope my life reflects the incredible role you both had in shaping it. Jessi – you provided the ultimate competition: a little sister who not only got better grades than me, but also was the most popular kid in school and yet remained down to earth and kind. I'm so very proud of the woman you've become and I hope we never grow too old to steal cookie batter out of each other's bowls. Connor – I think the best way to summarize our relationship is to count the number of eye-rolls Camille performs when we're in a room together. You're the best friend I've ever had and I've yet to meet someone who has a better sense of humor or sense of character than you. I'm very proud of the person you're turning into and I cannot wait to see what life has in store for you. Finally, I want to thank Camille specifically for her patience and proofreading abilities – without you this thesis would be chock-full of typos and grammatical errors. I love you all so much and without you I would not be the man I am today.

Dissertation Abstract

Influenza is an enveloped negative sense RNA virus encapsulated in a lipid bilayer derived from the host cell plasma membrane. Lipids play diverse and crucial roles for many viruses, including influenza. Previous studies have shown that influenza infection depends on cellular lipids, including the sphingolipids sphingomyelin and sphingosine. Here we examined the role of a third sphingolipid, glucosylceramide, in influenza infection following CRISPR/Cas9-mediated knockout of its metabolizing enzymes: glucosylceramide synthase (UGCG) and glucosylceramidase (GBA). We first confirmed the knockouts (in HEK 293 and A549 cells) by both western blotting and lipid mass spectrometry. We next observed diminished influenza infection in all four KO cell lines using a PR8 GFP reporter virus. We further showed that the reduction in infection correlates with impaired virus entry, using β -lactamase reporter particles. To examine whether glucosylceramide homeostasis is similarly required for other viruses, we compared entry mediated by the glycoproteins of influenza, VSV, Ebola, and Measles in GBA and UGCG knockout cells. Among these, GBA and UGCG loss significantly inhibited entry of particles bearing the glycoproteins of both influenza and Ebola, viruses that enter the cytoplasm through late endosomes. Consistent with the defect in late endosomal virus entry, we found that influenza particles in GBA knockout cells were impaired in trafficking to late endosomes (via colocalization with Lamp1). As an extension, we found that trafficking of epidermal growth factor to late endosomes as well as degradation of epidermal growth factor receptor were impaired in GBA knockout cells.

Collectively our findings suggest that glucosylceramide is critically important for normal endocytic trafficking of viruses such as influenza as well as cellular cargos including growth factor receptors. In the viral context, modulation of glucosylceramide levels may represent a novel accompaniment to strategies to antagonize 'late penetrating' viruses, including influenza.

TABLE OF CONTENTS

DEDICATION	IV
ACKNOWLEDGEMENTS	V
DISSERTATION ABSTRACT	VII
TABLE OF CONTENTS	IX
LIST OF FIGURES AND TABLES	XI
LIST OF ABBREVIATIONS	XII
CHAPTER 1 - INTRODUCTION	1
1.1 Aim of Dissertation	2
1.2 Strategy and Summary of Dissertation	2
1.3 Influenza	4
1.3.1 History	4
1.3.2 Influenza Structure.....	5
1.3.3 Influenza Life Cycle.....	6
1.3.4 Influenza Vaccine and Therapies	10
1.4 Endocytosis	11
1.5 Sphingolipids	16
CHAPTER 2 – MATERIALS AND METHODS	21
CHAPTER 3 – GLUCOSYLCERAMIDASE MAINTAINS INFLUENZA INFECTION BY REGULATING ENDOCYTOSIS	33
3.1 Summary	34
3.2 Importance	35
3.3 Introduction	35
3.4 Results	38
3.4.1 Glucosylceramide metabolism regulates influenza infection	38
3.4.2 Changes in Sphingolipid Species in GBA Knockout Cells	42
positive controls (Bafilomycin and NH ₄ Cl) to confirm changes in pH. Using this technique, we determined that the pH in endosomes in GBA KO cells was not detectably different than that in WT cells (Fig. 3.7). These data suggest that ourobserve viral entry phenotype is not due to changes in the acidification process of the endosome.....	52
3.4.4 Glucosylceramidase regulates influenza trafficking along the endocytic pathway.....	52
3.4.5 Glucosylceramidase regulates epidermal growth factor receptor trafficking along the endocytic pathway.....	55
3.5 Discussion	59
3.6 Acknowledgements	62

CHAPTER 4 – GLUCOSYLCERAMIDE SYNTHASE MAINTAINS INFLUENZA INFECTION.....	64
4.1 Abstract	65
4.2 Introduction	65
4.3 Results and Discussion	68
4.3.1 Glucosylceramide synthase regulates influenza infection.....	68
4.3.2 Glucosylceramide synthase regulates entry of influenza and other endocytosed viruses.....	75
CHAPTER 5 - DISCUSSION.....	81
5.1 Summary of Results	82
5.2 Implications for Sphingolipid Biology	85
5.2.1 Glucosylceramidase.....	92
5.2.2 Glucosylceramide Synthase.....	95
5.2.3 GlcCer Versus Other Sphingolipids.....	98
5.3 Implications for Cellular Endocytosis	100
5.3.1 Membranes and Vesicles.....	100
5.3.2 Trafficking.....	102
5.3.3 Endo-lysosome biogenesis.....	106
5.4 Implications for Viral Infections	108
5.4.1 Viral Entry.....	108
5.4.2 Viral Exit.....	109
5.4.3 Other Viruses.....	113
5.4.4 Implications for Influenza Therapeutics.....	114
CHAPTER 6 – REFERENCES.....	118
VITA.....	134

LIST OF FIGURES AND TABLES

FIGURE 1.1 STRUCTURE OF INFLUENZA VIRUS.	7
FIGURE 1.2 INFLUENZA LIFE CYCLE.	8
FIGURE 1.3 FUSION OF ENVELOPED VIRUSES IN ENDOSOMES.....	14
TABLE 1.1 SITE AND FUSION-TRIGGERING MECHANISM FOR REPRESENTATIVE ENVELOPED VIRUSES.....	15
FIGURE 1.4 THE SPHINGOLIPID PATHWAY.	17
FIGURE 3.1 ROLE OF SPHINGOLIPIDS IN INFLUENZA VIRUS INFECTION.	39
FIGURE 3.2 GLUCOSYLCERAMIDASE REGULATES INFLUENZA INFECTION.	41
FIGURE 3.3 ANALYSIS OF LIPID LEVELS IN GBA KNOCKOUT CELLS.....	43
TABLE 3.S1 FULL SPHINGOLIPID PROFILES OF GBA KNOCKOUTS.	44
FIGURE 3.4 INFLUENZA M1 GENE EXPRESSION IS TIME AND TRYPSIN DEPENDENT IN GBA KO CELLS.	46
FIGURE 3.5 LOSS OF GBA REDUCES INFLUENZA VIRUS FUSION IN ENDOSOMES.	47
FIGURE 3.6 LOSS OF GBA REDUCES ENTRY MEDIATED BY THE GLYCOPROTEINS OF OTHER ENDOSOME-ENTERING ENVELOPED VIRUSES, WITH MINIMAL EFFECTS ON ENTRY MEDIATED BY THE GLYCOPROTEINS OF MEASLES VIRUS, A PLASMA-MEMBRANE ENTERING VIRUS.	50
FIGURE 3.7 LOSS OF GBA DOES NOT DETECTABLY ALTER LYSOSOMAL PH.....	51
FIGURE 3.8 TRAFFICKING OF INFLUENZA TO LATE ENDOSOMES IS IMPAIRED IN GBA KO CELLS.	53
FIGURE 3.9 TRAFFICKING OF EGF TO LATE ENDOSOMES IS IMPAIRED IN GBA KO CELLS.	54
FIGURE 3.10 EGFR DEGRADATION IS IMPAIRED IN GBA KO CELLS.....	56
FIGURE 3.11 LOSS OF GBA UPREGULATES CATHEPSIN B ACTIVITY.....	58
FIGURE 4.1 SPHINGOLIPIDS AND INFLUENZA VIRUS INFECTIONS.	69
FIGURE 4.2 CRISPR/CAS9 MEDIATED KNOCKOUT OF GLUCOSYLCERAMIDE SYNTHASE.	70
FIGURE 4.3 GLUCOSYLCERAMIDE SYNTHASE REGULATES INFLUENZA INFECTION.	71
FIGURE 4.S1 A549 UGCG KO CELLS EXHIBIT HAPLOINSUFFICIENCY.	73
TABLE 4.S1 FULL SPHINGOLIPID PROFILES OF UGCG KNOCKOUTS.	74
FIGURE 4.4 UGCG MAINTAINS ENTRY OF MULTIPLE VLPs.....	76
FIGURE 4.5 UGCG MAINTAINS INFECTION OF MULTIPLE PSEUDOVIRUSES.	78
TABLE 5.1 LIST OF MUTATIONS CREATED IN UGCG AND GBA.....	89
FIGURE 5.1 ECTOPIC EXPRESSION OF UGCG OR GBA MAY NOT RECAPITULATE WILD-TYPE LIPID STATUS.	90
FIGURE 5.2 HYPOTHESIZED SPHINGOLIPID METABOLIC ENZYMES.	93
TABLE 5.3 PROPOSED FUTURE EXPERIMENTS.....	116

LIST OF ABBREVIATIONS

AP1	Activator protein 1
ATP	Adenosine triphosphate
B₄GALT1	Beta-1,4-galactosyltransferase 1
Baf	Bafilomycin
BHK	Baby hamster kidney
βlaM	βeta-lactamase M1
CatB	Cathepsin B
CatL	Cathepsin L
cDNA	Complementary DNA
Cer	Ceramide
CRISPR	Clustered regularly interspaced short palindromic repeats
cRNA	Complementary RNA
DiOC18	3,3'-Diocetadecyloxacarbocyanine perchlorate
DMEM	Dulbecco's modified eagle medium
DNA	Deoxyribonucleic acid
DPM1	Dolichyl-phosphate mannosyltransferase subunit 1
EBOV	Ebola virus
EBOV-GPΔ	Ebola virus glycoprotein with mucin-like domain deleted
EEA1	Early endosome antigen 1
EGF	Epidermal growth factor
EGFR	Epidermal growth factor receptor
FBS	Fetal bovine serum
FDA	Food and Drug Administration
FRET	Förster resonance energy transfer
GAPDH	Glyceraldehyde 3-phosphate dehydrogenase
GBA	Glucosylceramidase
GFP	Green fluorescent protein
GlcCer	Glucosylceramide
gRNA	Guide RNA
HA	Hemagglutinin
HEK	Human embryonic kidney
HEPES	4-(2-hydroxyethyl)-1-piperazineethanesulfonic acid
HM	HEPES-MES
IAV	Influenza A virus
KO	Knockout
Lamp1	Lysosome-associated membrane protein 1
Lamp2	Lysosome-associated membrane protein 2
LBPA	Lysobisphosphatidic acid

M1	Matrix protein 1
M2	Matrix protein 2
Measles F	Measles virus fusion protein
Measles HN	Measles virus hemagglutinin–neuraminidase protein
MES	2-(N-morpholino)ethanesulfonic acid
MOI	Multiplicity of infection
mRNA	Messenger RNA
NA	Neuraminidase
NF-κB	Nuclear factor kappa-light-chain-enhancer of B cells
NOCO	Nocodazole
NS1	Nonstructural protein 1
OMEM	Opti-modified eagle medium
Oct-1	Octamer binding protein 1
PBS	Phosphate-buffered saline
PCR	Polymerase chain reaction
PEI	Polyethylenimine
PFAM	Paraformaldehyde
PPMP	Palmitoylamino-3-morpholino-1-propanol
PR8	Influenza A virus (A/PR/8/1934(H1N1))
qPCR	Quantitative PCR
R18	Octadecyl rhodamine B
Rab5	Ras-related protein Rab-5A
Rab7	Ras-related protein Rab-7A
RNA	Ribonucleic acid
S1P	Sphingosine-1-phosphate
SE	Standard error
sgRNA	Single guide RNA
TPCN2	Two pore segment channel 2
trVLP	Transcription- and replication-competent virus-like particle
UGCG	Glucosylceramide synthase
VLP	Virus-like particle
vRNA	Viral RNA
vRNP	Viral ribonucleoprotein
VSV	Vesicular stomatitis virus
VSV-G	Vesicular stomatitis virus glycoprotein
WSN	Influenza A virus (A/WSN/1933(H1N1))
WT	Wild type

CHAPTER 1 - INTRODUCTION

1.1 Aim of Dissertation

This work was undertaken in the hope of further understanding the relationship between human influenza virus and host sphingolipids. By forming a collaboration between the viral entry lab of Dr. Judith White and the sphingolipid biochemistry lab of Dr. Mark Kester, I aimed to examine this issue through the lens of virology with a solid foundation in sphingolipid biology. After performing a deep literature search I realized that no one had studied the possibility of glucosylceramide being involved in influenza-host pathology, and narrowed our focus to that particular sphingolipid.

1.2 Strategy and Summary of Dissertation

We sought to examine the relationship between glucosylceramide and influenza by performing full genetic knockouts of both the enzymes responsible for glucosylceramide metabolism: glucosylceramidase and glucosylceramide synthase. Previous studies into virus-sphingolipid interactions often relied on pharmacological inhibitor or RNAi mediated knockdown of sphingolipid enzymes, which we felt lacked the rigor of complete genetic ablation. Inhibitors often contain unknown secondary effects and RNAi usually resulted in only partial knockdown of the targeted proteins, leaving the possibility open for functional enzymes confounding experimental results. We decided to employ CRISPR/Cas9 due to its reported efficacy and chose two different cell lines for our experimental system. HEK 293 cells were chosen due to their ease of use and universal cell

biology applications, while A549 cells were chosen due to their increased physiological relevance and potential as optimal cells for microscope imaging.

After two years of effort, our knockouts were successfully generated and we moved on to determining what effect, if any, they had on influenza infections. After six months we found that all knockout cell lines tested displayed reduced influenza infections and furthermore, that all knockouts were less susceptible to entry of both influenza and other endosome-entering viruses. Naturally we sought to find a common mechanism to explain our findings, and turned our attention to the role glucosylceramide might play in cellular endocytosis.

Over the next 18 months we performed a number of microscopy assays, biochemical measurements, and flow cytometry techniques to uncover the mechanism associated with our observed phenotype and finally determined that cells with disrupted glucosylceramide homeostasis displayed dysfunctional endosome trafficking. We decided to publish our work and began writing up our results as we finished rounding out our story. However, as we were preparing to submit the manuscript we discovered an error in our data – the glucosylceramide synthase knockout cells had been mislabeled or switched out with glucosylceramidase knockouts in the A549 cell line. After combing back through the data and double checking dates of knockout confirmation against dates of the various data obtained, we determined that any and all mechanistic work involving A549 glucosylceramide synthase knockouts could not be trusted and therefore had to be removed from the manuscript.

Though it still remains unclear what exactly occurred to result in such a disheartening error, we were fortunate it was caught and rectified before publication. We decided to split our work into two parts: an entirely complete story centered on glucosylceramidase (found in **Chapter 3**), and the remaining verified data involving glucosylceramide synthase (found in **Chapter 4**). Together these two stories describe a previously unknown relationship between influenza and glucosylceramide; but more importantly they provide an extraordinary example of the importance of performing stringent and rigorous science in order to present the most accurate and reliable data possible.

1.3 Influenza

1.3.1 History

In the 5th century B.C.E., the Greek doctor Hippocrates described a disease that left victims with chills, a fever, and usually resulted in their death. In the seventh chapter of the sixth book of his *Epidemics*, Hippocrates described the symptoms of a plague in northern Greece:

In Perinthus, a great many were consumptive in the spring, occasioned in some by an epidemic cough, in the winter; and in others by the long continuance of disorders... A consumption seized him about thirty, and he died. The keeper of the wrestling-place ... after wrestling much with a stronger, and falling upon his head, went away and drank a great deal of cold water. He could get no sleep that night, was very restless, and cold in his extremes. The next day he went home; had no stool, though a suppository was put up; made water a little, whereas before he had made none; was bathed at night, but yet could get no sleep, or lie still, and was lightheaded. The third day, was cold in his extremes; grew hot, and sweated; but died this very day...

Many scholars agree that this was the first recorded instance of an infection by influenza virus (1). Due to the many similarities shared between influenza symptoms and other afflictions, it is hard to pinpoint the next mention of the disease. However, in 1580 a disease matching the description of influenza was reported to originate in Russia and rapidly sweep across Europe, infecting a large proportion of the populace (2). From that point there were numerous mentions of outbreaks and various plagues that could be attributed to influenza, before the 1918 pandemic that swept across the world and killed millions of people.

In 1918 a strain of influenza (later determined to be H1N1) spread quickly across the globe, killing approximately 50 million people (3). Considered one of the deadliest disease outbreaks in human history, the 1918 “Spanish flu” is second only to the Black Death of the 14th century in terms of sheer number of people killed (4). In response to the mass devastation it had on human society, researchers and governments began focusing their efforts on studying the cause of the 1918 pandemic. Over the next century the field of influenza research exploded as our modern understanding of virology began to take shape.

1.3.2 Influenza Structure

A member of the *Orthomyxoviridae* family, influenza virus is comprised of a protein capsid within a lipid bilayer envelope. Embedded within this lipid membrane are two surface proteins, hemagglutinin (HA) and neuraminidase (NA). HA binds to surface receptors on cells (sialic acid), while NA is responsible for budding off of new virions. The capsid protein is called the matrix protein

(M1). Within the capsid is the influenza genome, comprised of eight negative single stranded RNA genes encoding eleven viral proteins. These genes are wrapped around a nucleoprotein (NP) and an RNA polymerase subunit consisting of PB1, PB2, and PA proteins. Together, the NP and RNA polymerase subunit are called the viral ribonucleoprotein (vRNP) complex, and the vRNPs serve as the template for influenza genome replication (5) (**Fig. 1.1**).

The membrane of influenza is derived from the plasma membrane of host cells that the virus uses to encapsulate its capsid protein upon assembly and budding. Quantitation of the lipidomes of influenza virus grown in Madin-Darby canine kidney cells (MDCK) determined that these viral lipids were enriched in sphingolipids and cholesterol compared to host cell membranes, and supported the hypothesis that influenza virus assembles at lipid microdomains at the cell surface (6). Many studies have established the relationship between cholesterol and influenza budding, though the impact of sphingolipids on the entry stage of the viral life cycle is not as well understood (7–11).

1.3.3 Influenza Life Cycle

The influenza life cycle can be broadly classified into three main components: entry, replication, and exit (see **Fig.1.2** for a complete depiction). Infection of a host cell by influenza begins when HA binds to sialic acid on the host surface (12). Upon binding, the virus is internalized into a vesicle that later forms into the

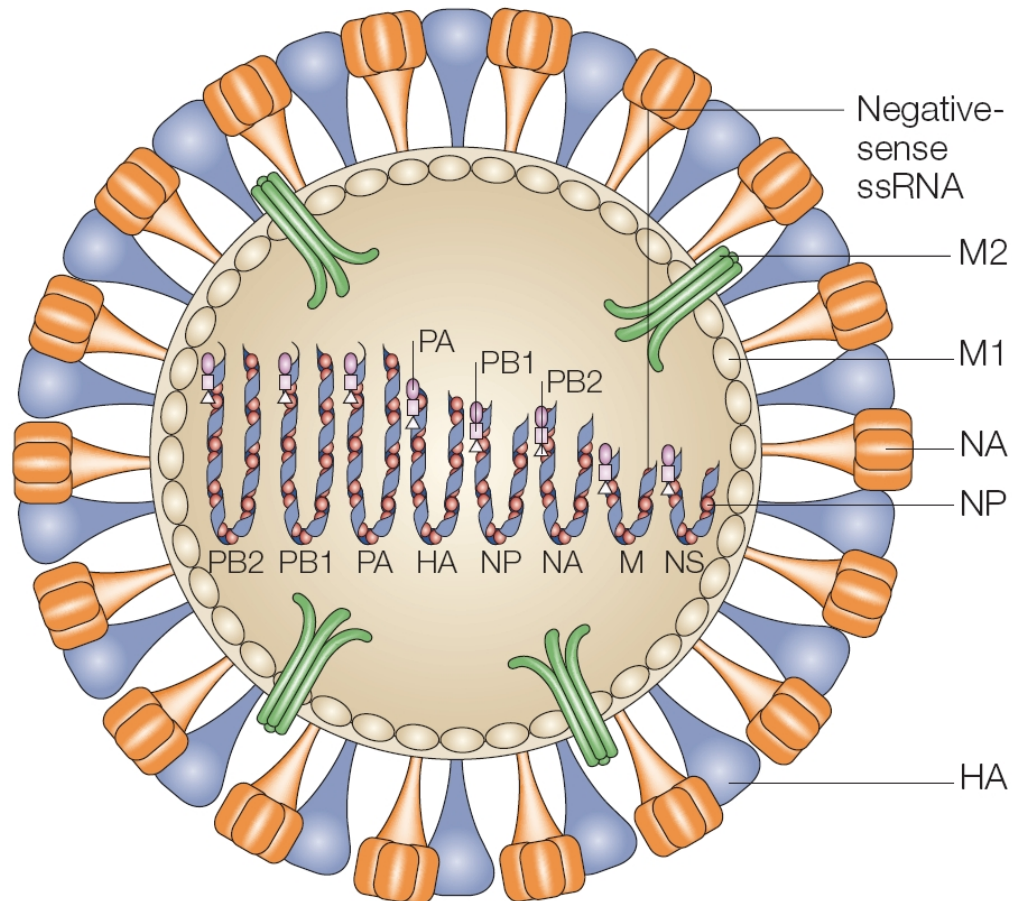


Figure 1.1 Structure of influenza virus.

Influenza virus is comprised of a protein capsid (made up of a matrix protein M1) within a lipid bilayer envelope. Embedded within this lipid membrane are two surface proteins, hemagglutinin (HA) and neuraminidase (NA). The influenza genome is comprised of eight negative single stranded RNA genes encoding eleven viral proteins. These genes are wrapped around a nucleoprotein (NP) and an RNA polymerase subunit consisting of PB1, PB2, and PA proteins. Adapted from Ref (13).

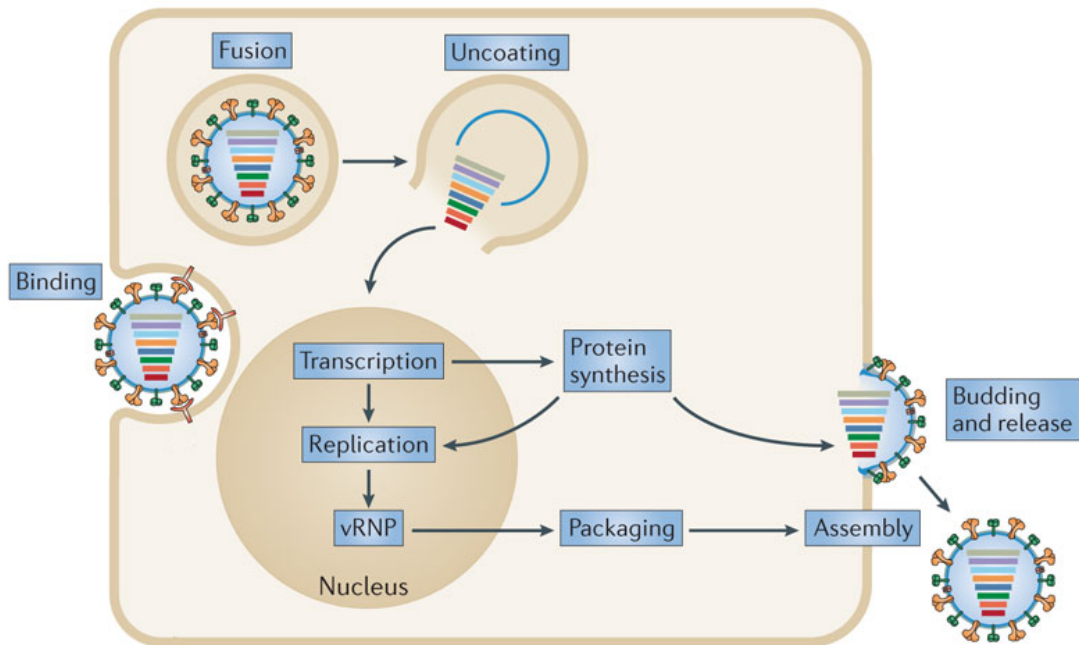


Figure 1.2 Influenza life cycle.

Influenza first binds to the cell surface before being internalized in an endosome. Following internalization the virus fuses to the endocytic vesicle and releases its genome into the host cell for replication. After the vRNA is replicated and new influenza proteins synthesized, the virus assembles at the plasma membrane and buds out as a new virion. Adapted from Ref. (14)

early endosome, characterized by expression of specific proteins such as early endosome antigen 1 (EEA1) and Ras-related protein Rab-5A (Rab5). This internalization process generally takes between 5-15 minutes (14).

As the endosome containing influenza proceeds down the endocytic pathway and matures into a late-endosome/lysosome, the pH of the endosomal compartment drops as a result of the action of several v-ATPases (16, 17). This acidification results in a conformational change in the HA protein, exposing the relevant fusion peptides and anchoring them into the endosome membrane (18–20). This anchoring brings the endosomal membrane next to the viral envelope, and facilitates the formation of a fusion pore between the two lipid membranes. The vRNPs are then released into the cytosol to initiate the replication phase of the viral life cycle.

Several nuclear localization signals are responsible for transporting the vRNPs to the host nucleus where genome replication can occur (21, 22). Because influenza is a negative stranded RNA virus, its genome must first be transcribed to positive sense RNA before proteins can be translated (23). Once the complimentary RNA (cRNA) is transcribed, new negative sense viral RNA (vRNA) is transcribed from the cRNA. These vRNAs serve as templates for subsequent synthesis of viral mRNA, which is synthesized through a complex system of 'cap snatching,' reviewed extensively by De Vlugt *et al.* (24).

Following mRNA synthesis and nuclear export, influenza proteins are translated entirely by host cellular machinery. Proteins involved in the vRNP complex are shuttled back into the nucleus to bind to newly synthesized vRNA, while HA, NA, and the second matrix protein (M2) are shuttled to the cell surface and embedded within the plasma membrane. Though the precise mechanism behind the subsequent assembly and transport of the full viral particle to the cell surface remains somewhat unclear, vRNPs and influenza capsid proteins make their way to the plasma membrane to prepare for exit from the host cell (25). Newly synthesized influenza particles have been shown to be enriched in sphingolipids and cholesterol, indicating they may assemble at the sites of lipid rafts (or lipid microdomains) (6). Upon assembly at the plasma membrane, influenza induces budding from the host cell by creating a curvature of the membrane, likely through protein-lipid interactions of HA and NA (26–29). As influenza buds from the cell surface, NA cleaves the glycosidic linkage between sialic acid and the viral envelope, releasing the virus from the cell (30).

1.3.4 Influenza Vaccine and Therapies

Every year influenza virus kills between 250,000 and 500,000 people (31, 32). While therapies and vaccines against the virus do exist, they are sometimes ineffectual due to antigenic shift of influenza (33). The influenza vaccine is traditionally a trivalent vaccine protecting against three strains of influenza A, though a quadrivalent vaccine exists that confers protection against an additional strain of influenza B (34). In 2009 a strain of H1N1 influenza with a unique combination of genes began circulating in the United States (35). Dubbed “swine

flu” due to its similarity to several porcine influenza strains, the seasonal influenza vaccine did not protect against this particular H1N1 virus and the resulting pandemic infected ~60 million people (36).

Current FDA-approved drugs against influenza target a variety of steps in the influenza life cycle. However, due to antigenic drift influenza has developed resistance against several of these therapeutics. Currently, drug studies involving influenza utilize a structural biology approach coupled with novel bioinformatics pipelines to develop pharmacological interventions that aim to circumvent the problem of drug resistance (37). In addition to targeting highly conserved areas of the virus, researchers are attempting to develop novel drugs that target host cellular machinery known to be essential for the viral life cycle, such as the endonuclease inhibitor Xofluza that was recently approved in Japan (38). However, these host-targeted drugs often have issues of cytotoxicity and are compromised by their side effects (39). As a result, novel avenues for influenza therapies must be investigated.

1.4 Endocytosis

Endocytosis is the primary method by which cells internalize surface proteins and extracellular molecules, and is a critical cellular process that is essential to maintaining cellular physiology and function. Upon internalization, endocytosed cargo is sorted to a variety of destinations and fates: some proteins or macromolecules are targeted for degradation by the lysosome, others are

returned to the cell surface via recycling endosomes, still others are localized throughout the cell according to their specific role (40, 41). Entire theses have been written on different endocytic mechanisms and pathways, and for the sake of brevity, this dissertation will primarily delve into the endocytic pathway from early endosomes to the lysosome.

The start of the endocytic pathway begins after a ligand binds to the cell surface and a portion of the cell membrane pinches off to create a vesicle that encapsulates the bound ligand. As the vesicle matures and becomes an early endosome, it displays specific protein markers such as Ras-related protein Rab-5A (Rab5) and early endosome antigen 1 (EEA1). The early endosome is also called the sorting endosome, as it can either mature into a late endosome and eventually a lysosome, or it can become a recycling endosome that transfers its cargo back to the plasma membrane (42). It is important to note that while each type of endosome has a unique identity and purpose within the cell, the separation between endosome types is not a hard and fast division. Endosome identity is quite fluid, and endosomes may display multiple markers at the same time, such as both early and late endosome surface proteins.

As the early endosome matures into the late endosome (characterized by expression of Ras-related protein Rab-7A, or Rab7), it begins to experience a drop in pH due to the action of the vacuolar ATPase. These hydrogen pumps increase the concentration of H⁺ within the endosome, thereby creating a more acidic environment (43). While most early endosomes are located near the

plasma membrane, late endosomes move closer to the perinuclear region of the cell and eventually create fusion events with lysosomes. These late endosome-lysosome hybrids are termed endolysosomes, and they are very difficult to distinguish from endosomes and lysosomes because they often contain markers of both late endosomes (Rab7) and lysosomes (lysosomal-associated membrane protein 1, Lamp1) (44). The endolysosome serves as the point-of-no return for endocytic cargo, as fusion with host lysosomes serves to degrade any cargo stored within the vesicle through a combination of lysosomal proteases and increasing acidity (45). For further reading into the maturation and trafficking of the endocytic pathway, see excellent reviews by Elkin *et al.* (40) and Kaksonen *et al.* (46).

Many viruses have evolved to hijack endocytosis for entry into host cells. Upon binding to their host surface receptors, these viruses are internalized into an endosome and are shuttled down the endocytic pathway similar to any other endosome cargos. However, in order to escape degradation by host lysosomes, these viruses may contain fusion proteins that result in merging of the viral membrane with host endosomes and subsequent release of the viral genome into the cytoplasm (**Fig. 1.3**). Viral fusion proteins can be triggered by several different events, including stimulation by low pH, host proteases, or binding to specific host receptors. For examples of endosomal virus fusion triggers, see **Table 1.1** (47).

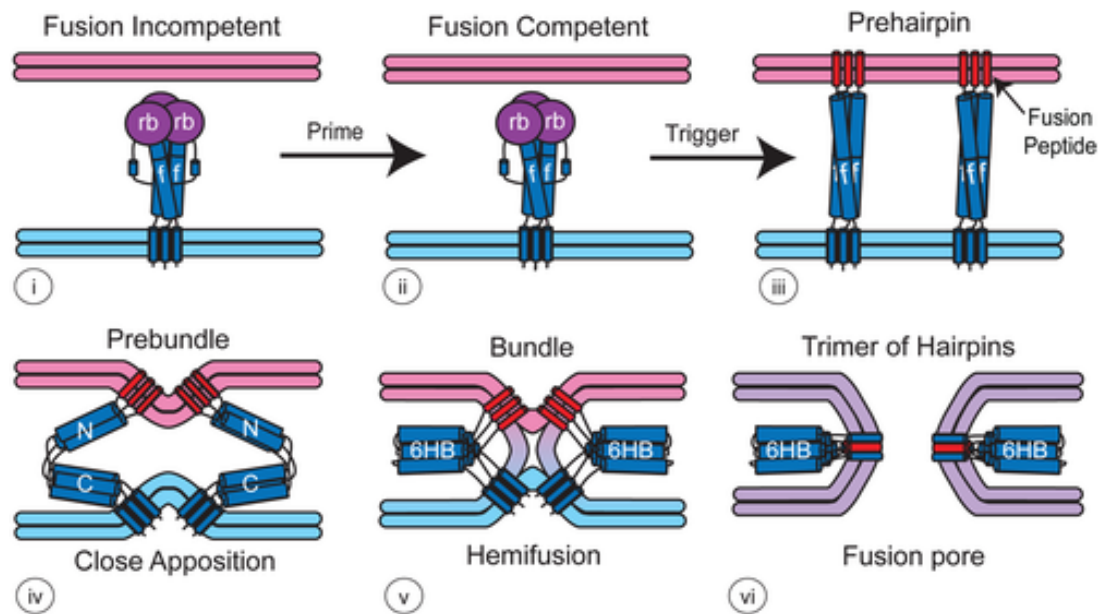


Figure 1.3 Fusion of enveloped viruses in endosomes.

This model represents a typical fusion sequence for enveloped endosome-entering viruses. Upon fusion triggering the fusion peptide draws the membranes for the virus and the endosome together and form a pore through which the viral genome is released into the cytosol. Adapted from Ref (47).

Family	Virus	Site	Trigger
Retroviridae	MLV	Plasma membrane	Receptor
Paramyxoviridae	PIV5	Plasma membrane	Receptor
Herpesviridae	HSV-1	Plasma membrane	Receptor
Coronaviridae	SARS	Plasma membrane or late endosome	Receptor + protease
Rhabdoviridae	VSV	Early endosome	Low pH
Togaviridae	SFV	Early endosome	Low pH
Bornaviridae	BDV	Early endosome	Low pH
Flaviviridae	TBE	Endosome	Low pH
Orthomyxoviridae	Influenza	Late endosome	Low pH
Arenaviridae	LCMV	Late endosome	Low pH
Bunyaviridae	UUKV	Late endosome	Low pH
Filoviridae	EBOV	Endolysosome	Low pH + additional cue(s)
Asfarviridae	ASFV	Late endosome	Low pH + additional cue(s)
Poxviridae	VV	Late endosome	Low pH + [additional cue(s)]
Arteriviridae	PRRSV	Early endosome	Low pH + [additional cue(s)]
Hepadnaviridae	HBV	Late endosome	

Table 1.1 Site and fusion-triggering mechanism for representative enveloped viruses.

Different viruses have evolved different fusion triggers. This table represents selected examples of specific viruses and their respective fusion triggers. Adapted from White and Whittaker (2016) (47).

1.5 Sphingolipids

Sphingolipids are a broad class of lipids involved in both cellular structure and cell signaling and are vital to numerous cellular functions, including proliferation, differentiation, and programmed cell death through apoptosis. Sphingolipid metabolism is performed through a variety of pathways, all of which shuttle through ceramide as the main hub (**Fig 1.4**). In *de novo* synthesis, serine and palmitoyl-CoA are combined by serine palmitoyltransferase to generate dihydrosphingosine, which is in turn converted to ceramide. In sphingomyelin hydrolysis, sphingomyelin lipids are catabolized by sphingomyelinase to generate ceramide. Finally, in the salvage pathway the signaling lipid sphingosine-1-phosphate (S1P) is dephosphorylated by S1P phosphatase and converted to sphingosine, which ceramide synthase then transforms into ceramide (48). Ceramide can be glycosylated by glucosylceramide synthase, and the resulting glucosylceramide serves as the precursor for a variety of long chain gangliosides. It is important to note that numerous enzymatic isoforms exist for virtually every step of sphingolipid metabolism, and thus studying the entire pathway is often a very complex endeavor (49).

Sphingolipid biology is a relatively new field, with most research only possible after the advent of new technologies in the 1980s and 90s (50). The bulk of studies on sphingolipids have thus far revolved around the context of cancer, as ceramide displays numerous pro-apoptotic properties while its derivatives (such as sphingosine-1-phosphate and GlcCer) are often pro-proliferation signaling

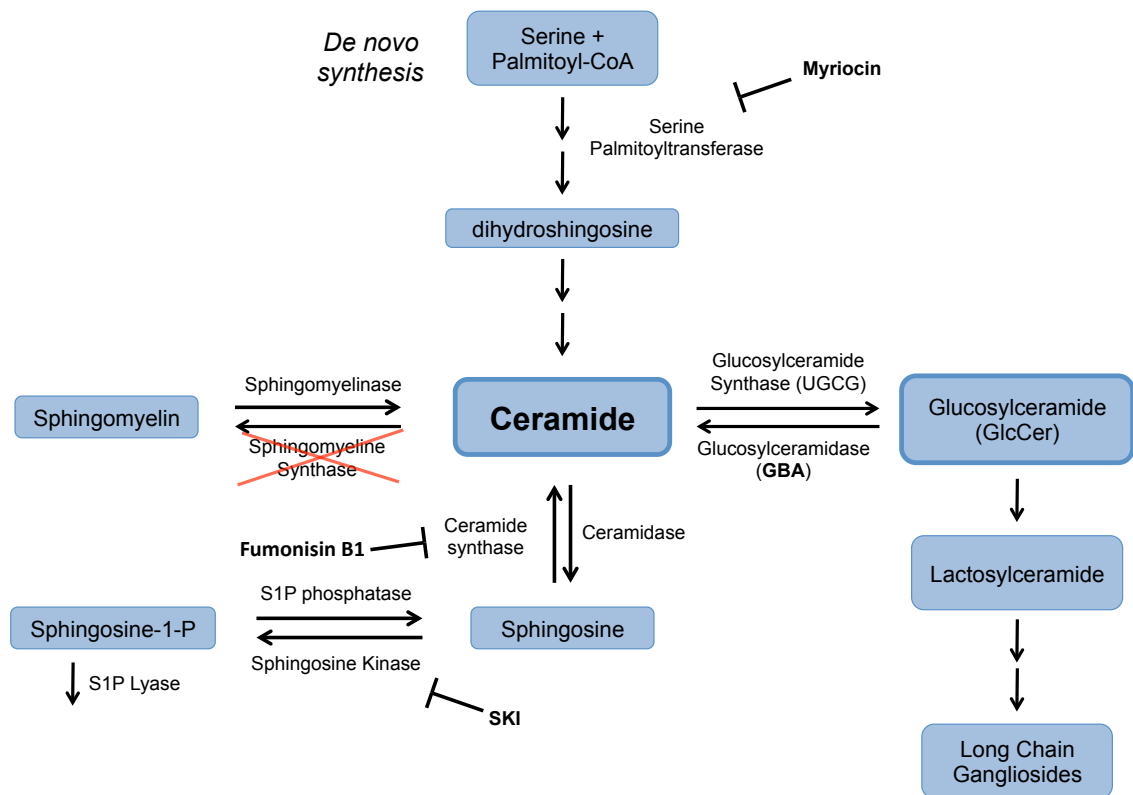


Figure 1.4 The sphingolipid pathway.

The sphingolipid pathway is a complex system involving numerous metabolites and enzymes. At the hub of the pathway is ceramide, which can be generated through *de novo* synthesis as well as a number of salvage mechanisms. Previous studies determined that deficiencies in sphingomyelin synthase (red X), as well as inhibition of serine palmitoyltransferase (with myriocin), sphingosine kinase (with SKI), or ceramide synthase (with fumonisin B1) result in reduced influenza infection.

molecules (49). Originally considered simply another component of cellular membranes, sphingolipids are now widely recognized as potent bioactive lipid species responsible for a plethora of regulatory pathways (51). For further reading regarding the metabolism and function of sphingolipids see several key reviews (49–55). One of the most prevalent human diseases directly linked to dysfunctional sphingolipid metabolism is Gaucher's disease, which occurs when mutations in glucosylceramidase (GBA) lead to accumulation of GlcCer in macrophages (56). Gaucher's disease is an autosomal recessive disorder with several identified mutations, and is currently treated through enzyme replacement therapy (57). In macrophages mutations in GBA result in a lysosomal storage disorder in which patient lysosomes are often increased in either size or number (58).

In the past two decades, multiple groups have explored the relationship between sphingolipids and viruses, discovering the diverse and critical role these lipids play in virus-host life cycles (59). During virus binding, sphingolipids may be involved in clustering virus receptors or may act as receptors themselves (60–63). The sphingolipid pathway has also been implicated in the entry of viruses including Ebola, bunya-, and caliciviruses. (64–66). In addition, sphingolipids may enhance replication of positive-sense single-stranded RNA viruses such as hepatitis C through interaction with their RNA polymerase (67, 68). Finally, sphingolipids may aid in the release of viruses from host cells, leading to enhanced infection of new hosts (69). Understanding the relationship between

viruses and host sphingolipids is therefore important to comprehending and treating viral infections.

Influenza and sphingolipids has been studied by numerous groups, and most studies focused on sphingomyelin and sphingosine-1-phosphate (S1P) (**Fig. 1.4**). Modulation of S1P by its metabolizing enzymes, sphingosine kinase and S1P lyase, altered influenza infections: S1P lyase overexpression interfered with, while sphingosine kinase overexpression increased, influenza infection in host cells (70). The same group later found that influenza infection leads to activation of sphingosine kinase. This activation led to upregulation of viral RNA synthesis and nuclear export of influenza ribonucleoprotein complexes (71). In addition, studies of cells that were deficient in sphingomyelin synthase demonstrated that influenza glycoproteins (HA and neuraminidase) displayed reduced transport from the cytosol to the cell surface. Finally, influenza infections were reduced upon pharmacological reduction of sphingomyelin infection (25).

Sphingolipid metabolism is a complex pathway, with numerous enzymes and lipids branching off from a central hub of ceramide. Ceramide is a pro-apoptotic molecule with a polar head group and a carbohydrate fatty acid chain. Both the head group and the fatty acid can be modified to generate numerous sphingolipid species (49). (**Fig. 1.4**). The glycosphingolipid glucosylceramide (GlcCer) is formed upon the the addition of a glucose molecule to ceramide's polar head group, and this reaction is catalyzed by the enzyme glucosylceramide synthase (UGCG), found primarily in the Golgi (73). The enzyme glucosylceramidase

(GBA) (found primarily in lysosomes) catalyzes, the catabolism of GlcCer to remove the glucose and create ceramide (27). Patients with mutations in GBA suffer from Gaucher disease, which is characterized as a lysosomal storage disorders (56, 75). Both UGCG and GBA have been implicated in maintaining the trafficking of glycolipids along the endocytic pathway (32). Though studies have examined the relationship of influenza and sphingomyelin, the glycosphingolipid arm of the pathway has so far been little-studied in the context of influenza. A recent haploid genetic screen revealed a role for UGCG in the infection of certain bunyaviruses in cell culture, (66), but to our knowledge no one has investigated the role of GlcCer in influenza infections.

CHAPTER 2 – MATERIALS AND METHODS

Cells

HEK 293 (human embryonic kidney; ATCC CRL-1573), HEK 293T/17 (ATCC CRL-11268), A549 (human lung carcinoma; ATCC CCL-185), and BHK-21 (baby hamster kidney; ATCC CCL-10) cells were grown in Dulbecco modified Eagle medium (DMEM) supplemented with 10% fetal bovine serum (FBS), 1% sodium pyruvate, 1% antibiotic/antimycotic, and 1% L-glutamine at 37°C (all from Gibco Life Technologies) with 5% CO₂.

CRISPR/Cas9 Gene Editing

gRNA targeting GBA and UGCG were selected using the CRISPR design tool developed by the Zhang laboratory at MIT and available at crispr.mit.edu. The gRNA was cloned into a Cas9-sgRNA (Addgene plasmid# 68463, deposited by Su-Chun Zhang) using BbsI. The resulting plasmid along with a plasmid encoding GFP was cotransfected into HEK 293 and A549 cells and sorted for positive GFP expression into single cells using an Influx flow cytometer. The cells, originally in wells of 96-well plates, were expanded, and the DNA from between 100-120 discrete clones was extracted and analyzed by PCR and subsequent gel electrophoresis. PCR was performed using primers flanking the regions of interest and designed to produce fragments of ~250-300 bp. Colonies with PCR products indicative of CRISPR activity (~5-10 per cell line) as compared to products from WT cells were maintained and analyzed by western blotting (for GBA protein) and mass spectrometry (for sphingolipid content).

Inhibitors and Other Reagents

Epidermal growth factor (EGF) (Cat# E9644), PPMP (Cat# P4194), and Bafilomycin A1 (Cat# B1793) were purchased from Sigma-Aldrich. EGF-Alexa Fluor 555 (Cat# E35350) was purchased from Thermo Fischer Scientific. BbsI was purchased from New England Biolabs (Cat# R0539S).

Influenza Viruses and VLPs, VSV Pseudoviruses, and EBOV trVLPs

Stocks of PR8 IAV were obtained from Charles River Laboratories. PR8 NS-GFP was kindly provided by Dr. Thomas Braciale at the University of Virginia (77). All influenza viruses were grown in embryonated chicken eggs, thereby cleaving HA₀ before any infection assays were performed (78, 79).

VSV-GFP pseudoviruses were produced using 5×10^5 BHK-21 cells plated in each of forty 10cm² dishes and transfected at ~75-80% confluency with plasmids encoding EBOV-GP Δ , Measles F and HN, or VSV-G using polyethylenimine (PEI; Polysciences, Inc Cat# 23966). Measles F plasmid was generously provided by Dr. Yusuke Yanagi of Kyushu University (80). The next day, cells were infected with pre-titered VSV- Δ G helper virus (from plaque eluate) encoding GFP for 1 hr at 37°C, washed extensively with PBS, and then cultured in growth medium overnight at 37°C. 24 hours post infection with helper virus, cell supernatants containing budded pseudovirus were collected, centrifuged twice (1360 x g/10 min) to clear debris, and concentrated ~50-fold using a Viva-Spin 20 300kDa concentrator. Finally, the concentrated pseudovirus was centrifuged through a 20% sucrose cushion (in HEPES-MES [HM] buffer containing 20 mM HEPES,

20 mM MES, 130 mM NaCl, pH 7.4) in an SW28 rotor for 2 hours at 112,398 x g at 4°C and then resuspended in 10% sucrose-HM. Pseudovirus stocks were stored at -80°C until use in subsequent experiments. Experiments using VSV-G and measles pseudoviruses were performed from a single prep, while experiments using EBOV pseudovirus were performed from several independent preps.

VSV-ΔG helper virus was produced as described previously (81). In brief, 5x10⁵ BHK-21 cells plated in five 10cm² dishes were transfected at ~75-80% confluency with 12 μg (per dish) of plasmid expressing VSV-G using PEI. ~24 hours later, the cells were infected with ~40 μl of VSV-ΔG-GFP plaque eluate (3.39 x 10⁸ infectious units/mL) in serum-free media for 1 h at 37°C. Cells were then washed extensively with PBS and incubated overnight in complete media at 37°C. The next day supernatants containing helper virus were collected, centrifuged for 10 min at 1070 x g to clear debris, and stored at -80°C.

Influenza M1-VLPs were produced by transfecting 1x10⁶ HEK 293T/17 cells in each of 5 10cm² dishes in complete media with no antibiotic/antimycotic using plasmids encoding βlaM1, and either WSN HA + WSN NA or VSV-G or EBOV-GPΔ using PEI. WSN is an H1N1 strain of influenza that is trypsin-independent *in vitro* (82). The βlaM1 plasmid was kindly provided by Dr. Adolfo Garcia-Sastre and the NIAID Centers of Excellence for Influenza Research and Surveillance (CEIRS) program (83). Media containing VLPs was harvested 24 and 48 hours post transfection and centrifuged twice to clear debris. The VLPs were then pelleted through a 20% sucrose cushion in HM buffer using an SW28 rotor for 2

hours at 112,398 x g at 4°C, and then resuspended in 10% sucrose-HM. VLPs were stored at -80°C.

Transcription/replication-competent viral-like particles (trVLPs) were prepared as described in (84). Briefly, HEK 293T/17 cells were transfected with pCAGGS-L, a tetracistronic minigenome plasmid, pCAGGS-VP35, pCAGGS-NP, pCAGGS-VP30, and pCAGGS-T7 polymerase. 24 hours post transfection the medium was replaced with fresh growth medium containing 5% FBS and cells were incubated at 37°C. 72 hours post transfection the medium was harvested, pooled, and centrifuged for 5 min at 800 x g to clear cellular debris.

IAV Reporter Infection Assay

WT and GBA or UGCG KO 293 and A549 cells were seeded in 96 well plates at a density of 3×10^4 cells per well. The next day cells were prechilled to 4°C for 15 minutes and then incubated with PR8 influenza encoding GFP fused to the N-terminus of NS1 (MOI of ~1) in growth medium without FBS or trypsin and centrifuged at 250 x g for 1 hour at 4°C. The cells were then incubated at 37°C. Approximately 16-18 hours post infection, cells were lifted with trypsin, fixed in 4% paraformaldehyde (PFAM), and assayed for GFP signal on an Attune NxT flow cytometer. Gates for positive GFP signal were created using uninfected cells to account for any background signal.

qPCR

WT and GBA or UGCG KO A549 cells were seeded in 24 well plates at a density of 5×10^4 cells per well. The next day cells were prechilled to 4°C for 15 minutes and then incubated with WT PR8 influenza in growth medium without FBS (with or without 1 µg/mL trypsin as indicated) and centrifuged at 250 x g for 1 hour at 4°C. The cells were then incubated at 37°C. At the indicated time points samples were harvested and RNA extracted using TRIzol reagent according to manufacturer's instructions (Thermo Fisher Scientific Cat#15596026). cDNA was generated using iScript cDNA synthesis (Bio-Rad Cat#1708891) according to manufacturer's instructions, and qPCR was performed with the following primers: IAV M1 forward (5'-CTTCTAACCGAGGTCGAAACG-3') and reverse (5'-GGCATTGTTGGACAAAGCGTCTA-3'). Relative expression of IAV M1 mRNA was calculated after normalization to endogenous reference gene beta-2-microglobulin (Bio-Rad pHSACID0015347).

Influenza M1-VLP Entry Assay

Cells were seeded in 96 well plates at a density of 3×10^4 cells per well. The next day cells were prechilled to 4°C for 15 minutes and then incubated with previously titered influenza M1-VLPs diluted in Opti-MEM I (OMEM) and centrifuged at 250 x g for 1 hour at 4°C. The cells were incubated at 37°C for 3 hours before addition of the β laM substrate CCF2-AM (Invitrogen, cat# K1032) in loading buffer (phenol red-free DMEM, 5 mM (HEK 293) or 20 mM (A549) probenecid (MP Biomedicals, cat# 156370), 2 mM L-glutamine, 25 mM HEPES, 200 nM bafilomycin) and incubated for an additional hour at room temperature.

Cells were then washed with PBS and allowed to incubate in loading buffer with 10% FBS overnight in the dark at room temperature. The following day, cells were lifted with trypsin, fixed in 4% PFAM, and analyzed for VLP entry as measured by CCF2-AM cleavage (resulting in FRET disruption and a color shift from green (518nm) to blue (447nm)) on an Attune NxT flow cytometer.

VSV Pseudovirus Infection Assay

Cells were seeded in 96 well plates at a density of 3×10^4 cells per well. The next day cells were prechilled to 4°C for 15 minutes and then incubated with VSV pseudoviruses in Opti-MEM I (OMEM) and centrifuged at 250 x g for 1 hour at 4°C. Cells were then washed and incubated for 18-24 hr at 37°C. The cells were then lifted, fixed, and analyzed for GFP expression via flow cytometry on an Attune NxT flow cytometer.

trVLP Infection Assay

Infection of HEK 293 cells by trVLPs was performed as described previously (84). Cells were seeded in opaque 96 well plates, and when the cells were approximately 50% confluent they were transfected with (per well) 13.88 ng pCAGGS-Tim1, 4.16 ng pCAGGS-VP30, 6.94 ng pCAGGS-VP35, 6.94 ng pCAGGS-NP, and 55.55 ng pCAGGS-L in order to support entry and replication of infecting trVLPs. 24 hours post transfection the medium was removed and trVLPs were added. Cells were incubated for 18-24 hours in growth medium at 37°C, before being analyzed using *Renilla*-Glo luciferase assay system (Promega Cat# E2710) on a GloMax plate reader.

Western Blotting

Cell samples were lysed in 1% SDS containing 5 mM EDTA, and 1 mM sodium vanadate (Sigma; Cat# S6508). These lysates were then resolved by SDS-PAGE and the proteins subsequently transferred to PVDF membranes. The membranes were then probed with the indicated primary antibodies followed by secondary antibodies coupled to horseradish peroxidase. Signals were visualized following incubation with a chemiluminescent horseradish peroxidase substrate. Images were captured with an Alpha-Innotech Fluorchem detector. For quantification, samples were normalized to signals for GAPDH in the lysates using Image Studio Lite.

Antibodies

Antibodies were purchased from the following sources: anti-EGFR (A-10), Santa Cruz Biotechnology (Cat# sc-373746); anti-GBA, Abcam (Cat# ab55080); anti-GAPDH (14C10) Cell Signaling Technology (Cat# 3683); anti-UGCG (M03), Abnova (Cat# H00007357); anti-Cathepsin B, Santa Cruz Biotechnology (Cat# sc-365558).

Lipid Mass Spectrometry and Enzyme Activity Assay

Lipids were extracted from cell lysates as described previously (85). Briefly, samples were centrifuged to remove debris, resuspended in a mixture of isopropanol: water: ethyl acetate (30:10:60) (with 20 pmol of internal standards added) and incubated for an hour at 37° C with shaking. Samples were centrifuged and the upper organic layer was transferred to a new tube before

being dried down under nitrogen gas. Samples were then resuspended in a reverse-phase LC-MS/MS solvent and analyzed on an Acquity I-Class/Xevo TQ-S micro IVD system. Mass spectrometry peaks were compared to internal standards and all data are represented as pmol of lipid/mg of protein. For the enzyme activity assay, cells were incubated with 5 μ M C6 ceramide nanoliposomes for 4 hours at 37°. Samples were then collected and lipids extracted. Lipids were analyzed by mass spectrometry for both C6 ceramide and C6 GlcCer concentration to determine the activity level of UGCG (85).

EGFR Degradation

WT and GBA KO A549 cells were seeded in 6 well plates at a density of 6×10^5 cells per well. The next day cells were washed twice with PBS and then incubated with 50 ng/mL EGF in growth media at 37°C for the indicated times. Cells were lysed and analyzed by western blotting as described above. For quantification, samples were normalized to the signal for GAPDH and then to 0 hour.

Cathepsin Activity Assays

In vitro Cathepsin B and Cathepsin L activities in HEK 293 cell lysates were measured as described previously (86, 87). Briefly, Cathepsin L activity was assayed with the Cathepsin B+L substrate Z-Phe-Arg-7-AMC (Calbiochem, Cat# 03-32-1501) in the presence of 1 μ M CA-074 (Calbiochem, Cat# 205530), a Cathepsin B inhibitor. Cathepsin B was measured in the same manner using Z-Arg-Arg-7-AMC (Calbiochem, Cat# 219392) and no inhibitor. *In vivo* Cathepsin

B activity in HEK 293 cells was measured using Magic Red-(RR)₂ (BioRad Cat# ICT937) stain as per the manufacturer's instructions.

Influenza Fusion Assay

Influenza PR8 was dually labeled as described previously (88, 89) with 3,3'-dioctadecyloxycarbocyanine (DiOC18) and octadecyl rhodamine B (R18) at final concentrations of 0.2 and 0.4 μ M, respectively. The reaction mixture was vortexed vigorously and left to incubate for one hour at room temperature before being filtered through a 0.22 μ m filter. Labeled virus particles were then bound to pre-chilled cells at an MOI \sim 5 (by pre-titered visual inspection) at 4°C for 15 minutes. Titering was determined by performing a standard curve of labeled particles and comparing the concentration of particles added to the average number of particles/cell in imaging by visual inspection. Following binding, cells were washed three times with cold PBS before being placed at 37°C for 40 minutes. Cells were then fixed in 4% paraformaldehyde for 20 minutes and imaged. Images were acquired on a Nikon Eclipse TE2000-E microscope equipped with a Yokogawa CSU 10 spinning-disk confocal unit and a 512-by-512 Hamamatsu 9100c-13 EM-BT camera using a 60x/1.45 numerical aperture (NA) Nikon Plan APO Apo TIRF oil immersion objective. Non-fused influenza particles appear red, as the green signal of DiOC18 (Em, 501 nm) is suppressed by a combination of self-quenching and FRET from DiOC18 to R18 (Em, 578 nm). In contrast, fused particles appear green, due to loss of FRET and self-quenching. Images were processed for Gaussian background subtraction, and then by automated particle counting for the number of red and green particles using

ImageJ. The number of green particles was then divided by the number of red particles to obtain the reported ratio of fused to non-fused events for each field.

Trafficking Assays

Cells were transfected with GFP-Lamp1 (Addgene plasmid# 34831, deposited by Esteban Dell'Angelica) using Lipofectamine 2000 (Invitrogen, cat# 11668-030) and incubated overnight in growth media. The next day, PR8 influenza was incubated with 1 μ M R18 for 1 hour at room temperature as described previously (90). Labeled viruses were filtered through a 0.22 μ m filter and then immediately bound to pre-chilled cells at an MOI > 1 at 4°C for 15 minutes. For EGF trafficking, Alexa Fluor 555-EGF was bound to pre-chilled cells at 4°C for 15 minutes at a final concentration of 100 ng/mL. Following binding with either fluorescently labeled IAV or fluorescently labeled EGF, cells were washed three times with PBS followed by the addition of prewarmed media lacking IAV or EGF and placed at 37°C for 40 minutes. Cells were then fixed in 4% paraformaldehyde containing 5 μ g/mL of Hoescht 33342 (Thermo Fischer Scientific Cat#H3570) for 20 minutes before imaging. Images were acquired on a Nikon Eclipse TE2000-E microscope equipped with a Yokogawa CSU 10 spinning-disk confocal unit and a 512-by-512 Hamamatsu 9100c-13 EM-BT camera. Samples were acquired using a 100x/1.45 numerical aperture (NA) Nikon Plan Apo TIRF oil immersion objective.

To quantify colocalization of IAV or EGF with Lamp1, 100 independent images per experiment from two independent experiments were captured. Each image

was uniformly processed for Gaussian background subtraction and then for the Mander's coefficient of colocalization of IAV or EGF with Lamp1 using the automated JACoP plugin in ImageJ. To quantify the number of IAV or EGF particles, each image was uniformly processed for Gaussian background subtraction and then particles were counted using the automated particle analysis tool in ImageJ.

Measurement of (endo)lysosomal pH

pH of lysosomes was measured using a FITC-dextran conjugate as described previously (91). Cells were plated at a density of 9000 cells/cm² in 35mm dishes and incubated in cell culture medium containing 0.1 mg/mL FITC-dextran for 72 hours. Cells were then pulsed in medium without FITC-dextran for 2 hours, lifted by trypsinization and washed with PBS. Cells were then resuspended in PBS and analyzed on a BD four color FACSCalibur flow cytometer by exciting with a 488 nm laser and collecting emission data at 530 (FL1) and 610 nm (FL2). The FL1/FL2 ratios of samples were compared to a standard curve generated using cells incubated with pH calibrated Britton-Robinson buffers containing 50 mM sodium azide, 50 mM 2-deoxyglucose, and 10 μ M nigericin.

CHAPTER 3 – GLUCOSYLCERAMIDASE MAINTAINS INFLUENZA INFECTION BY REGULATING ENDOCYTOSIS

The text included in this chapter has been adapted from the following publication:

Glucosylceramidase Maintains Influenza Infection By Regulating Endocytosis.

Kelly Drews, Michael P. Calgi, William Casey Harrison, Camille M. Drews, Pedro Costa-Pinheiro, Jeremy Joseph Porter Shaw, Kendra A. Jobe, Elizabeth A. Nelson, John D. Han, Todd Fox, Judith M. White, Mark Kester

Journal of Virology Mar 2019, JVI.00017-19; **DOI:** 10.1128/JVI.00017-19

3.1 Summary

Influenza is an RNA virus encapsulated in a lipid bilayer derived from the host cell plasma membrane. Previous studies showed that influenza infection depends on cellular lipids including the sphingolipids sphingomyelin and sphingosine. Here we examined the role of a third sphingolipid, glucosylceramide, in influenza infection following CRISPR/Cas9-mediated knockout of its metabolizing enzyme glucosylceramidase (GBA). After confirming GBA knockout of HEK 293 and A549 cells by both western blotting and lipid mass spectrometry, we observed diminished infection in both KO cell lines by a PR8 (H1N1) GFP reporter virus. We further showed that reduction in infection correlated with impaired influenza trafficking to late endosomes, and hence fusion, and entry. To examine whether GBA is required for other enveloped viruses, we compared entry mediated by the glycoproteins of Ebola, influenza, vesicular stomatitis, and measles viruses in GBA knockout cells. Entry inhibition was relatively robust for Ebola and influenza, modest for VSV, and mild for measles, suggesting a greater role for viruses that enter cells by fusing with late endosomes. As the virus studies suggested a general role for GBA along the endocytic pathway, we tested and found that trafficking of epidermal growth factor to late endosomes, as well as degradation of its receptor, were impaired in GBA knockout cells. Collectively our findings suggest that GBA is critically important for endocytic trafficking of viruses as well as cellular cargos including growth factor receptors. Modulation of glucosylceramide levels may therefore represent a novel accompaniment to strategies to antagonize 'late penetrating' viruses, including influenza.

3.2 Importance

Influenza is a viral pathogen responsible for the second largest pandemic in human history. A better understanding of how influenza enters host cells may lead to more efficacious therapies against emerging strains of the virus. Here we show that the glycosphingolipid metabolizing enzyme glucosylceramidase is required for optimal influenza trafficking to late endosomes and consequent fusion, entry, and infection. We also provide evidence that promotion of influenza entry by glucosylceramidase extends to other endosome-entering viruses and is due to a general requirement for this enzyme. Finally, we demonstrate that glucosylceramidase maintains efficient trafficking of endogenous cargos such as the EGF receptor along the endocytic pathway, and hence we hypothesize that optimal levels of glucosylceramide regulate cellular endocytosis. This work therefore has implications for the basic process of endocytosis as well as pathogenic processes including virus entry.

3.3 Introduction

Between three and five million people are infected with influenza A virus (IAV) worldwide each year, with one quarter to half a million cases resulting in death. While therapies against influenza exist, they are often administered too late to provide patient relief. Vaccines against the virus are produced each year, but may provide limited coverage against isolates arising from antigenic shift, such as occurred during the 2009 H1N1 pandemic, which is estimated to have killed up to 575,000 people (92). IAV is a negative sense RNA virus belonging to the family *Orthomyxoviridae* and is an enveloped virus that derives its lipid-bilayer

membrane as the virus buds through the host plasma membrane during virus assembly. To infect a cell, influenza employs its hemagglutinin (HA) protein to bind to sialic acid moieties on the target cell surface and then is taken into the cell by endocytosis (93). As the virus travels along the endocytic pathway, the acid environment prevailing in endosomes prompts conformational changes in HA, leading to viral membrane fusion with a late endosomal membrane (at pH ~5.0 to 5.7 depending on the strain) and subsequent genome release into the cytoplasm to initiate replication (47, 94–97). Hence, proper endosomal trafficking and pH are crucial to the influenza life cycle (98–100).

The membrane of influenza contains sphingolipids, a class of bioactive signaling molecules broadly distributed in mammalian cells and integral to multiple cell functions (53). Sphingolipids have also been shown to play diverse roles in virus-host interactions (59), including promoting virus binding (60–63), entry (64–66), replication (67, 68), and new particle release (69). Several laboratories have explored the relationship between influenza virus and sphingolipids, notably sphingosine-1-phosphate (S1P) and sphingomyelin (**Fig. 3.1**). Overexpression of S1P lyase lowered, while overexpression of sphingosine kinase increased, influenza infection in host cells (70). Moreover, influenza infection was shown to activate sphingosine kinase, generating sphingosine-1-phosphate, which was shown to increase viral RNA synthesis and nuclear export of influenza ribonucleoprotein complexes (71). Cells deficient in sphingomyelin synthase displayed reduced transport of the influenza glycoproteins (HA and neuraminidase) to the cell surface, and pharmacological reduction of

sphingomyelin with myriocin led to decreased influenza infection (25). These studies suggest that sphingolipid metabolism may provide an important target for discovery of future influenza therapeutics.

At the hub of sphingolipid metabolism is ceramide, an apoptosis-inducing molecule that can be modified at both its polar head group and carbohydrate chain to generate numerous sphingolipid species (49) (**Fig. 3.1**). Ceramide is converted to the glycosphingolipid glucosylceramide (GlcCer) by the addition of a glucose moiety catalyzed by the enzyme glucosylceramide synthase (UGCG), which is found primarily in the Golgi (73). Conversely, catabolism of GlcCer to remove the glucose group is performed by glucosylceramidase (GBA), which is reported to be primarily found in lysosomes (27). Mutations in GBA are well-studied genetic determinates of Gaucher disease, one of the most common lysosomal storage disorders (56, 75). While GBA has been implicated in trafficking of membrane glycolipids along the endocytic pathway (32), there have not been studies on the role of GBA in endocytic cargo trafficking. Moreover, while several studies have focused on the conversion of sphingomyelin to ceramide in the context of viral infections (**Fig. 3.1, pink shading**) (60, 64, 65, 101–103), little attention has been focused on the glucosylceramide arm of sphingolipid metabolism (**Fig. 3.1, green shading**). One recent study employing a haploid genetic screen revealed a role for UGCG in infections by specific bunyaviruses, but not by other viruses tested (66). And, to our knowledge no one has investigated the role of GBA in any viral infection.

In this study, we explored the role of GBA in influenza entry and infection by genetically knocking it out using CRISPR/Cas9. We found that cells deleted for GBA displayed reduced influenza trafficking to late endosomes and consequent fusion, entry, and infection, suggesting that GBA, and by extension optimal levels of its substrate lipid, GlcCer, are critical for maintaining the influenza life cycle in host cells. We also provide evidence that GBA is required for the entry of other viruses that enter cells by endocytosis as well as for the proper trafficking and disposition of normal cellular vesicular cargos destined for late endosomes including EGF and its receptor.

3.4 Results

3.4.1 Glucosylceramide metabolism regulates influenza infection

Previous studies have demonstrated that certain enzymes along the sphingolipid pathway (**Fig. 3.1**) are important for influenza infection; cells exposed to inhibitors of serine palmitoyltransferase or sphingosine kinase, as well as cells deficient in sphingomyelin synthase, displayed reduced influenza infection (70–72). The role of glucosylceramidase (GBA) or its substrate, glucosylceramide (GlcCer), has not been explored in influenza infections. To examine the role of GBA in influenza infection, we generated knockout (KO) cell lines lacking GBA using clustered regularly interspaced short palindromic repeats with Cas9 (CRISPR/Cas9) gene editing. CRISPR/Cas9 was performed in two cell lines, HEK 293 and lung epithelial A549 cells derived from an adenocarcinoma. HEK 293 cells were chosen for their ease of and broad use in cell biology, while A549 cells were chosen as they,

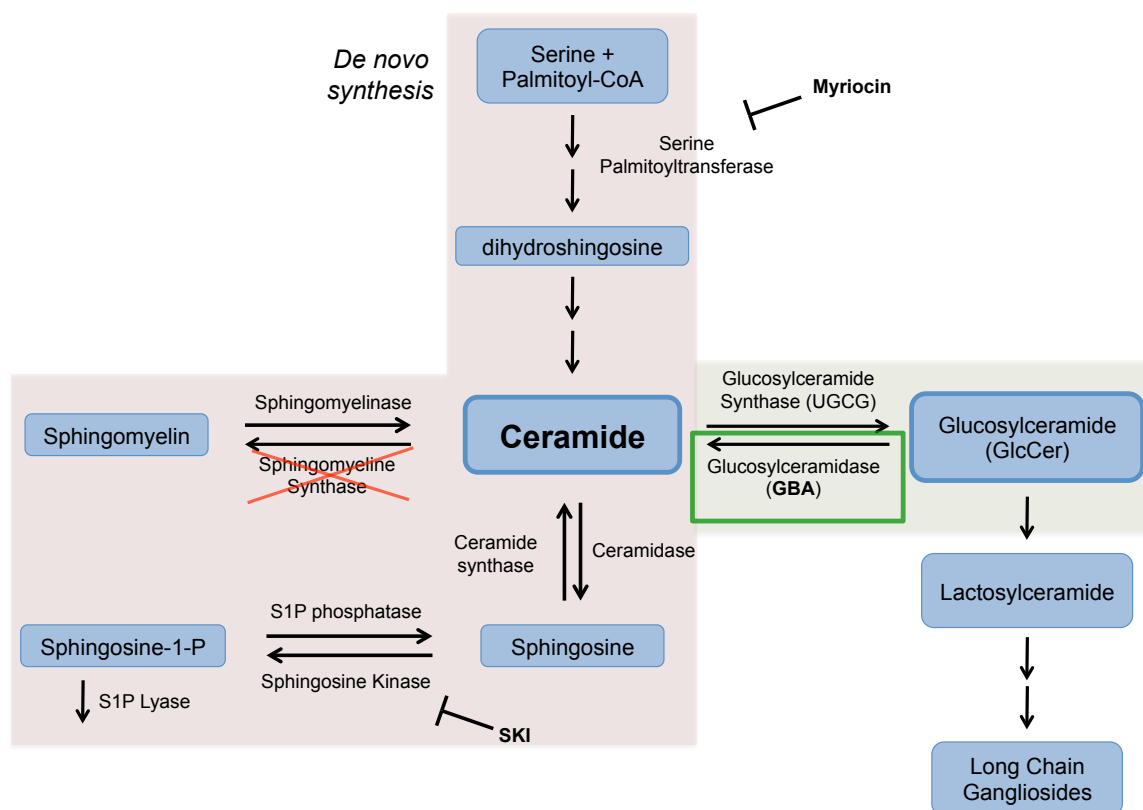


Figure 3.1 Role of sphingolipids in influenza virus infection.

The sphingolipid pathway involves numerous enzymes and lipids, most of which shuttle through ceramide as the pathway hub. Previous studies showed that deficiencies in sphingomyelin synthase as well as inhibition of serine palmitoyltransferase or sphingosine kinase led to decreased influenza infection (red shading) (70, 71, 104). However, the glycosphingolipid arm of the sphingolipid pathway (green shading) has not yet been studied in the context of influenza. We specifically examined glucosylceramidase (green box) to determine the effects of glucosylceramide metabolism on influenza infections.

being derived from lung epithelia, are considered more physiologically relevant for influenza research.

After performing CRISPR/Cas9 gene editing (**Fig. 3.2A**) and isolating individual clones, cells were analyzed for expression of GBA by western blot analysis and for the resulting concentration of GlcCer by mass spectrometry. In both HEK 293 and A549 cells CRISPR/Cas9 targeting resulted in complete loss of GBA protein as detected by western blotting (**Fig. 3.2B**). Mass spectrometry revealed that in both HEK 293 and A549 cells, GBA KO resulted in ~3-4 fold increase in GlcCer levels (**Fig. 3.2C and D**).

After confirming functional KO of GBA in the two cell lines described above, we examined the effect of loss of GBA on influenza infection. As seen in **Fig. 3.2E and F**, GBA KO in HEK 293 cells resulted in ~50% decrease in PR8 influenza infection, while in A549 cells GBA KO resulted in ~70% decrease.

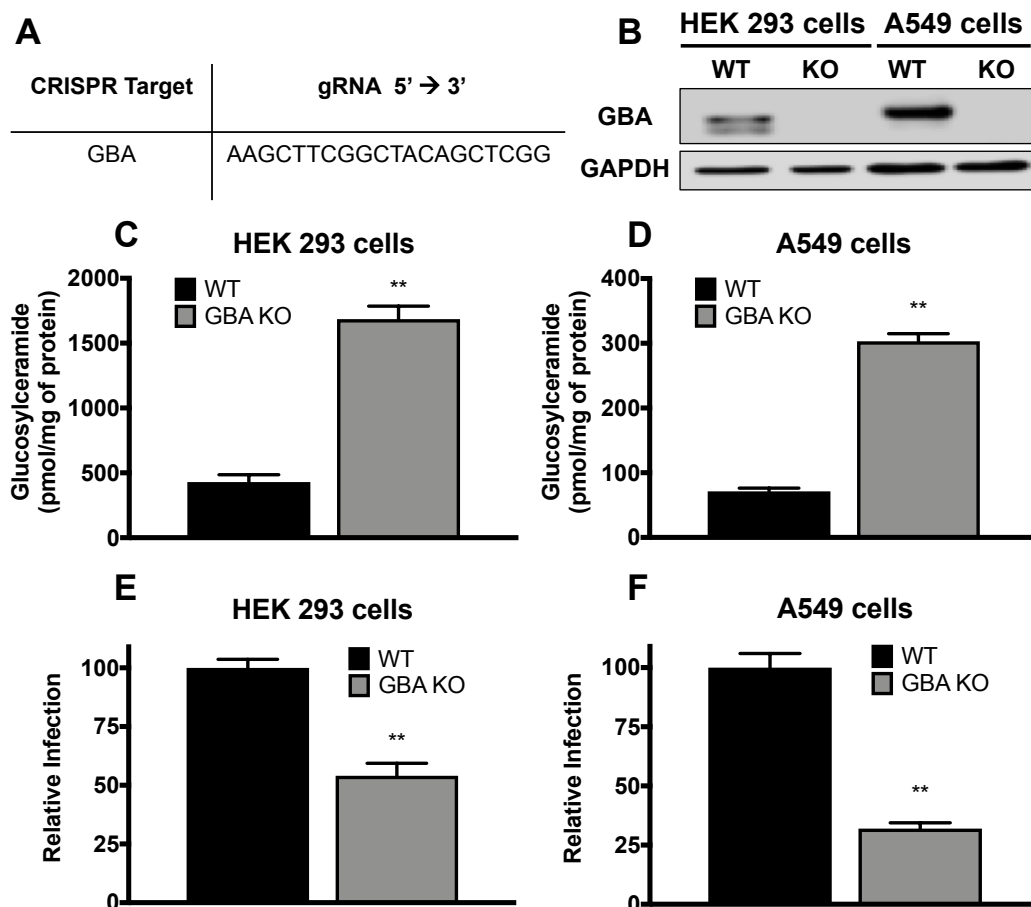


Figure 3.2 Glucosylceramidase regulates influenza infection.

HEK 293 and A549 cells were transfected with plasmids encoding Cas9-sgRNA targeting GBA and a plasmid containing GFP. Single cell colonies were selected for successful transfection as measured by GFP expression and expanded. **(A)** The gRNA used to target GBA is listed. **(B)** Complete loss of GBA protein expression was confirmed by western blot analysis of lysates of both HEK 293 and A549 cell colonies **(C,D)** Lipids were extracted from the cells and analyzed by mass spectrometry. Consistent with KO status, total GlcCer levels were raised in both HEK 293 and A549 GBA knockouts. Data represent the mean values of six biological replicates \pm SE. Loss of GBA activity was confirmed using a direct enzyme assay (data not shown). **(E,F)** Cells in triplicate samples were infected at 4° with PR8 influenza encoding an NS1-GFP chimeric protein and then incubated for ~18 hours at 37°C. The cells were then harvested, fixed, and analyzed for GFP expression by flow cytometry. In both HEK 293 and A549 cell lines GBA knockout resulted in decreased influenza infection compared to WT as measured by NS1-GFP expression. Data represent the mean \pm SE, n=6 experiments. ** p<0.01 using a Mann-Whitney non-parametric test. The growth rates of WT and GBA KO cells were similar over the duration studied (up to 4 days) (data not shown).

3.4.2 Changes in Sphingolipid Species in GBA Knockout Cells

As noted above, loss of GBA resulted in an expected increase in GlcCer levels. Surprisingly, this was not accompanied by a corresponding decrease in ceramide levels (**Fig. 3.3A and B**). Moreover, major changes in downstream ceramide metabolites such as sphingosine-1-phosphate and sphingomyelin were not noted. Taken together, we hypothesize that the lack of change in ceramide levels is due to compensatory *de novo* synthesis of ceramide, consistent with the increase seen in dihydrosphingosine (**Fig. 3.3A and B**), an intermediate metabolite in *de novo* synthesis (**Fig. 3.1 and Fig. 3.3C**, in purple). Interestingly, GBA KO cells displayed an even greater fold change in glucosylsphingosine (**Fig. 3.3A and B**), although the total mass of glucosylsphingosine is hundreds fold lower than that of glucosylceramide. Little is known regarding the metabolism of glucosylsphingosine, but its increase suggests a potential new role for GBA in the catabolism of glucosylsphingosine (**Fig. 3.3C**). A full list of all sphingolipids analyzed can be found in **Table 3.S1**.

3.4.3 Glucosylceramidase regulates entry of influenza and other endocytosed viruses

The reduction in influenza infection observed in GBA KO cells (**Fig. 3.2E and F**) could be due to defects at different stages of the viral life cycle. To begin to identify the step requiring GBA, we first analyzed IAV Matrix Protein 1 (M1) mRNA after 24 hours in cells incubated in media lacking trypsin, in order to limit IAV infections to one cycle of replication. GBA KO cells exhibited reduced IAV M1

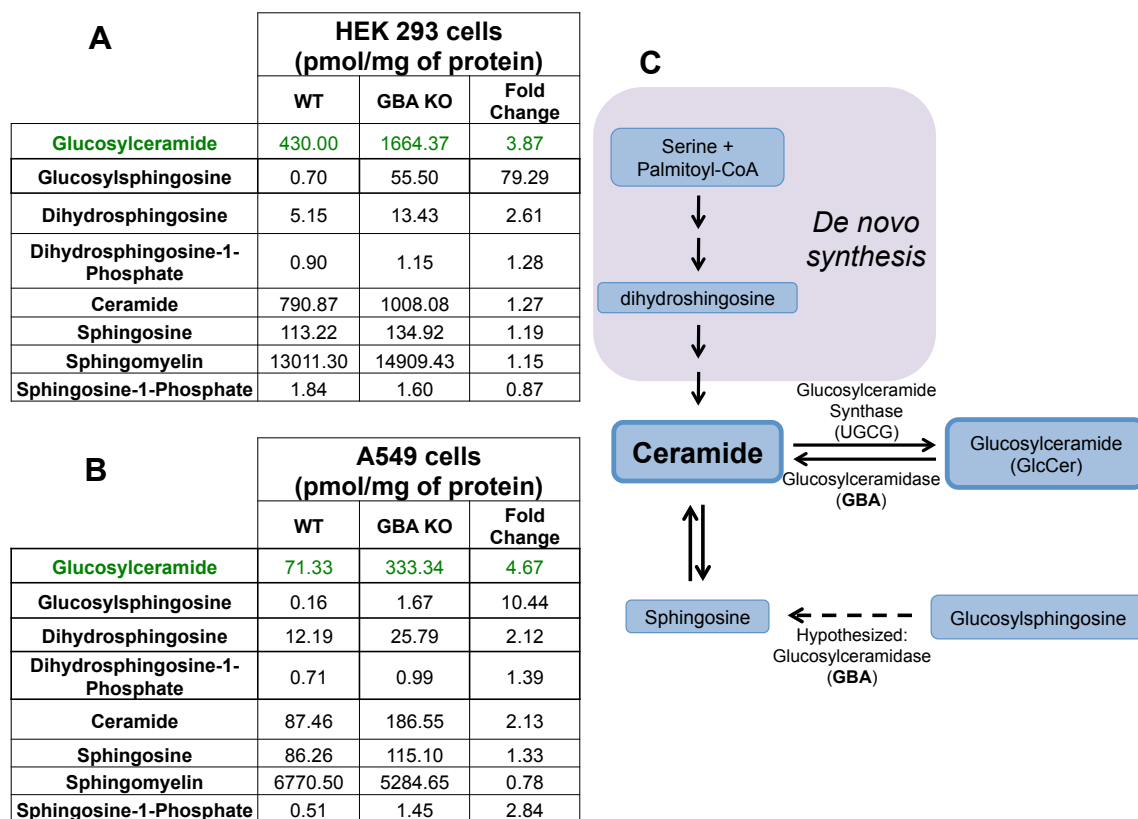


Figure 3.3 Analysis of Lipid Levels in GBA knockout cells.

(A,B) Sphingomyelin, ceramide, glucosylceramide, glucosylsphingosine, sphingosine, and sphingosine-1-phosphate were analyzed by mass spectrometry in all knockout cells and compared to their WT counterparts. Mass spectrometry peaks were compared to internal standards and all data are represented as pmol lipid/mg of protein (mean values shown, n=6). The data for GlcCer are the same as those displayed graphically in **Fig. 3.2C and D**. **(C)** Mass spectrometry data indicate GBA may utilize glucosylsphingosine as a secondary substrate (indicated by dashed arrow). *De novo* synthesis of ceramide is indicated by purple shading.

	HEK 293 cells (pmol/mg protein)			A549 cells (pmol/mg protein)		
	WT	GBA KO	Fold Change	WT	GBA KO	Fold Change
Sphingosine	113.22	134.92	1.19	86.26	115.10	1.33
Dihydrosphingosine	5.15	13.43	2.61	12.19	25.79	2.12
Sphingosine-1-Phosphate	1.84	1.60	0.87	0.51	1.45	2.85
Dihydrosphingosine-1-Phosphate	0.90	1.15	1.28	0.71	0.99	1.40
Hexosylsphingosine	0.70	55.50	79.29	0.16	1.67	10.42
Ceramide C16	35.51	38.50	1.08	39.61	59.65	1.51
Ceramide C18	35.75	102.03	2.85	4.03	8.25	2.05
Ceramide C20	15.92	41.58	2.61	0.41	0.92	2.22
Ceramide C22	101.60	153.11	1.51	1.35	3.51	2.60
Ceramide C22:1	15.77	41.34	2.62	1.03	1.26	1.22
Ceramide C24	141.73	121.58	0.86	2.53	5.93	2.35
Ceramide C24:1	429.57	495.86	1.15	37.91	105.76	2.79
Ceramide C26	2.44	2.17	0.89	0.30	0.41	1.38
Ceramide C26:1	12.58	11.91	0.95	0.28	0.85	3.06
Ceramide Totals	790.87	1008.08	1.27	87.46	186.55	2.13
Glucosylceramide C16	68.09	300.36	4.41	33.33	139.34	4.18
Glucosylceramide C18	8.02	50.90	6.34	3.19	14.45	4.53
Glucosylceramide C20	15.81	121.30	7.67	0.74	2.70	3.65
Glucosylceramide C22	77.22	337.22	4.37	3.25	15.90	4.89
Glucosylceramide C22:1	17.09	139.16	8.14	1.71	4.65	2.72
Glucosylceramide C24	76.48	164.12	2.15	2.74	14.74	5.37
Glucosylceramide C24:1	161.86	537.34	3.32	25.70	139.19	5.42
Glucosylceramide C26	0.68	2.45	3.61	N.D.	N.D.	N.D.
Glucosylceramide C26:1	4.74	11.52	2.43	0.67	2.36	3.53
GlcCer Totals	430.00	1664.37	3.87	71.33	333.34	4.67
Sphingomyelin C16	7871.70	7880.64	1.00	4773.83	3275.53	0.69
Sphingomyelin C18	1078.78	2290.01	2.12	386.14	286.62	0.74
Sphingomyelin C20	918.54	1232.56	1.34	130.51	110.36	0.85
Sphingomyelin C22	716.32	845.06	1.18	243.56	244.17	1.00
Sphingomyelin C22:1	224.62	349.47	1.56	61.35	59.70	0.97
Sphingomyelin C24	350.12	329.35	0.94	164.10	231.90	1.41
Sphingomyelin C24:1	1816.23	1951.44	1.07	985.50	1045.43	1.06
Sphingomyelin C26	6.29	5.89	0.94	8.29	15.25	1.84
Sphingomyelin C26:1	28.71	25.02	0.87	17.22	15.69	0.91
Sphingomyelin Totals	13011.30	14909.43	1.15	6770.50	5284.65	0.78

Table 3.S1 Full sphingolipid profiles of GBA knockouts.

Sphingomyelin, ceramide, glucosylceramide, sphingosine, and sphingosine-1-phosphate were analyzed by mass spectrometry in all knockout cells and compared to WT. Averages from five biological replicates are listed. Mass spectrometry peaks were compared to internal standards and all data are represented as pmol lipid/mg of protein.

expression after 24 hours (**Fig. 3.4A**). We next analyzed IAV M1 mRNA at two timepoints post infection in the presence of trypsin (to cleave the HA precursor and therefore permit production of infectious particles). After 8 hours, GBA KO cells displayed reduced IAV M1 expression compared to WT cells, but no difference was seen at 24 hours (**Fig. 3.4B**), indicating that multiple cycles of infection resulted in a rescue of the observed reduction in influenza infection. These data suggest that the observed reduction in influenza infection seen in **Fig. 3.2E and F** is limited to one cycle of replication, likely at the level of virus entry.

To test whether GBA regulates influenza virus entry (through endosomes) we monitored fusion of A/PR/8/34 influenza (H1N1) labeled with octadecyl rhodamine B chloride (R18) and 3,3'-dioctadecyloxycarbocyanine (DiOC18). Fusion results in a shift in fluorescence emission from red (R18, 586 nm) to green (DiOC18, 510 nm) due to separation of the probes upon fusion and dilution into the endosome membrane (88, 89). As seen in **Fig. 3.5A**, in WT cells there were ~3.5 fused influenza particles for every non-fused particle, while in the GBA KO cells the corresponding ratio was less than 1. The results in **Fig. 3.5** indicate that GBA is necessary for influenza particles to fuse in endosomes and suggest that the observed reduction in influenza infection (**Fig. 3.2E and F and Fig. 3.4**) is due to a defect in the entry phase of the viral life cycle.

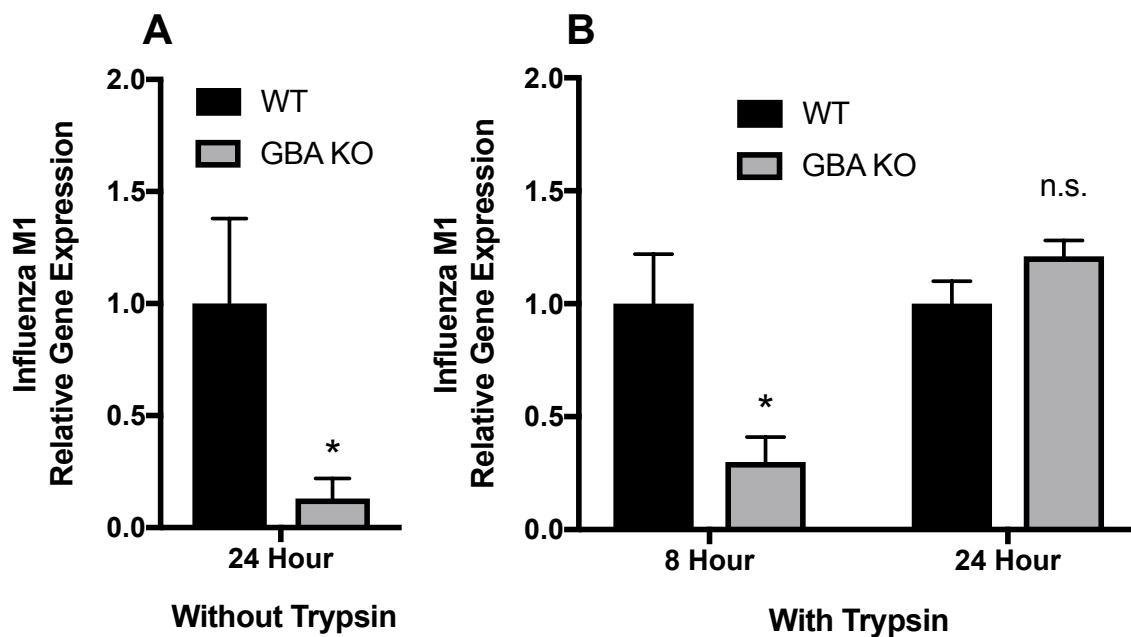


Figure 3.4 Influenza M1 gene expression is time and trypsin dependent in GBA KO cells.

WT and GBA KO cells in triplicate samples were incubated at 4° with PR8 influenza and then incubated for 8 or 24 hours at 37°C with or without trypsin in the medium. Samples were collected and mRNA extracted, cDNA generated, and relative gene expression analyzed by qPCR. **(A)** GBA KO cells display a reduction in influenza M1 expression when incubated without trypsin, and therefore limited to one cycle of influenza infection. **(B)** Influenza M1 expression is reduced after 8 hours in GBA KO cells in the presence of trypsin, but after 24 hours the expression matches that of WT cells.

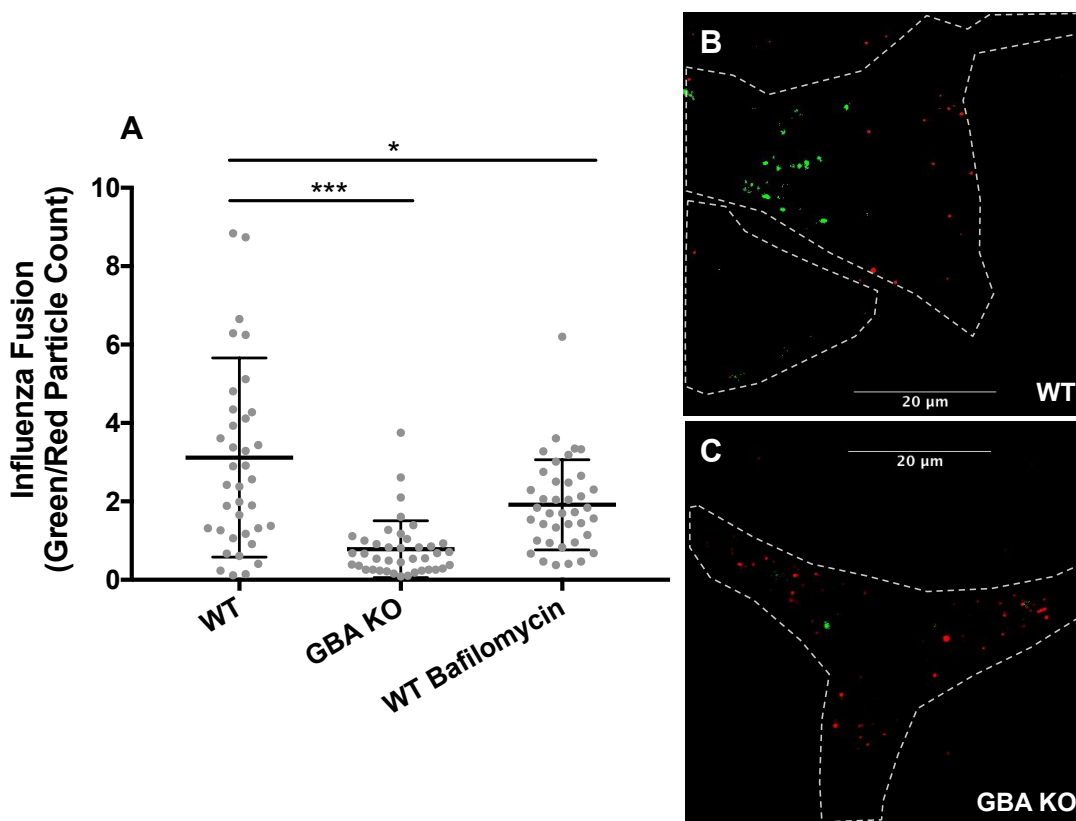


Figure 3.5 Loss of GBA reduces influenza virus fusion in endosomes.

Influenza was labeled with R18 (red) and DiOC18 (green) and then added to prechilled A549 cells at 4° for 15 min. Cells were then washed, incubated at 37°C for 30 min, fixed, and imaged at 60X magnification. The number of green (indicating a fused virus) and red (indicating an unfused virus) particles were then analyzed using ImageJ particle analysis. WT cells pretreated with 100 nM bafilomycin, an endosome acidification inhibitor, for 1 hr served as a positive control. **(A)** The ratio of fused to unfused particles was measured by automated counting of the number of green particles divided by the number of red particles on an image by image basis from 2 experiments (n = 40 fields for each treatment). Each data point represents the total number of green particles divided by the total number of red particles for 1 image field, and the bars indicate mean values \pm SD. (see Materials and Methods for details) **(B,C)** Representative images. Cell outlines were marked by visual examination. * $p < 0.05$, *** $p < 0.001$ using a Mann-Whitney non-parametric test.

We next asked if entry of other endocytosed enveloped viruses is impacted by loss of GBA. To do this, we generated virus like particles (VLPs) with an influenza Matrix-1 (M1)- β -lactamase (β -lam) core and bearing different viral glycoproteins on their surfaces: VSV G, which directs fusion in early endosomes (pH \sim 6.0), WSN influenza HA, which directs fusion in late endosomes (pH \sim 5.0-5.5), and Ebola GP, which direct fusion in endolysosomes (pH \sim 4.5-5.0) (105, 89, 106). WT and GBA KO cells were incubated with the VLPs and assayed for VLP entry using a fluorescent β -lam substrate in conjunction with flow cytometry (**Fig. 3.6A and B**). Interestingly, entry mediated by VSV-G was reduced in HEK 293 GBA KO cells, but unaffected in the corresponding A549 KO cells. Entry mediated by the HA of WSN influenza was reduced in both the HEK 293 and A549 GBA KO cells, consistent with the PR8 infection (**Fig. 3.2E and F and Fig. 3.4**) and fusion (**Fig. 3.5**) data. Entry mediated by EBOV-GP was also reduced in both KO cell lines, and trended towards a lower extent of entry than entry mediated by the glycoproteins of WSN influenza or VSV. These findings suggest that other viruses that enter cells through endosomes depend on GBA and further support the hypothesis of a greater entry inhibition for viruses that fuse with later endosomes, suggesting that GBA may affect endosome maturation and/or acidification. The differing results for VSV-G-VLPs between A549 and HEK 293 GBA KO cells may indicate a cell type dependence for GBA in the early endocytic pathway, as it is well established that expression of sphingolipids enzymes differ depending on tissue type (107).

To further explore the breadth of viruses whose entry is affected by GBA, we employed pseudoviruses with a VSV core and displaying the glycoproteins of measles virus, which fuses at neutral pH at the cell surface or the glycoproteins of the VSV and EBOV, which enter cells through endosomes. Infections by VSV pseudoviruses bearing the VSV and EBOV glycoproteins were decreased in GBA KO cells (**Fig. 3.6C and D**), as seen with their corresponding influenza M1-VLPs (**Fig. 3.6A and B**). In contrast, infection by pseudoviruses bearing the glycoproteins of measles virus appeared less dependent on GBA. These findings support the contention that virus entry through endosomes, particularly through late endosomes, is dependent on functional GBA and by extension, optimal levels of GlcCer. Interestingly, we tested the role of GBA in EBOV infections using EBOV transcription-replication competent VLPs (trVLPs), which recapitulate the full Ebola lifecycle and can be used under BSL2 conditions (108). As seen in **Fig. 3.6E**, loss of GBA strongly reduced Ebola trVLP infection even after multiple cycles of replication. These trVLP data contrast the finding in **Fig. 3.4** that the effect of GBA on influenza infection is limited to viral entry. Taken together, **Fig. 3.4** and **Fig. 3.6E** suggest that the role of GlcCer in viral assembly and/or budding may be virus-specific.

As the observed decreases in entry by viruses that fuse in late endosomes could be due to a defect in endosome acidification, we measured the pH of endosomes in GBA KO cells. To accomplish this we employed a dual-emission ratiometric technique after feeding cells FITC-dextran, which fluoresces at different intensities depending on the lysosomal pH (91). We utilized two independent

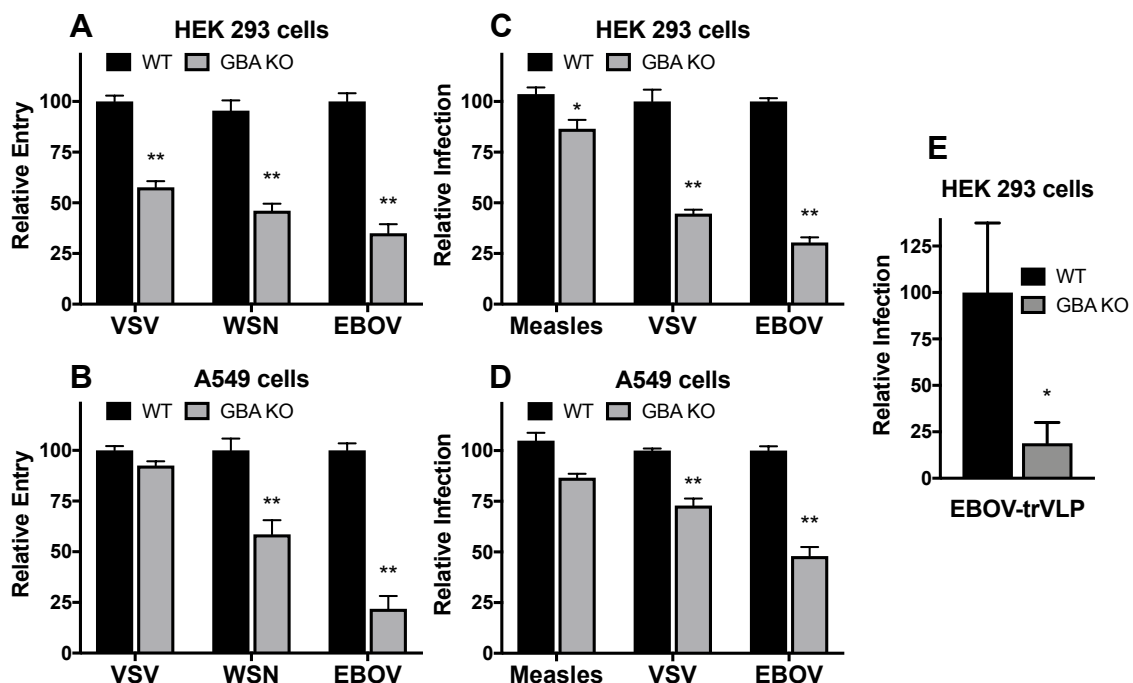


Figure 3.6 Loss of GBA reduces entry mediated by the glycoproteins of other endosome-entering enveloped viruses, with minimal effects on entry mediated by the glycoproteins of measles virus, a plasma-membrane entering virus.

(A,B) Influenza virus like particles (VLPs) bearing the VSV-G, WSN HA/NA, or EBOV-GP Δ glycoproteins were generated on a β laM1 backbone as described in the Materials and Methods. VLPs were added to prechilled cells, and the complexes were centrifuged at 4° for 1 hr, incubated for 3 hr at 37°C, and then incubated for 1 hr at room temperature in the dark in the presence of a fluorescent β -lactamase substrate. Cells were washed and the following day were harvested, fixed, and analyzed for β -lactamase activity via flow cytometry. (See Materials and Methods for details.) Data represent the mean \pm SE, n=6 experiments. (C,D) VSV pseudoviruses bearing the Measles-F and HN, VSV-G, or EBOV-GP Δ glycoproteins and encoding GFP were generated and bound to prechilled cells by centrifugation at 4°C for 1 hour. The pseudovirus-cell complexes were then incubated at 37°C for 24 hours, after which they were lifted, fixed, and analyzed for GFP expression via flow cytometry. Data represent the mean \pm SE, n=6 experiments. *p<0.05, ** p<0.01 using a Mann-Whitney non-parametric test. (E) WT and GBA KO HEK 293 cells were infected with EBOV trVLPs for 24 hr at 37°C and infection was assayed as described in the Materials and Methods. Data represent the mean \pm SE, n=5. * p<0.05 using a Mann-Whitney non-parametric test.

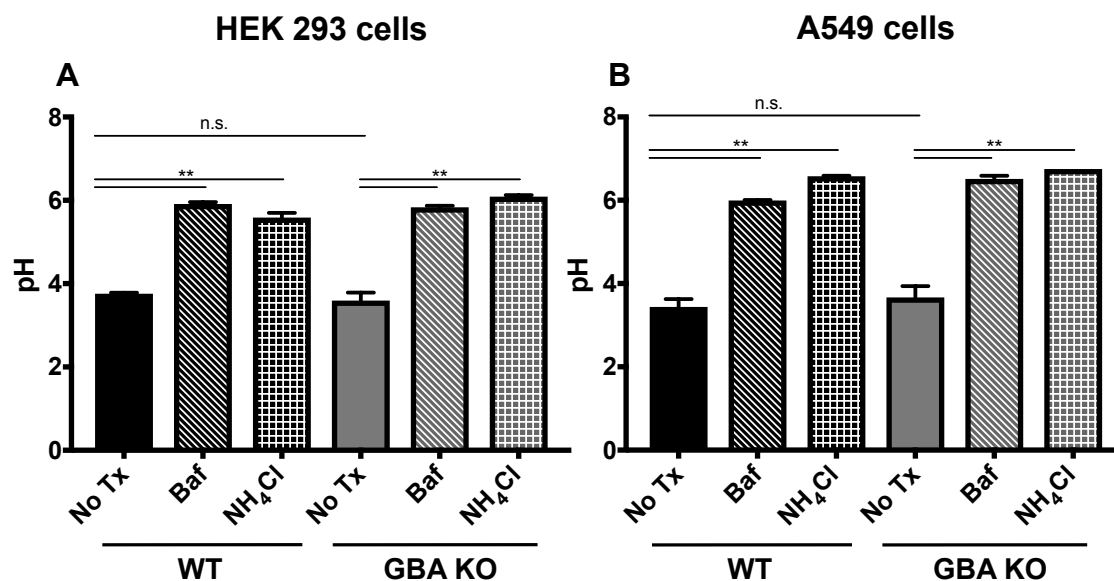


Figure 3.7 Loss of GBA does not detectably alter lysosomal pH.

Cells were incubated with FITC-dextran for 72 hours followed by a 2 hour pulse in medium without FITC-dextran. Cells were pretreated with bafilomycin (Baf) or NH₄Cl where indicated for 1 hour at 37°C to serve as positive controls. Following the dextran-free pulse, cells were analyzed by flow cytometry. Samples were compared to a standard curve of pH controls to determine lysosomal pH, as described in the Materials and Methods. Data represent the mean \pm SE, n=5 experiments.

positive controls (Bafilomycin and NH_4Cl) to confirm changes in pH. Using this technique, we determined that the pH in endosomes in GBA KO cells was not detectably different than that in WT cells (Fig. 3.7). These data suggest that our observed viral entry phenotype is not due to changes in the acidification process of the endosome.

3.4.4 Glucosylceramidase regulates influenza trafficking along the endocytic pathway

It is well established that influenza virus traffics to late endosomes for fusion (109). In addition, GlcCer has been implicated in lipid transport along the endocytic pathway (76). We therefore asked if GBA is important for trafficking of influenza particles to late endosomes. We transfected WT and GBA KO A549 cells with Lamp1-GFP and then infected the cells with R18-labeled influenza virus (red). In WT cells at 40 min post-warming influenza could be visualized in Lamp1⁺ (green) late endosomes in a high percentage of cells (**Fig. 3.8A and B**). In contrast, colocalization was reduced in GBA KO cells (**Fig. 3.8A and C**), albeit not as strongly as in WT cells treated with nocodazole (**Fig. 3.8A**), a microtubule inhibitor known to block trafficking between early and late endosomes. The observation that equivalent numbers of influenza particles were seen in WT and GBA KO cells (**Fig. 3.8D**) indicates that there is not a defect in influenza binding to GBA KO cells, but rather a defect in trafficking along the endocytic pathway.

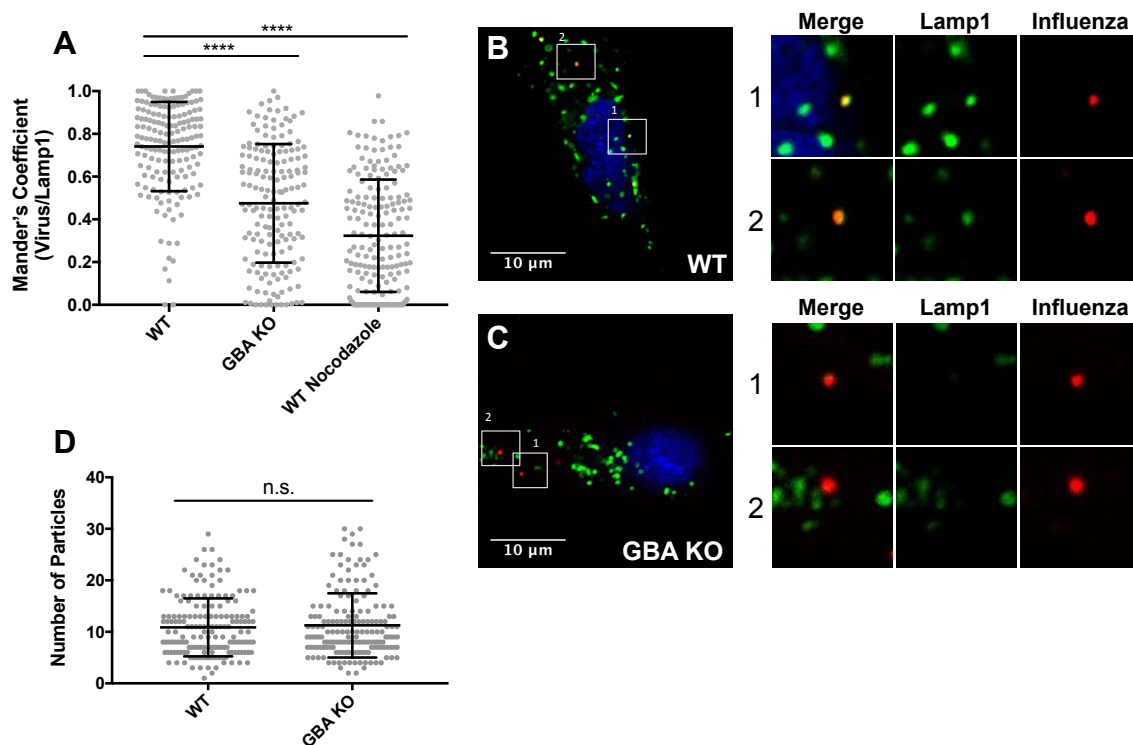


Figure 3.8 Trafficking of influenza to late endosomes is impaired in GBA KO cells.

A549 cells were transfected with Lamp1-GFP one day prior to experiments. WT cells were pretreated with 40 μ M nocodazole (as a positive control) for 1 hr where indicated. Influenza (PR8) was labeled with R18 and then added to prechilled cells at an MOI \sim 10 at 4 $^{\circ}$ for 15 min. Cells were washed, incubated at 37 $^{\circ}$ C for 40 min, fixed and imaged at 100X magnification. **(A)** Average Manders colocalization coefficients of influenza with Lamp1 (\pm SD) from 2 experiments (n = 100 fields in each experiment). Each data point represents the Manders colocalization coefficient for 1 image field, with one cell per image. **(B,C)** Representative micrographs of cells infected with R18-labeled influenza. Numbered white boxes are enlarged to the right of each panel. Examples are of colocalized particles in the WT cells and examples of non-colocalized particles in the knockout cells. **(D)** Total number of influenza virions in each image analyzed in **Fig. 3.8A**. **** $p < 0.0001$ based on a Mann-Whitney non-parametric test.

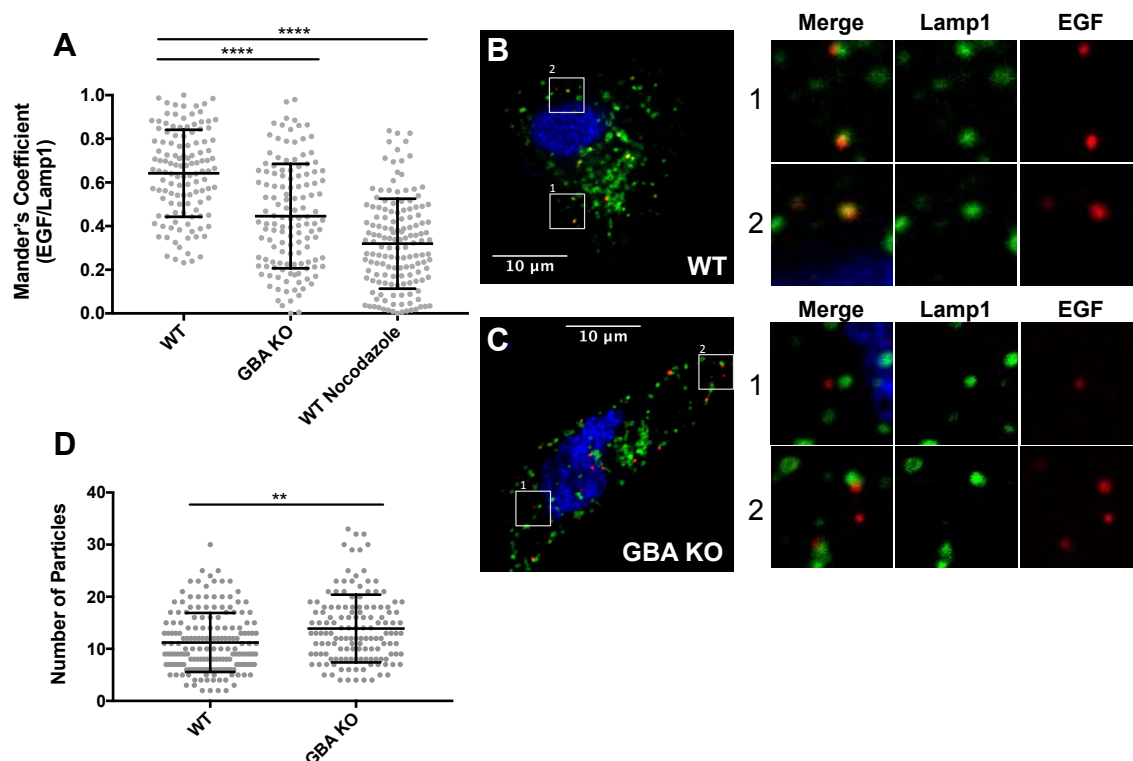


Figure 3.9 Trafficking of EGF to late endosomes is impaired in GBA KO cells.

A549 cells were transfected with Lamp1-GFP and pretreated with nocodazole as in Figure 6. EGF-555 (100 ng/mL) was added to cells prechilled to 4° for 15 min. Cells were then washed, incubated at 37°C for 40 min, fixed, and imaged. **(A)** Average Manders colocalization coefficients of EGF with Lamp1 (\pm SD) from 2 experiments ($n = 100$ fields in each experiment). Each data point represents the Manders colocalization coefficient for 1 image field, with one cell per image. **(B,C)** Representative micrographs of cells incubated with EGF-555. White boxes are enlarged to allow better qualitative visualization. Examples of colocalized particles pictured in the WT cells **(B)** and examples of non-colocalized particles pictured in the knockout cells **(C)**. **(D)** Total number of EGF particles in each image analyzed in **Fig. 3.9A**. ** $p < 0.01$, **** $p < 0.0001$ using a Mann-Whitney non-parametric test.

3.4.5 Glucosylceramidase regulates epidermal growth factor receptor trafficking along the endocytic pathway

In view of the findings on influenza trafficking, we next asked if GBA is required for proper trafficking of non-viral cargo along the endocytic pathway. We utilized the same approach as in **Fig. 3.8**, but with fluorescently tagged epidermal growth factor (EGF) (red) (**Fig. 3.9**). Similar to influenza, in WT cells at 40 min post-warming, EGF was seen in a high percentage of Lamp1⁺ (green) endosomes, while colocalization was reduced in GBA KO cells. As for influenza, the decrease in colocalization of EGF with Lamp1 was not as severe as seen in WT cells treated with nocodazole (**Fig. 3.9A**). There was no decrease in the number of EGF particles in GBA KO vs. WT cells (**Fig. 3.9D**; a small increase was seen), indicating a post-binding requirement for GBA for proper trafficking of EGF.

Following binding of EGF to its receptor (EGFR) at the cell surface, the EGF-EGFR complex is transported to lysosomes and degraded by proteases including cathepsins (110). Since EGF trafficking was impaired in GBA KO cells, we asked if degradation of EGFR is also impaired. To do this, media containing EGF was added to cells at 37°C, and at various times the cells were harvested, lysed, and analyzed for the presence of EGFR by Western blot analysis. As seen and quantified in **Fig. 3.10**, and consistent with the EGF trafficking data (**Fig. 3.9**), degradation of EGFR was notably impaired in GBA KO cells.

We proposed that the defect in EGFR degradation in GBA KO cells (**Fig. 3.10**) is due to a defect in EGFR trafficking (**Fig. 3.9**) as opposed to a defect in endosome

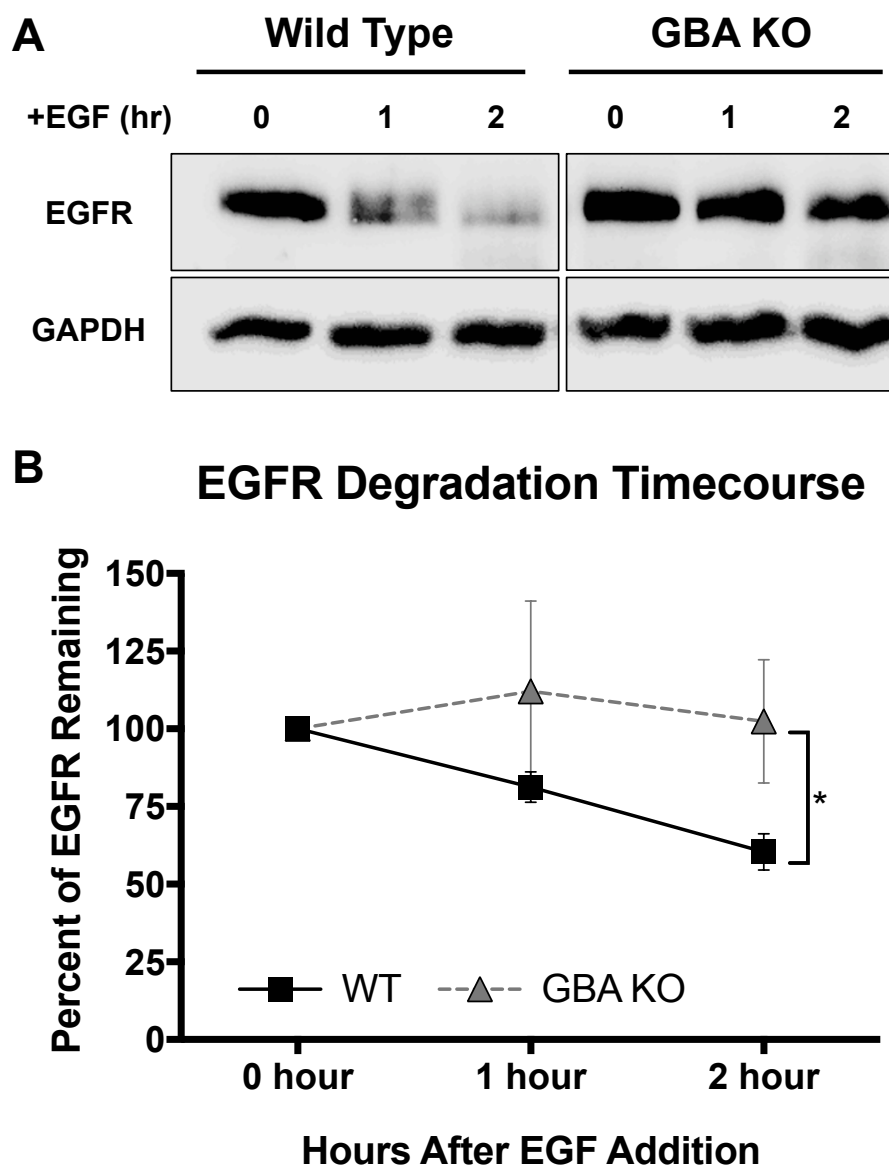


Figure 3.10 EGFR Degradation is impaired in GBA KO Cells.

EGF (50 ng/mL) was added to cells and the cells incubated at 37°C. At the indicated times, cell lysates were prepared and subjected to SDS-PAGE and Western blotting for EGFR. **(A)** Representative Western blot. **(B)** Quantitation of Western Blots indicated a significant difference in EGFR remaining at 2 hr post addition of EGF in GBA KO cells as compared to WT. Values are normalized to the intensity of GAPDH and presented as a percentage of EGFR remaining as compared to cells without EGF stimulation. Data represent the mean \pm SE, n=6 experiments. * $p < 0.05$ using a Mann-Whitney non-parametric test.

acidification (**Fig. 3.7**) or cathepsin activities. To test the latter possibility, we examined the levels of two cysteine proteases normally found in lysosomes, Cathepsin B (CatB) and CatL. This was done *in vitro*, following cell lysis and adjustment to an acidic pH for CatB and CatL using fluorescent peptide substrates, and, additionally for Cat B, in live cells using Magic Red-(RR)₂ (111). Unexpectedly, GBA KO cells displayed an ~3.5-fold increase in CatB activity as compared to WT cells in the *in vitro* assay (**Fig. 3.11A**). CatB activity was also increased in the live cell assay, but not to as great an extent (**Fig. 3.11B**). Consistently, we observed an increase in CatB protein levels in GBA KO cells (**Fig. 3.11C**). CatL activity in cell lysates displayed no significant difference in KO as compared to WT cells (**Fig. 3.11D**). Taken together, these data suggest that diminished cathepsin expression and/or activity are not the cause of dysfunctional EGFR degradation in GBA KO cells, and further support our proposed mechanism of impaired endosome trafficking. The mechanism behind the unexpected increase in CatB activity and expression in GBA KO cells may be a result of defects in CatB localization, as lack of CatB in lysosomes could lead to upregulation of CatB production as a compensatory mechanism. Further investigation is necessary to better understand the mechanism and implications for these findings

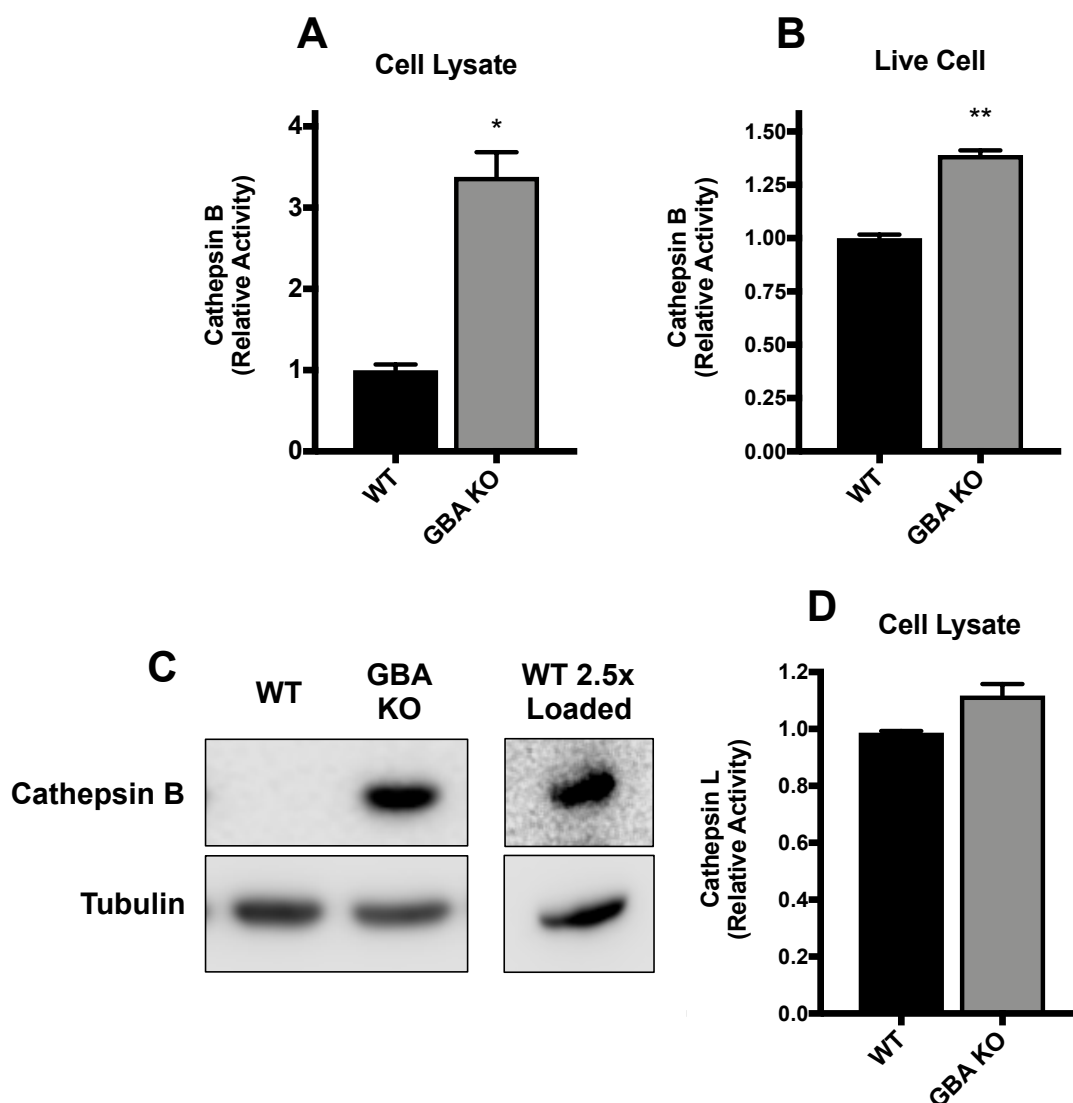


Figure 3.11 Loss of GBA upregulates Cathepsin B activity.

(A,D) WT and GBA KO A549 cells were lysed and analyzed for cathepsin B activity following incubation with a cathepsin B specific substrate for 1 hour at 37°C, as described in the Materials and Methods. Data represent the mean \pm SE, n=5 experiments. **(B)** Cathepsin B activity *in vivo* in A549 cells was determined using the Magic Red-(RR)₂ cathepsin activity assay as per the manufacturers instructions. Data represent the mean \pm SE, n=5 experiments. **(C)** Cathepsin B was probed by Western Blot and found to be undetectable in A549 WT samples but readily detectable in GBA KO cells. Loading 2.5X the amount of lysate resulted in CatB detection in the WT cells. **(D)** WT and GBA KO cells were lysed and processed as in **(A)**, but incubated with a cathepsin L specific substrate and analyzed for cathepsin L activity as described in the Materials and Methods. * p<0.05, ** p<0.01 using a Mann-Whitney non-parametric test.

In summary, our findings suggest that GBA and optimal levels of GlcCer are required to regulate trafficking along the endocytic pathway of viruses and endogenous cargos, particularly to later stages of the pathway. Consequently, when GBA is missing, endocytosed enveloped viruses show diminished fusion, entry, and infection, and critical growth factor receptors are not degraded, a process required for proper growth control. Collectively the findings presented in **Figs. 3.7-11** indicate that the defect in viral entry (and consequent infection) and EGFR degradation seen in GBA KO cells is not due to lowered levels of cathepsins or impaired endosome acidification, but rather to a defect in trafficking of cargos to degradative endosomes/lysosomes.

3.5 Discussion

In this study we established a role for glucosylceramidase (GBA) in the regulation of endocytosis of viral and cellular cargos, firstly for endosomal entry and infection by influenza virus. We established that the defect in influenza infection in GBA KO cells is due to defects in delivery to late endosomes and consequent fusion and entry into the cytoplasm. Consistently we observed defects in entry mediated by the glycoproteins of other enveloped viruses that enter cells through endosomes (47); VLPs and pseudoviruses bearing VSV, influenza, and Ebola (EBOV) glycoproteins displayed decreased entry into GBA KO cells, with minimal effects seen on entry mediated by the glycoproteins from a virus (measles) that fuses and enters the cell through the plasma membrane. Interestingly, the trend was for greater reliance on functional GBA for viruses that enter through later, more acidic, endosomes (47, 112–115). Based on these findings, we hypothesized

that GBA and optimal levels of GlcCer are required, in general, for proper trafficking of cargo along the endocytic pathway, particularly to late endosomes. Indeed, we found that trafficking of not only influenza particles but also EGF and its receptor (to Lamp1⁺ endosomes) is impaired in GBA KO cells, which in the latter case correlated with significantly delayed degradation of EGFR. Collectively our findings strongly suggest that GBA regulates normal trafficking of cargo along the endocytic pathway.

We note that loss of GBA led to inhibition in single but not multi-cycle influenza infections (**Fig. 3.4**), suggesting that the perturbations to the sphingolipid pathway in our GBA KO cells may have consequences for IAV assembly or exit, findings that require further investigation. Indeed, a 2012 study demonstrated that the membrane of IAV may be enriched in sphingolipids, indicating a role for these lipids in the exit of the virus from host cells (6). We hypothesize that if influenza exit from GBA KO cells is increased as compared to WT, or if the viral particles that bud from in KO cells display an enhanced entry phenotype, multiple cycles of infection results in recovery of influenza entry in GBA KO cells.

Oft-times altering the function of one enzyme in the sphingolipid pathway results in compensation that makes it challenging to pinpoint a single lipid species as the cause of a particular cellular phenotype (116). We found, by mass spectrometry of lipids, that removal of GBA in both HEK 293 and A549 cells results in a significant increase in GlcCer mass. As such, we hypothesize that it is excess

GlcCer and not changes in other sphingolipids that is responsible for the observed phenotypes. We did not note a decrease in ceramide levels, nor did we note major changes to non-glycosylated ceramide metabolites, such as sphingomyelin and sphingosine-1-phosphate (**Fig. 3.3**). We hypothesize this is due to a compensatory increase in *de novo* synthesis of ceramide from serine and palmitoyl-CoA (**Fig. 3.1 and Fig. 3.3C**). Indeed, increases in *de novo* synthesis may be responsible for the increase in dihydrosphingosine we observed in both GBA KO cell lines. We also noted an elevation in glucosylsphingosine levels, albeit a much smaller change in mass compared to GlcCer. Little is known about the metabolism of glucosylsphingosine, but several recent studies indicate that it may serve as a biomarker for Gaucher disease, a lysosomal storage disorder characterized by mutations in GBA (117–119). Our data suggest that GBA may catabolize both GlcCer and glucosylsphingosine (**Fig. 3.3C**), suggesting a more global role for GBA in sphingolipid biology and pathophysiology.

Even though we suggest that GBA is a major regulator of influenza infectivity, we cannot exclude other GlcCer metabolizing enzymes. A previous study showed that glucosylceramide synthase (UGCG) is required for entry by one type of bunyavirus (severe fever with thrombocytopenia syndrome virus), but not for another (Rift Valley) or for other enveloped viruses tested (VSV and EBOV) (66). Consistent with our work, these prior findings point to an optimal level of GlcCer being important for (certain) viral infections. Yet, our findings expand a need for optimal levels of GlcCer to other, potentially many, enveloped viruses that enter

cells through late endosomes as well as to important endogenous endocytic cargo including EGF and its receptor.

It is well established that lipids are heterogeneously distributed throughout cells (120). Specialized lipid microdomains in various membrane compartments facilitate cellular organelle function and organization, including in endosomes (121). Sphingolipids in particular have been shown to be enriched in endosomes (122), and perturbations to the sphingolipid pathway result in abnormal endosome size, location, and function (123–126). GlcCer has been implicated in altering the physical properties of membranes, for example, increased GlcCer results in decreased membrane fluidity (127, 128). In addition, a recent paper demonstrated that cells taken from patients with Gaucher disease displayed restricted lateral lipid mobility and exhibited reduced rates of transferrin receptor endocytosis (129). Coupled with our findings, these reports suggest that the disruption in endocytosis that we observe in GBA KO cells for critical cargos including pathogenic viruses and growth factor receptors may be due in part to an alteration in the biophysical properties of cellular membranes and possibly a result of internalization defects. Hence, targeting GBA might prove beneficial as part of strategies to ameliorate viral infections that utilize the endocytic pathway.

3.6 Acknowledgements

We thank the UVA Flow Core for all of their technical assistance and data collection, including Michael Solga, Claude Chew, Alexander Wendling, Lesa Campbell, and Joanne Lannigan. We thank Ryan D'Souza and Adam Green for

assistance with microscopy and image analysis. Thomas Braciale and MarthaJoy Spano were invaluable in providing GFP-PR8 influenza as well as other reagents. Finally, we thank Christine Hulseberg and Maya Cabot for experimental advice.

CHAPTER 4 – GLUCOSYLCERAMIDE SYNTHASE MAINTAINS INFLUENZA INFECTION

The text included in this chapter has been adapted from the following publication:

Glucosylceramidase Maintains Influenza Infection By Regulating Endocytosis

Drews KC, Calgi MP, Harrison WC, Drews CM, Costa-Pinheiro P, Shaw JJP, Jobe KA, Han JD, Fox T, White JM, and Kester M.

PLoS One, Preparing For Submission (2019).

4.1 Abstract

Influenza is an enveloped virus wrapped in a lipid bilayer derived from host cells. Influenza infection has been shown to be dependent on cellular lipids, including sphingolipids such as ceramide and sphingomyelin. Here we examine the role of glucosylceramide in influenza infection by knocking out the enzyme responsible for its synthesis, glucosylceramide synthase (UGCG). We observed diminished influenza infection in HEK 293 and A549 UGCG functional knockout cells and we further demonstrated that the block to influenza infection in UGCG knockout cells is at the level of entry. Finally, we observed that other enveloped, endosome-entering viruses have impaired entry into UGCG knockout cells, suggesting a broader role for this enzyme in viral-host interactions. We recently showed that glucosylceramidase, the enzyme that converts glucosylceramide back to ceramide, is required for proper endocytic trafficking, entry and infection by influenza virus (130). Collectively these findings suggest that an optimal level glucosylceramide is critical for the entry of influenza and other pathogenic viruses.

4.2 Introduction

Influenza A virus is the causative agent of influenza respiratory disease, and is responsible for infecting between three and five million people worldwide each year. In 1918 an influenza pandemic resulted in one of the deadliest disease outbreaks in human history, killing an estimated 50 million people (3). While a vaccine against influenza virus is produced annually, antigenic shift may result in influenza strains that circumvent vaccine efficacy and result in worldwide pandemics, such as the 2009 H1N1 pandemic (92).

A negative sense RNA virus belonging to the family *Orthomyxoviridae*, influenza is an endosome-entering enveloped virus that is encapsulated in a lipid membrane derived from host cells. Inserted in the lipid envelope are influenza's two glycoproteins: hemagglutinin (HA) and neuraminidase (NA). During infection, influenza virus first binds to host cellular receptors through its HA protein and the virus is then internalized into an endosome. As the endosome acidifies to a pH of ~5.0-5.7, HA undergoes conformational shifts and leads to fusion between the viral membrane and the endosomal membrane (47, 94–97). Upon successful viral fusion, the influenza genome is released into the cytoplasm and shuttled into the nucleus to undergo replication (21, 22).

The lipid membrane of influenza is enriched in sphingolipids, a major class of signaling molecules characterized by their sphingosine backbone (53). Sphingolipids have been studied in the context of numerous viruses, and have been found to be critical to all stages of viral life cycles, including virus binding (60–63), entry (64–66), replication (67, 68), and new particle release (69). Several studies in the past decade investigated the role of specific sphingolipids in influenza infection, including sphingomyelin (104), ceramide (131), and sphingosine-1-phosphate (70, 71) (**Fig. 4.1**). Most recently, we determined that deletion of glucosylceramidase (GBA) leads to reduced influenza entry and impaired cellular endocytosis (130). Taken together, these studies suggest a need to further understand the role for sphingolipids in viral-host interactions.

Sphingolipid metabolism is complex involving numerous enzymes and intermediary lipids, all of which shuttle through ceramide as a main hub (49) (**Fig. 4.1**). Though several distinct salvage pathways exist, ceramide metabolism is primarily driven through the condensation of serine and palmitoyl-CoA by the enzyme serine palmitoyltransferase (51). Upon addition of a glucose molecule by glucosylceramide synthase (UGCG), ceramide is converted into the glycosphingolipid glucosylceramide (GlcCer), a pro-survival signaling molecule and a precursor lipid for higher order gangliosides (132). GlcCer is a relatively understudied sphingolipid in the context of viral infections, as most research focuses on sphingomyelin, the far more abundant sphingolipid, which is found primarily in plasma membranes. (60, 64, 65, 101–103). In addition to our study on GBA and GlcCer in influenza infection, another recent study explored the role for UGCG and GlcCer in bunyavirus infections, and found that inhibition of UGCG led to reduction in bunyavirus entry. However, to our knowledge UGCG has never been studied in the context of influenza virus (66). Here we used CRISPR/Cas9 to genetically knock out UGCG and thereby determine its role in influenza entry and infection. We found that UGCG KO cells displayed a reduction in influenza infection and entry, as well as reductions in entry of other endosome-entering viruses.

4.3 Results and Discussion

4.3.1 Glucosylceramide synthase regulates influenza infection

Previous studies demonstrated that loss of expression or inhibition of several sphingolipid-metabolizing enzymes leads to reductions in influenza infection (**Fig. 4.1**). We recently discovered that glucosylceramidase (GBA) is required for optimal influenza entry (130) and we hypothesized that glucosylceramide synthase (UGCG), which converts glucosylceramide back to ceramide, may also play a role in the influenza life cycle (green box). When we inhibited UGCG using PPMP we observed a decrease in infection by PR8 influenza encoding NS1-GFP, as monitored by flow cytometry for GFP expression (**Fig. 4.2A**). We next employed CRISPR/Cas9 to knockout UGCG (see **Fig. 4.2B** for gRNA sequence) in HEK 293 and A549 cells and determined the functional status of UGCG in putative knockout lines. We assayed for UGCG enzyme activity by incubating cells with C6 ceramide, a synthetic analogue of ceramide, and measuring the levels of C6 ceramide and C6 GlcCer. Functional UGCG would convert C6 ceramide to C6 GlcCer, as seen in WT cells. However, in both HEK 293 and A549 UGCG KO cells conversion of C6 ceramide to C6 GlcCer was not seen, indicating a full ablation of UGCG functional activity (**Fig. 4.2C and D**). We next measured the endogenous levels of GlcCer in both WT and KO cells and determined that HEK 293 UGCG KO display significantly decreased GlcCer levels, and that GlcCer is undetectable in A549 UGCG KOs (**Fig. 4.2E and F**). Finally, to determine if knockouts of UGCG affect influenza infection, we used the GFP-encoding PR8

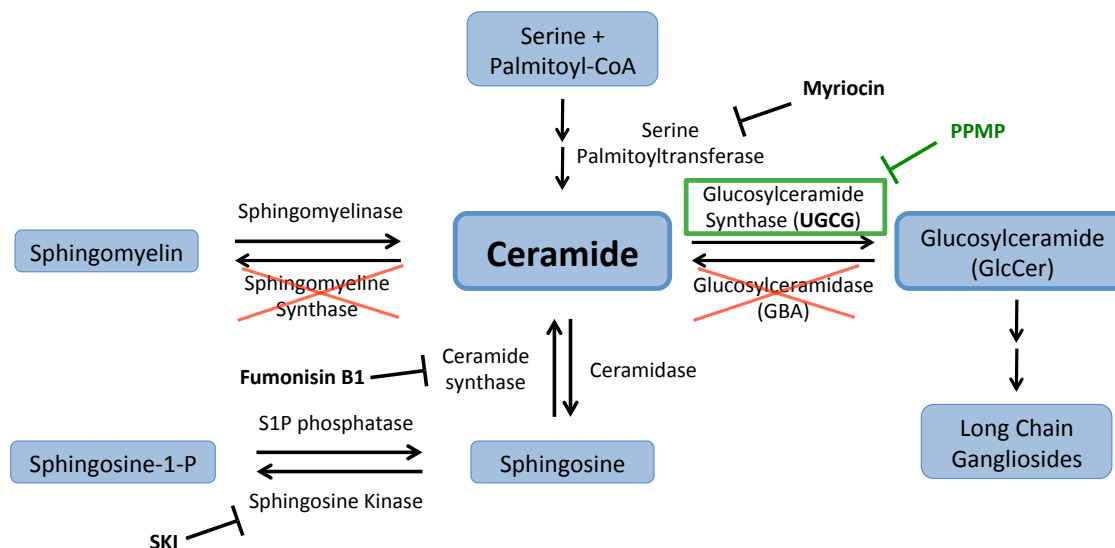


Figure 4.1 Sphingolipids and influenza virus infections.

Several studies demonstrated that inhibition of different enzymes in the sphingolipid pathway resulted in reduced influenza infection. Pharmacological inhibition of serine palmitoyltransferase and sphingosine kinase, as well as genetic manipulation of sphingomyelin synthase and glucosylceramidase led to decreased influenza infection (23, 24, 75, 128). We sought to determine the effect of UGCG (green box) on influenza infection by using the pharmacological inhibitor PPMP as well as knocking out the enzyme in two different cell lines.

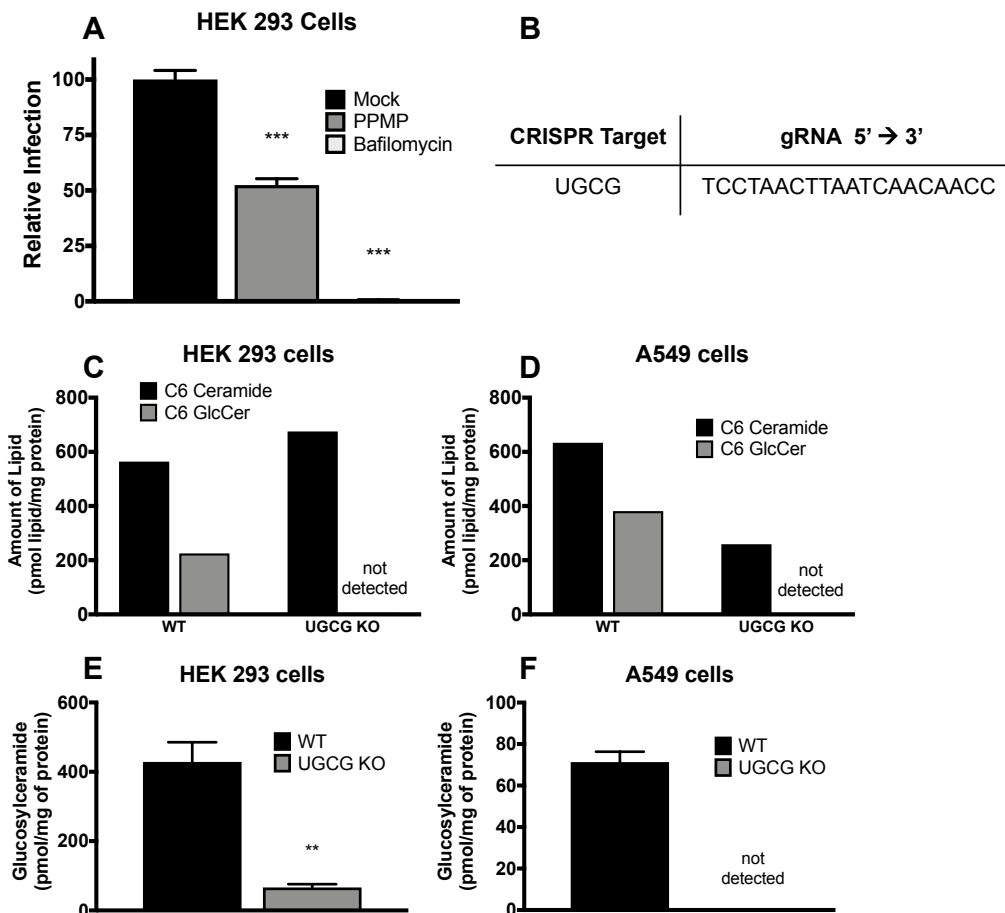


Figure 4.2 CRISPR/Cas9 mediated knockout of glucosylceramide synthase.

(A) HEK 293 cells were pretreated with 20 μ M PPMP (for 48 hours) or 100 nM bafilomycin (for 1 hour) before being infected with PR8 influenza encoding an NS1-GFP chimeric protein in the presence of the indicated drug. Samples were analyzed by flow cytometry for GFP expression. PPMP-treated samples exhibited a 50% reduction in GFP signal compared to WT, indicating a role for UGCG in influenza infection. Data represent the mean values of 4 biological replicates \pm SE. (B) HEK 293 and A549 cells were transfected with a plasmid encoding Cas9-sgRNA targeting UGCG. Single cell-colonies were expanded and monitored for successful UGCG knockout. (C,D) Loss of UGCG activity was confirmed by incubating cells with 5 μ M C6 ceramide nanoliposome for 4 hours. Cells containing functional UGCG are able to convert the C6 ceramide to C6-GlcCer, as seen in WT samples. Putative HEK 293 and A549 UGCG KO cells transfected displayed no C6-GlcCer, indicating a complete loss of UGCG activity. (E,F) Lipids from WT and putative KO cells were analyzed by mass spectrometry. In agreement with the measured enzyme activity in (C,D), levels of total endogenous GlcCer were significantly reduced in both HEK 293 and A549 KO cells as compared to WT. (mean \pm SE ; n=6). ** p<0.01 using a Mann-Whitney non-parametric test.

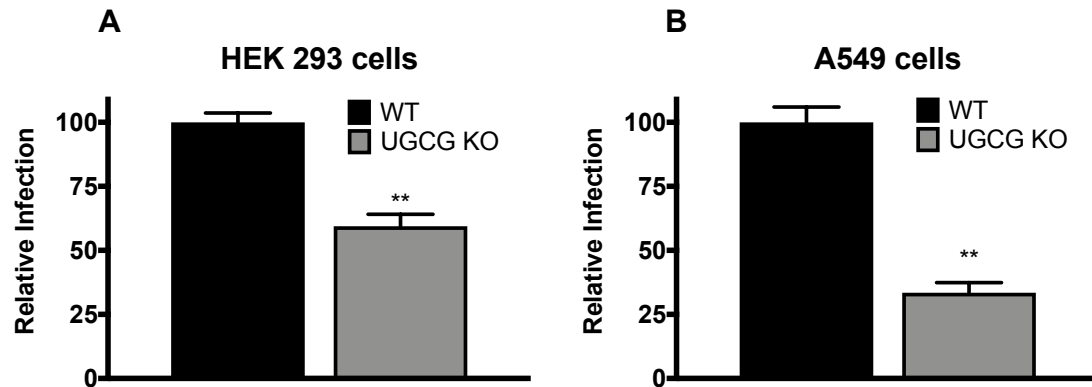


Figure 4.3 Glucosylceramide synthase regulates influenza infection.

Cells were infected with influenza as in **Fig. 4.2A**, and analyzed ~18-24 hours later by flow cytometry. **(A)** HEK 293 UGC KO cells exhibited an ~40% reduction in influenza infection as compared to WT, while **(B)** A549 UGCG KO cells exhibited ~70% reduction in influenza infection as compared to WT. (mean \pm SE ; n=6). ** p<0.01 using a Mann-Whitney non-parametric test.

influenza as in **Fig. 4.2A**. As seen in **Fig. 4.3A and B**, influenza infection levels were decreased in both HEK 293 and A549 UGCG KO cells compared to WT cells. Further experiments are needed to determine if deletion of UGCG inhibits multiple cycles of influenza infection, as GlcCer may play a positive role in influenza assembly and/or release, as suggested by our recent work (130) and by findings that the membrane in influenza is enriched in glycosphingolipids (6).

After performing gene editing we assessed for loss of UGCG protein by western blot (**Fig. 4.S1A**). Consistent with the results of lipid mass spectrometry (**Fig. 4.2C-F**), there was no detectable UGCG protein in HEK 293 UGCG KO cells. However, despite the indicated KO of enzyme activity (**Fig. 4.2C-F**), A549 UGCG KO cells displayed a western blotting band for UGCG, albeit in reduced amount compared to WT cells. To address this apparent contradiction between the western blot data and the mass spectrometry findings of complete loss of UGCG activity, we performed next-generation sequencing to determine the exact genetic alterations that had occurred in the A549 UGCG KO cells. We determined that those cells displayed a heterozygous phenotype (**Fig. 4.S1B**), with one allele mutated by the CRISPR/Cas9 activity to contain a premature stop codon (**Fig. 4.S1C**) while the other allele remained unaltered. We hypothesize that the induced mutation (stop codon) resulted in haploinsufficiency, as the functional activity of UGCG was completely lost in A549 KO cells (**Fig. 4.2C-F**). A full list of sphingolipid species analyzed can be found in **Table 4.S1**. As expected, levels of all GlcCer species decreased in UGCG KO cells, confirming loss of UGCG function.

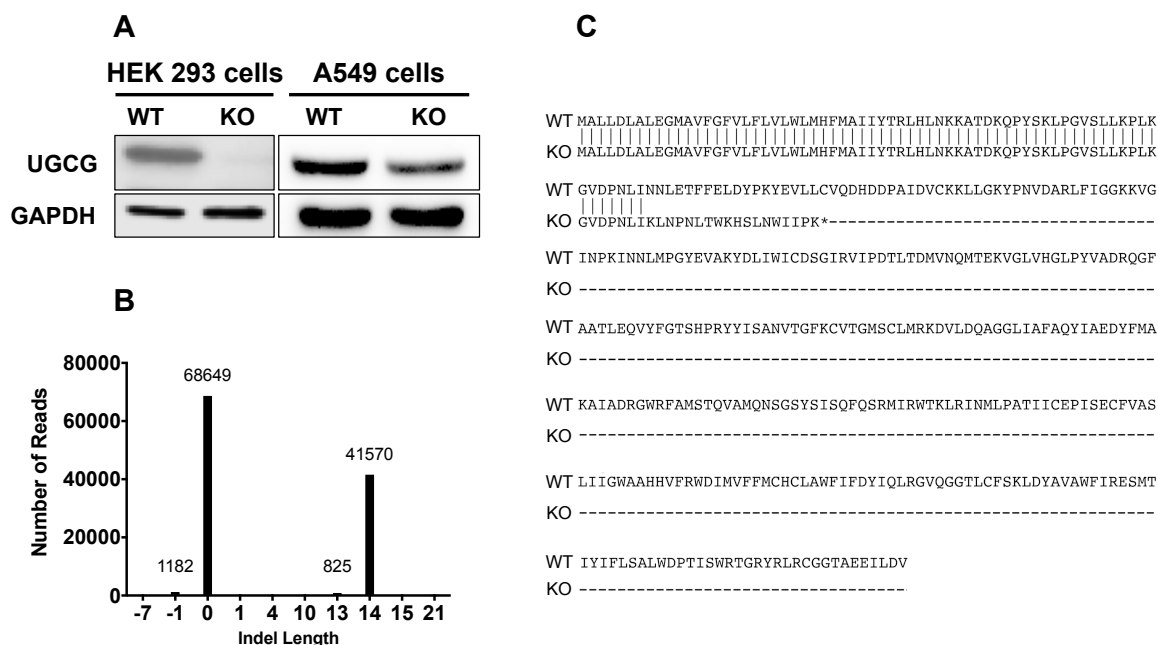


Figure 4.S1 A549 UGCG KO cells exhibit haploinsufficiency.

(A) Complete loss of UGCG expression was confirmed in HEK 293 cells, however, A549 cells display only a reduced level of UGCG. (B) Next generation sequencing indicated the presence of a heterozygous 14 base pair insertion in the A549 UGCG KO cells, suggesting that the loss of UGCG activity seen in Fig. 4.2D and F may be the result of haploinsufficiency. (C) Analysis of the CRISPR-modified UGCG allele in A549 cells reveals a frameshift mutation beginning at N68 and terminating in an early stop codon at the C86 position.

	293			A549		
	WT	UGCG KO	Fold Change	WT	UGCG KO	Fold Change
Sphingosine	111.50	36.27	0.33	86.26	166.19	1.93
Dihydrosphingosine	5.09	1.81	0.36	12.19	38.35	3.15
Sphingosine-1-Phosphate	1.70	25.08	14.77	0.51	0.99	1.93
Dihydrosphingosine-1-Phosphate	0.88	1.36	1.55	0.75	1.31	1.74
Hexosylsphingosine	0.67	0.41	0.61	0.19	0.29	1.53
Ceramide C16	32.70	40.94	1.25	33.44	34.66	1.04
Ceramide C18	37.19	37.80	1.02	3.43	4.28	1.25
Ceramide C20	17.67	6.81	0.39	0.34	0.45	1.35
Ceramide C22	115.50	54.37	0.47	1.15	1.76	1.53
Ceramide C22:1	15.45	7.22	0.47	0.89	2.54	2.85
Ceramide C24	155.91	146.76	0.94	2.20	3.13	1.43
Ceramide C24:1	384.97	194.61	0.51	31.94	59.77	1.87
Ceramide C26	2.62	3.37	1.29	0.26	0.56	2.15
Ceramide C26:1	13.50	7.38	0.55	0.24	0.96	4.00
Ceramide Totals	775.52	499.25	0.64	73.88	108.12	1.46
Glucosylceramide C16	71.11	24.98	0.35	28.56	N.D.	N.D.
Glucosylceramide C18	7.87	1.86	0.24	2.72	N.D.	N.D.
Glucosylceramide C20	17.69	1.23	0.07	0.64	N.D.	N.D.
Glucosylceramide C22	83.96	7.28	0.09	2.91	N.D.	N.D.
Glucosylceramide C22:1	18.64	1.01	0.05	1.46	N.D.	N.D.
Glucosylceramide C24	78.06	11.25	0.14	2.41	N.D.	N.D.
Glucosylceramide C24:1	147.36	17.86	0.12	21.85	N.D.	N.D.
Glucosylceramide C26	0.72	0.17	0.24	N.D.	N.D.	N.D.
Glucosylceramide C26:1	4.66	0.66	0.14	0.58	N.D.	N.D.
GlcCer Totals	430.06	66.31	0.15	61.15	N.D.	#VALUE!
Sphingomyelin C16	8589.64	6251.15	0.73	4164.63	8087.13	1.94
Sphingomyelin C18	1209.58	1194.49	0.99	341.60	675.41	1.98
Sphingomyelin C20	1055.36	541.38	0.51	115.96	188.50	1.63
Sphingomyelin C22	817.54	802.26	0.98	218.37	368.16	1.69
Sphingomyelin C22:1	259.74	134.07	0.52	53.99	209.19	3.87
Sphingomyelin C24	382.17	625.26	1.64	144.76	312.34	2.16
Sphingomyelin C24:1	2011.61	1648.51	0.82	881.30	3877.56	4.40
Sphingomyelin C26	6.68	13.87	2.08	6.99	11.47	1.64
Sphingomyelin C26:1	31.69	45.24	1.43	15.18	68.46	4.51
Sphingomyelin Totals	14364.01	11256.24	0.78	5942.78	13798.25	2.32

Table 4.S1 Full sphingolipid profiles of UGCG knockouts.

Sphingomyelin, ceramide, glucosylceramide, sphingosine, and sphingosine-1-phosphate were analyzed by mass spectrometry in all knockout cells and compared to WT. Averages from five biological replicates are listed. Mass spectrometry peaks were compared to internal standards and all data are represented as pmol lipid/mg of protein.

However, a corresponding increase in ceramide levels was not consistently observed. We hypothesize that knocking out UGCG leads to modulations in the pathway that maintain ceramide levels: through increased sphingosine-1-phosphate metabolism in HEK 293 cells and increased sphingomyelin metabolism in A549 cells. These data suggest that consequent to knocking out UGCG, cells undergo compensatory sphingolipid metabolism in a cell type or tissue specific manner. It is been established that sphingolipids enzyme are differently expressed in different tissue types, suggesting that the origin of HEK 293 cells compared to A549 cells may explain the difference in sphingolipid profiles observed (107). Further investigations into disrupted sphingolipid metabolism are required to test the proposed compensatory mechanisms that maintain ceramide levels in the context of UGCG ablation.

4.3.2 Glucosylceramide synthase regulates entry of influenza and other endocytosed viruses

We hypothesized that the reduction in influenza infection in UGCG KO cells was due to a reduction in influenza entry into the cells. To address this we generated virus like particles (VLPs) containing an influenza Matrix-1 (M1)- β -lactamase (β -lam) core bearing the HA and NA glycoproteins of WSN influenza, which fuses with host endosomes at pH \sim 5.0-5.9 (133). We extended the screen to include influenza Matrix-1 VLPs displaying the glycoproteins of vesicular stomatitis virus (VSV), which fuses with host early endosomes (pH \sim 6.0), and Ebola (EBOV), which fuses with host endolysosomes (pH \sim 4.5-5.0) (105, 89, 106). We determined that both WSN influenza HA/NA and EBOV GP VLPs displayed

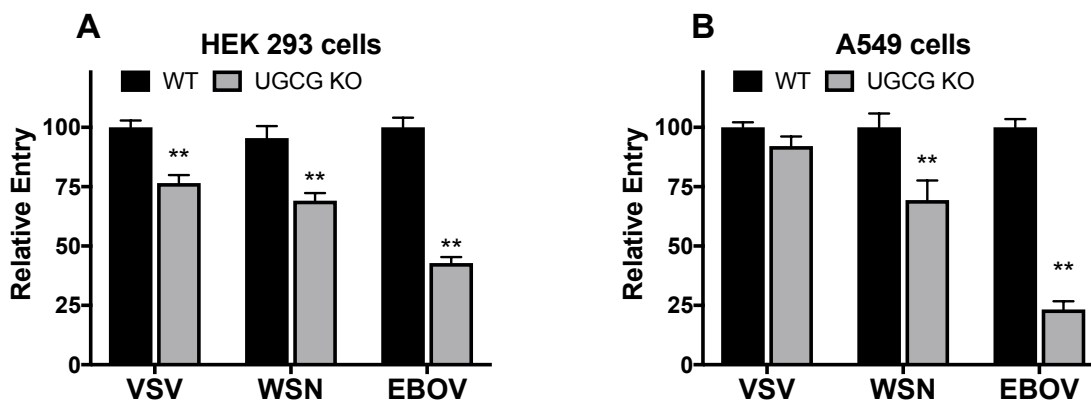


Figure 4.4 UGCG maintains entry of multiple VLPs.

Virus like particles (VLPs) were generated on a β laM1 backbone with the envelope proteins of the virus of interest. Prechilled cells were spun at 4° with the VLP for 1 hour, incubated for 3 hours at 37° , and then incubated for 1 hour at room temperature in the presence of the β laM substrate. Cells were washed and the following day were harvested, fixed, and analyzed for β -lactamase activity via flow cytometry. **(A,B)** VSV entry was significantly reduced in HEK 293 UGCG knockout cells, though unaffected in A549 KO cells. WSN influenza entry was reduced in all knockout cells, consistent with the findings in **Fig. 4.3**. EBOV entry was reduced in all knockout cells, to a greater extent than WSN or VSV (mean \pm SE ; n=6). ** p<0.01 using a Mann-Whitney non-parametric test.

reduced entry into both HEK 293 and A549 UGCG KO cells compared to WT cells. VSV-G VLPs displayed reduced entry into HEK 293 UGCG KOs, but not into A549 UGCG KOs (**Fig. 4.4A and B**), which may be due to the different tissue origins of these cells and their different sphingolipid profiles (**Table 4.S1**).

To further explore the extent to which UGCG mediates viral infections, we employed a VSV pseudovirus system and examined how pseudoviruses bearing the glycoproteins of VSV, EBOV, and measles (a virus that employs its H and F proteins to fuse at the plasma membrane) infect UGCG KO and WT cells. As seen in **Fig. 4.5A and B**, and similar to the results seen with influenza Matrix-1 VLPs, VSV G-mediated pseudovirus infection was reduced in HEK 293 UGCG KOs, but unaffected in A549 UGCG KOs; EBOV pseudovirus infection was reduced in both UGCG KO cell lines tested. In contrast, measles H/F-mediated pseudovirus infection was not inhibited in HEK 293 UGCG KOs, and was even increased in A549 UGCG KO compared to WT cells. We hypothesize that this increase in measles infection may be due to the different sphingolipid profiles of A549 and HEK 293 UGCG KO cells (**Table 4.S1**). A549 UGCG KO cells are enriched in sphingomyelin, a major component in lipid rafts. A 2004 study found that measles virus enters cells at sites of lipid rafts, indicating that A549 UGCG cells may present a plasma membrane composition more conducive to measles binding and subsequent entry (134).

These results indicate a role for UGCG in influenza entry, and suggest roles in the entry of other endosome-entering viruses, particularly ones that enter late in the

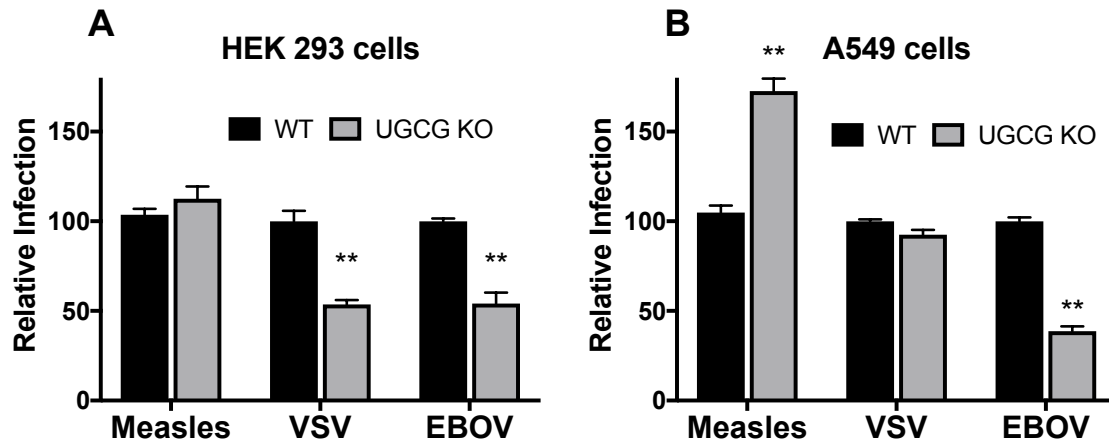


Figure 4.5 UGCG maintains infection of multiple pseudoviruses.

Pseudoviruses were generated using a VSV-GFP backbone and the envelope proteins of the virus of interest. Prechilled cells were spun at 4° with the pseudovirus for 1 hour, washed, and the following day were harvested, fixed, and analyzed GFP expression via flow cytometry. **(A,B)** VSV-Measles infection was unaffected in HEK 293 UGCG knockout cells, but increased the A549 UGCG knockout cells. VSV-G infection was decreased in HEK 293 UGCG knockouts but unaffected in A549 UGCG knockout cells, consistent with the findings in **Fig. 4.4**. VSV-EBOV infection was decreased in all knockouts tested (mean ± SE ; n=6). ** p<0. 01 using a Mann-Whitney non-parametric test.

endocytic pathway. Based on our previous work (130) we further propose that impairment in entry of 'late penetration' viruses (47) in UGCG KO cells is due to a general impediment of normal endocytic trafficking. This conclusion is concordant with that of Drake *et al.*, who demonstrated a role for UGCG in infections by specific bunyaviruses at a post-internalization step, which they suggested to be endosome trafficking or virus-endosome fusion (66).

Previously, we found that deleting GBA, the enzyme that converts GlcCer (the primary product of UGCG enzymatic activity) to ceramide (**Fig. 4.1**) increases GlcCer levels and impairs endosome trafficking and influenza entry (130). Here we found that knocking out UGCG decreases GlcCer levels (in both HEK 293 and A549 cells), impairing entry of endosome-entering viruses. This suggests that specific amounts of GlcCer may be needed for optimal endocytic trafficking.

Interestingly, ablation of UGCG activity in HEK 293 and A549 cells did not result in the same changes in sphingolipid species between the two cell lines. While both cell types displayed reduced levels of GlcCer (as expected), ceramide levels were not correspondingly elevated. We hypothesize that because ceramide is a pro-apoptotic molecule (49), cells attempt to limit any buildup of this bioactive lipid by converting it to either sphingomyelin or sphingosine. In HEK 293 UGCG KO cells sphingomyelin levels are comparable to those in WT cells, but sphingosine-1-phosphate levels increase 7-fold, indicating that blocking the GlcCer production by removing UGCG shunts sphingolipid production to sphingosine-1-phosphate. However, A549 UGCG KOs display an increase in

sphingomyelin, the most prevalent sphingolipid found in cells, predominantly in the plasma membrane (135). Perhaps the elevated sphingomyelin levels in A549 UGCG KO cells contribute to the increase in entry we observed for measles (**Fig. 4.5B**), the virus tested that enters by fusion with the plasma-membrane (136).

In summary, the findings presented in this study demonstrate a previously undiscovered role for UGCG in influenza entry. By both pharmacological inhibition and genetic ablation, cells deficient in UGCG activity display reduced influenza entry and infection, as well as reduced entry and infection of other endosome-entering viruses such as Ebola. These results suggest that UGCG may provide an intriguing candidate for further study in the context of viral entry, as well as a novel target for future influenza therapies.

CHAPTER 5 - DISCUSSION

5.1 Summary of Results

The major significance of this body of work is that we established a link between glucosylceramide (GlcCer) and virus entry. We did this by knocking out the two enzymes responsible for GlcCer metabolism and testing the resulting cell lines for susceptibility to viral infection.

In brief, CRISPR/Cas9 was employed to create genetically modified HEK 293 and A549 cell lines lacking either glucosylceramidase (GBA) or glucosylceramide synthase (UGCG). By transiently transfecting in the Cas9-sgRNA-encoding plasmid we attempted to limit the potential off-target effects of continually expressing CRISPR machinery, and by co-transfecting a plasmid encoding for GFP we were able to sort for positive transfection events. Following sorting, we screened putative knockout clones for DNA alterations (by conducting rounds of PCR), for GBA and UGCG protein (by western blotting), and for lipid alterations (by mass spectrometry). From ~100 clones per cell line, we identified 4-5 clones that appeared to display successful knockout status. To confirm loss of enzyme function we devised a screen that selected for cells that lost the ability to metabolize synthetic lipid substrates. Though the entire CRISPR process was relatively straightforward, the endeavor took over two years due to complications arising from the cloning and validation processes.

Upon successfully knocking out GBA and UGCG, we next sought to determine the susceptibility of the respective cell lines to influenza infection. A PR8 influenza encoding GFP fused to the N-terminus of NS1 (kindly provided by Tom Braciale)

allowed for robust, reproducible data using flow cytometry. All four cell lines tested (HEK 293 GBA KO, HEK 293 UGCG KO, A549 GBA KO, and A549 UGCG KO) displayed reduced susceptibility to influenza infection, suggesting a role for GlcCer in the influenza life cycle.

In order to determine if the reduced influenza infection phenotype was due to a reduction in influenza entry we utilized a β -lactamase M1 (β laM) assay, which measures entry of influenza virus like particles (VLPs) into the cytoplasm. In all KO cell lines tested influenza VLPs displayed significantly reduced entry, which was later confirmed using an influenza fusion assay. Because influenza enters cells through the endocytic pathway, we hypothesized that other endosome-entering viruses would display the same phenotype in the GBA and UGCG KO cells. We generated VLPs displaying Ebola glycoprotein (enters at endolysosomes) as well as VLPs displaying VSV glycoprotein (enters at early endosomes) and tested their ability to enter the KO cells. We found that Ebola VLP entry was decreased compared to WT in all cell lines (which corroborated with infection assays performed using VSV-EBOV pseudoviruses), while VSV VLP entry was only reduced in HEK 293 KO cells (both UGCG and GBA) as compared to WT. These data suggested that GlcCer was involved in the endocytic pathway, though perhaps more potently at different stages in HEK 293 and A549 cells. Unfortunately, due to a technical error in maintaining the UGCG KO cells, the following mechanistic data is limited to GBA KO cells. To determine if the defect in entry of endosome-entering viruses translated to a cellular endocytic process, we compared degradation of EGFR (upon addition of exogenous EGF) in WT and

GBA KO cells. We found that EGFR degradation was slowed and attenuated in the KO cells, further suggesting that GlcCer is needed to maintain endocytosis.

Broadly speaking, the viral and EGFR phenotypes we observed could be due to two main defects in endocytosis: trafficking and/or acidification. We hypothesized that acidification of endosomes in GBA KO cells may be impaired, as GBA mutations in patients cause Gaucher's disease, a well-documented lysosomal storage disorder. However, upon testing the pH of cellular endo-lysosomes in GBA KO cells we did not detect a significant difference in their acidity as compared to WT cells (though a recent study found a correlation between GBA and endocytic pH) (137). As a result, we hypothesized that GBA KO cells exhibited an endosomal trafficking defect.

To examine endosomal trafficking we performed a series of colocalization experiments in which cells were first transfected with Lamp1-GFP, and then incubated with either red fluorescent EGF or red fluorescent PR8 influenza. After allowing endocytosis for 40 min, cells were fixed and imaged for colocalization between EGF and Lamp1 or PR8 and Lamp1. GBA KO cells displayed a significant reduction in colocalization events as compared to WT cells, suggesting that GlcCer is involved in trafficking along the endocytic pathway. We confirmed that the reduction in observed colocalization was not the result of defects in influenza or EGF binding to the cell surface; the number of R18-labeled influenza particles was the same in both WT and GBA KO cells, while the number of EGF particles was slightly increased in GBA KO cells. Taken together, our data suggest

that GlcCer maintains influenza infection through regulation of endosome trafficking.

5.2 Implications for Sphingolipid Biology

A consequence of altering enzyme expression or activity within the sphingolipid pathway is reverberations of lipid flux throughout the entire pathway. In addition, each fatty-acid containing sphingolipid (namely ceramide, sphingomyelin, and GlcCer) contains numerous variations in the carbohydrate chain length of their fatty acid functional group, with each of these species potentially responsible for a variety of cellular functions. Thus the premise of knocking out a sphingolipid metabolic enzyme and assigning a singular lipid cause to any resulting phenotype is intrinsically flawed. One possible method to address such concerns is to knock out or alter enzyme activity in multiple cell types and determine what lipid changes are conserved across each cell line tested, as we have begun to do by using both HEK 293 and A549 cells. Yet the effects of other lipids other than glucosylceramide cannot be ruled out and therefore it is necessary to examine the lipid changes in the entire pathway in order to form the strongest possible hypothesis to explain the data.

Knocking out enzymes in metabolic systems and observing a cellular phenotype naturally leads to an assumption that the enzyme's function is the underlying driver for that phenotype. However, such an assumption does not take into account the possibility that the enzyme in question serves a secondary role in the cell, perhaps as a scaffolding protein or an intracellular receptor. One way to

address that question is by adding back the enzyme either as a functional or catalytically inactive mutant (while still maintaining protein folding and structure) and assessing if the phenotype is rescued. In our case this experiment may serve as a method of determining whether the reductions in influenza infection we observe in UGCG and GBA KO cells are due to a lipid versus a protein mechanism.

In any protein knockout system a classic experiment is to perform an addback/rescue of the relevant protein to determine if such an experiment would restore the WT phenotype. Performing an addback of either GBA or UGCG to their respective KO cells is fairly straightforward from a technical standpoint, however, it is difficult to add the correct amount of enzyme to recapitulate WT lipid status. Ectopic expression of GBA may result in overexpression of the enzyme, pushing the cells towards a state similar to knocking out UGCG, and vice versa, and therefore disrupting optimal levels of GlcCer (**Fig. 5.1**). Our preliminary data indicate that both GBA and UGCG KO cells exhibit reduced levels of influenza infection and therefore any rescue experiment must successfully restore WT lipid levels in order to be considered a physiologically relevant addback.

Two main methods exist for adding back proteins to knockout cells in a manner that might allow for restoration of WT lipid levels: transient transfection of plasmids encoding the protein that was knocked out and reintroduction of the

knocked out protein via viral transduction. With the transient transfection method, we can perform a titration of plasmids encoding either GBA or UGCG into their respective KO cell lines. We can use western blots to determine the optimal amount of GBA/UGCG plasmid to transfect that most closely resembles protein levels of GBA/UGCG in WT cells. We could then determine whether the transient reintroduction of the knocked out protein restored WT lipid levels. However, one drawback to this method is that it relies heavily on achieving high transfection efficiencies. Lipid levels in cells that are not successfully transfected could potentially mask any changes in the cells that were transfected. Co-transfection of a GFP expression plasmid would enable us to sort cells that were successfully transfected thereby circumventing the issue posed by untransfected cells. However, protein expression resulting from transient transfections will eventually be depleted as the cells grow and divide and the plasmid is lost. Therefore, this approach may not lend itself well to analysis by western blot, mass spec, and flu infections. Instead, reintroduction of the knocked out protein via viral transduction may be a more viable option for us to truly examine whether rescue of the knocked out proteins results in influenza infections comparable to WT cells. We would first incorporate the gene encoding GBA or UGCG into a lentiviral or retroviral backbone that contains a selection marker and then transduce our knockout cells such that the GBA or UGCG gene is inserted into the cellular genome. With this approach, we will be able to achieve a stable population of knockout cells containing the addback protein. Utilization of an inducible promoter in this system, would allow for titration of the inducing agent in order to control the expression levels of the addback protein. Finally, it is important to

note that different viral vectors result in different expression levels of encoded proteins (136). Therefore, other viral vectors may be explored should initial results fail to recapitulate WT lipid status.

To address whether our observed phenotype of reduced influenza infection is due to GBA or UGCG function (and therefore, sphingolipids), or if these enzymes have some as yet unknown role in other cellular functions, we attempted to create catalytically inactive mutants of both GBA and UGCG. After obtaining plasmids encoding the WT version of either GBA or UGCG we used QuikChange PCR to create single point mutations with the goal of rendering the resulting mutated protein catalytically dead and yet still able to fold and express correctly. Amino acids were chosen as candidates for mutation based on either known Gaucher's disease mutations in GBA (for GBA), or on a paper that attempted to identify the active site of UGCG (for UGCG) (137, 138). Specific mutations chosen and oligonucleotides used to induce the point mutants are displayed in **Table 5.1**. After confirming (through sequencing) the mutations were correctly induced in the respective GBA or UGCG plasmids, we sought to express the addback proteins in GBA or UGCG KO cells through a lentiviral vector. However, we failed to achieve a stable cell population of cells and due to time constraints we decided to forge ahead with submitting the manuscripts in Chapters 3 and 4 without the addback data.

Gene	Mutation	Oligonucleotide (5' - 3')	
UGCG	D144A	F	ctggaattactcttattccactagcacaaatccatataagatcatac
		R	gtagatcttatatggattgtgctagtgggaataagagtaattccag
UGCG	K124A	F	tcatatcctggcattaaattattaattgcaggattaatgccaactttttgccacc
		R	ggtggcaaaaaagttggcattaatcctgcaattaataattaatgccaggatatga
UGCG	R272A	F	gtagtttggccacctgatcattgctggattgaaactgagaaattgaat
		R	attcaatttctcagtttcaatccgcaatgatcaggtggaccaaactac
UGCG	R275A	F	gttaattcgtagtttggccacgcgatcattctggattgaaactga
		R	tcagttcaatccagaatgatcgcgtggaccaaactacgaattaac
UGCG	W276A	F	catgtaattcgtagtttggccacctgatcattctggattgaaac
		R	gtttcaatccagaatgatcagggcgaccaaactacgaattaacatg
GBA	E274K	F	cagcagaaggcttatttctcagctgtcactgccaga
		R	tctgggcagtgcagctgaaaataagccttctgctg
GBA	P284T	F	ccaggcactggaagggtatccactcaacag
		R	ctgttgagtgatacacttccagtgctgg
GBA	N227I	F	tcaccgctccaatggttcttgagccaagtggg
		R	cccacttgctcaagaccattggagcgggta
GBA	P198S	F	gctcggatgaatcaggcttattcttgagcttggtatcttcc
		R	ggaagataccaagctcaagataagcctgattcaccgagc
GBA	W351S	F	aaagtcagggtacgaatgtacagcaatgcatgaaca
		R	tgttcatggcattgctgtacattcgtacctggacttt
GBA	S405R	F	gaggttcgtgatgatcctgtggctgtactgc
		R	gcagtacagccacaggatcatcacgaacctc

Table 5.1 List of mutations created in UGCG and GBA.

Mutations in GBA or UGCG were created using QuikChange PCR and the indicated oligonucleotides. Confirmation of each mutation was verified via sequencing.

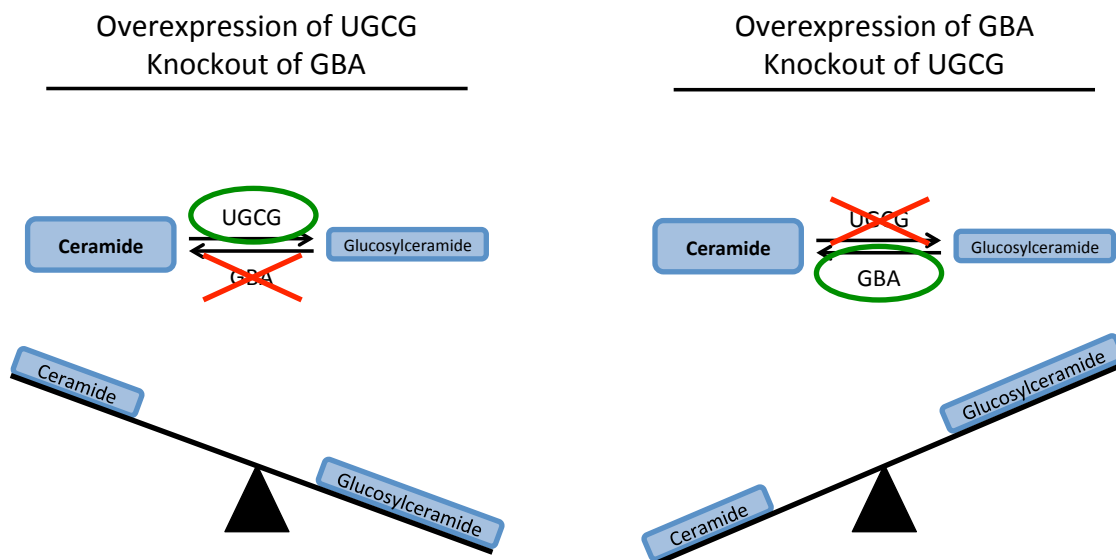


Figure 5.1 Ectopic expression of UGCG or GBA may not recapitulate wild-type lipid status.

Addition of ectopic UGCG may result in the same phenotype as cells deficient in GBA: increased GlcCer levels as compared to WT cells. Conversely, addition of ectopic GBA may result in same phenotype as cells deficient in UGCG: decreased GlcCer levels as compared to WT cells. As a result, recapitulating WT lipid status in KO cells is an extremely challenging endeavor and may not be feasible.

In lieu of adding back the enzymes responsible for GlcCer metabolism, it is possible to addback the lipids themselves. However, to do so poses a multitude of challenges from a technical standpoint. First and foremost, there are nine different species of GlcCer due to their various fatty acid chain lengths, and our observed phenotype could be due to one or several of these species. In addition, should a different lipid be responsible for the reductions in influenza infection we observed, adding back GlcCer may have no effect whatsoever, or it may result in increased metabolism of a different sphingolipid and thereby confound our results. In total, our mass spectrometry measurements account for 32 different sphingolipid species (including nine ceramides and nine sphingomyelins), making it extremely challenging to pinpoint the precise lipid to addback. In addition, there may be a combination of lipids that are responsible for our observed phenotype. Finally, adding lipids to cells is technically difficult as lipids' biophysical properties (namely their hydrophobicity and polarity) ensure that not all the lipids added to the cells will be successfully incorporated into the appropriate cell structures (including membranes and vesicles). As a result, the possibility of recapitulating wild-type lipid status is fairly remote and therefore may not provide much insight despite the large amount of time, resources, and effort spent in such an endeavor. Nevertheless, we attempted to add C16 GlcCer in the hopes of performing a rescue experiment and restore influenza infection levels in HEK 293 KO cells to those of WT cells. In our hands exogenous C16 GlcCer addition resulted in rounding of cells and subsequent cell detachment, rendering any resulting data unusable. Refinement of lipid add back techniques and strategies may result in enhanced efficacy and requires further investigation.

5.2.1 Glucosylceramidase

Upon successful ablation of GBA activity in HEK 293 and A549 cells, the expected increase of GlcCer was observed. However, in both cases ceramide levels were not reduced, suggesting that the cells may generate ceramide through a different mechanism in order to compensate for the loss of GBA. The increase in dihydrosphingosine, a lipid only produced through the *de novo* synthesis pathway, indicates that *de novo* synthesis may be responsible for maintenance of ceramide within GBA KO cells (**Fig. 5.2**).

De novo synthesis of dihydrosphingosine begins with the condensation of serine and palmitoyl-CoA by serine palmitoyltransferase to form 3-ketodihydrosphingosine, an indispensable reaction in the formation of sphingolipids (138). The increased *de novo* synthesis in GBA KO cells may be the result of several factors, including upregulation of serine palmitoyltransferase at either a transcriptional or translational level, increased availability of substrates such as serine or palmitoyl-CoA, or increased enzyme activity through the aid of an as-yet-unidentified cofactor(s). To address these possibilities a series of experiments are necessary:

Experiment 5.2.1.a – *Serine labeling and tracking via mass spectroscopy to confirm activation of de novo synthesis in GBA KO cells.* Serine can be labeled with ^{13}C , which is a heavy carbon that allows it to be easily identified even when the carbon in question is incorporated into other molecules, including sphingolipids. The percentage of ceramide derived from *de novo* synthesis can be

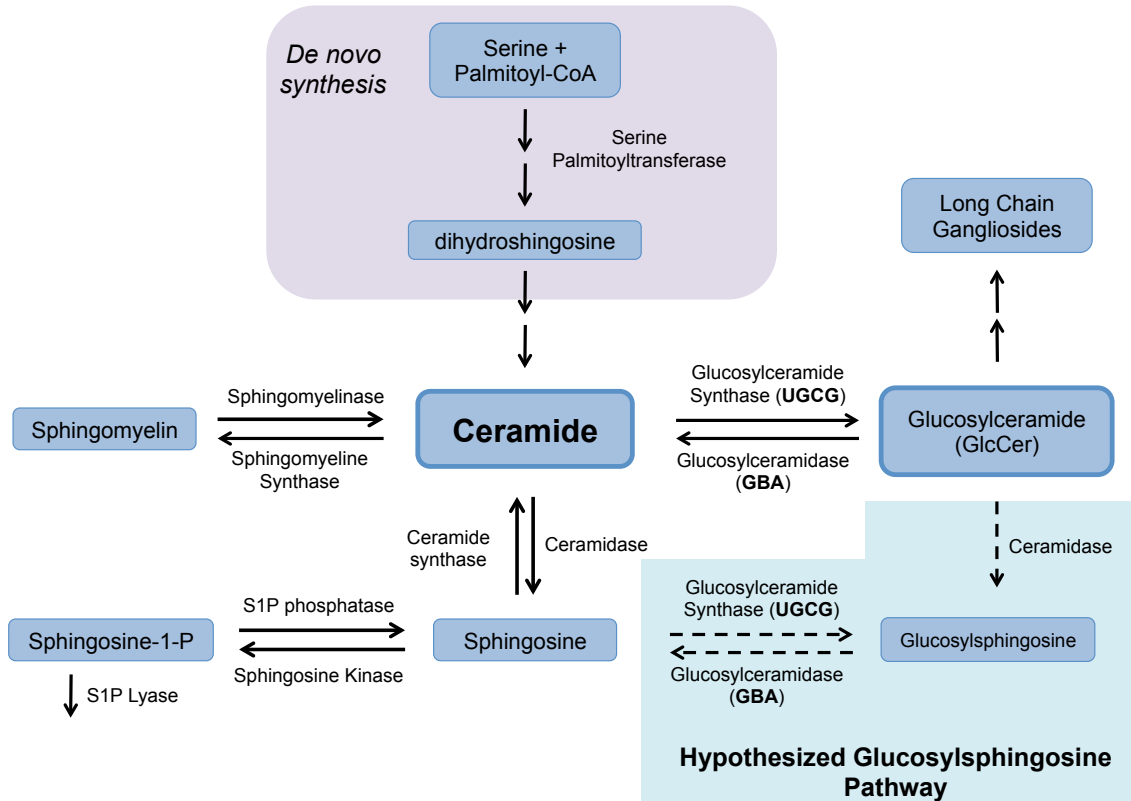


Figure 5.2 Hypothesized sphingolipid metabolic enzymes.

We hypothesize that the increases in ceramide we observe in GBA KO cells is a result of increased *de novo* synthesis (purple box), as dihydroshingosine levels increased as well. In addition, we hypothesize that glucosylsphingosine is catabolized by GBA (blue box) and generated either by UGCG or one of the ceramidase enzymes.

estimated by incubating cells with serine-¹³C and then analyzing their lipids using mass spectrometry.

Experiment 5.2.1.b – *Protein and mRNA expression of serine palmitoyltransferase.* Analysis of protein abundance (by western blot) and mRNA expression (by qPCR) will determine if the increase in *de novo* synthesis of ceramide (as evidenced by the accompanied increase in dihydrosphingosine) is correlated with increased expression of the primary driver of *de novo* synthesis, serine palmitoyltransferase (though it is possible that other enzymes along the *de novo* pathway are upregulated as well, and this pathway may need to be further examined).

Experiment 5.2.1.c – *Measurement of substrate abundance for de novo synthesis.* Analysis of serine and palmitoyl-CoA abundance will determine if the increase in *de novo* synthesis of ceramide is correlated with an increased abundance of the substrates of *de novo* synthesis.

Regardless of the exact mechanism behind the increase in *de novo* synthesis, ceramide's position as the hub of sphingolipid metabolism suggests that any alterations to ceramide metabolism may have effects on downstream lipids such as sphingomyelin and sphingosine. Indeed, sphingosine levels are slightly upregulated in both GBA KO cell lines, while sphingomyelin is increased in HEK 293 GBA KOs, and slightly decreased in A549 GBA KOs (perhaps due to differences in cellular tissue origins).

One important and unexpected discovery from these studies is the potential role of GBA in glucosylsphingosine metabolism. In both HEK 293 and A549 cells lacking GBA, glucosylsphingosine levels rise dramatically, indicating that GBA may play a role in the metabolism of this little-studied sphingolipid. Though the functional role of glucosylsphingosine remains unclear, several recent studies implicated it as a biomarker for Gaucher's disease (118, 139, 140). These reports are in alignment with our findings, as Gaucher's disease is attributed to mutations in the GBA enzyme (56). We hypothesize that GBA is responsible for catabolism of glucosylsphingosine by removing its glucose molecule and converting the lipid into sphingosine (**Fig. 5.2**). The possible routes for anabolism of glucosylsphingosine are further discussed in section **5.1.2**.

Experiment 5.2.1.d – *Tracking glucosylsphingosine-d7 to identify possible glucosylsphingosine catabolic enzymes.* Incubating GBA KO cells with a commercially available labeled glucosylsphingosine and then tracking that label via mass spectrometry will confirm if GBA is the sole enzyme responsible for catabolism of glucosylsphingosine or if another enzyme is capable of catabolizing this sphingolipid as well. For this particular experiment, the limitations described above are less pressing, as the results do not depend on an efficacious delivery of glucosylsphingosine into the cell; the bare minimum will suffice.

5.2.2 Glucosylceramide Synthase

Knockouts of UGCG exhibited significantly reduced expression of endogenous GlcCer, and completely lost the ability to synthesize C6 GlcCer when incubated with C6 ceramide (**Fig 4.2C and D**). We hypothesized that UGCG KO cells

would display a corresponding increase in endogenous ceramide levels. However, ceramide either decreased (in the case of HEK 293 UGCG KO) or remained roughly the same (in the case of A549 UGCG KO). These data suggest that upon losing the ability to convert ceramide into GlcCer, the UGCG KO cells instead shuttled excess ceramide into other sphingolipids such as sphingosine-1-phosphate and sphingomyelin, which we observed in our data (**Table 4.S1**).

Unlike in the case of GBA KOs, the sphingolipid changes in UGCG KOs varied greatly between HEK 293 and A549 cells. As a result, assigning a singular lipid responsible for the reduction in influenza infection in UGCG KOs may be impossible without further study. Yet if we examine each cell line individually certain trends emerge. In HEK 293 UGCG KO cells almost all sphingolipids are reduced, including dihydrosphingosine. We initially hypothesized that ceramide levels would rise after knocking out UGCG, as GlcCer is one of the main downstream products of ceramide metabolism. However, because ceramide is a pro-apoptotic sphingolipid it follows that the cell might compensate for the loss of UGCG by reducing the overall metabolism of sphingolipids. In contrast to HEK 293 UGCG KO cells, A549 UGCG KO cells exhibit a stark increase in sphingomyelin levels, doubling the total mass of this already prevalent sphingolipid. Sphingomyelin serves as an important class of phospholipid within cell membranes, comprising between 2-15% of the membrane (141). Because A549 UGCG KOs exhibit such a large increase in sphingomyelin it suggests that their cell membrane compositions may be highly enriched in sphingolipids compared to WT A549 cells, which may result in modified infection levels for

viruses that enter host cells via the plasma membrane (such as measles) according to those viruses' reliance on sphingolipids as sites of binding and/or fusion.

Experiment 5.2.2.a – *Analysis of plasma membrane sphingolipid composition.* Plasma membranes may be isolated from whole cell lysates (fractionated by sonication) using differential ultra-centrifugation through a sucrose gradient (142). Should that method fail to yield sufficiently pure membranes, other methods of plasma membrane isolation have been published, including methods based on adhesion to plastic surfaces as well as combinations of cell surface labeling and crosslinking (143, 144). Isolating the plasma membranes of A549 cells and analyzing the sphingolipid composition of UGCG KO cells as compared to WT will help determine how UGCG maintains membrane lipid ratios.

We predicted that if glucosylsphingosine is catabolized by GBA, it may be synthesized by UGCG. If true, we would expect that cells deficient in UGCG would also be deficient in glucosylsphingosine as compared to WT cells. However, we did not detect any decreases in glucosylsphingosine in UGCG KO cells as compared to WT. As a caution, because the baseline levels of glucosylsphingosine are so low in both HEK 293 and A549 cells, any potential differences in the UGCG KOs may be below the limits of detection. An alternative to UGCG as the catalyzing enzyme for glucosylsphingosine is the ceramidases. These enzymes remove the fatty acid group of ceramide, converting it into sphingosine. An early

study into glucosylsphingosine metabolism suggested that patients with Farber disease (deficient in acid ceramidase) accumulated less glucosylsphingosine than patients with WT acid ceramidase, providing evidence for the role of the ceramidases in the synthesis of glucosylsphingosine (145). We hypothesize that the ceramidases act upon GlcCer, removing its fatty acid group and converting it directly into glucosylsphingosine (**Fig. 5.2**).

Experiment 5.2.2.b – *Tracking sphingosine-d7 and glucosylceramide-d5 to determine the lipid precursor to glucosylsphingosine.* Incubating GBA KO cells with both labeled sphingosine and labeled GlcCer will determine the lipid precursor for glucosylsphingosine, and by extension, the likely enzyme responsible for its anabolism. Importantly, the labels for sphingosine and GlcCer must be located on different carbons within the sphingosine backbone, in order to differentiate one from the other as the lipids are metabolized. Such lipids are currently available for purchase from Avanti Polar Lipids.

5.2.3 GlcCer Versus Other Sphingolipids

One major difficulty that arises when studying sphingolipids is trying to assign an observed phenotype to a specific sphingolipid. Upon knocking out, inhibiting, or silencing any of sphingolipid metabolizing enzymes, changes throughout the sphingolipid pathway occur, and the levels of the various specific sphingolipids may dramatically rise or fall as cells try to compensate. Thus, ignoring the rest of the pathway and claiming all of our observed influenza infection decreases are due to disruption of GlcCer homeostasis is presumptuous and must be further examined.

In any interconnected system, one method of narrowing down which component(s) may be responsible for an observed effect is to try to replicate the effect in different scenarios and to check if the hypothesized cause remains consistent across each scenario. In our case we sought to knock out UGCG or GBA in multiple cell lines, reasoning that if we observed a phenotype in both cell lines we could examine their lipid profiles and determine what lipid changes, if any, were comparable in each cell line. As shown in the sphingolipid **Table 3.S1**, in GBA KO cells GlcCer, ceramide, dihydrosphingosine, and glucosylsphingosine all rose in both cell lines tested. As such, claiming that our observed phenotype is due to GlcCer cannot be based solely on the lipid profiles. As **Table 4.S1** demonstrates, in UGCG KO cells only GlcCer and sphingosine-1-phosphate exhibited the same increase or decrease across both HEK 293 and A549 cell lines. As sphingosine-1-phosphate is a potent signaling molecule, alterations in its mass may have a large effect on cellular functions, including endocytosis.

After examination of all of our data, we attempted to determine how knocking out enzymes that performed opposing actions resulted in a similar decrease in influenza infections. We hypothesized that a balance of lipids was necessary to maintain infection of influenza, and that disruption of that balance was responsible for the reduction in influenza infection observed in all of the cell lines tested. The importance of maintaining the right balance of key molecules has been shown in several other cellular systems. For instance, tightly regulated signaling pathways often require a homeostatic state to maintain proper cell

function (such as Notch signaling), and both up- and down-regulation of specific proteins has been shown to cause constitutive Akt signaling (146, 147). In the context of homeostasis, examination of the lipid profiles of GBA and UGCG KOs did yield one consistent theme: of all the lipids analyzed, only GlcCer was consistently increased (in the case of GBA KOs) or decreased (in the case of UGCG KOs).

GlcCer serves as the foundational lipid for a variety of higher order glycolipids, including lactosylceramide, GM3, and GMD3. Disruptions in GlcCer levels may result in disruptions in the homeostasis of any number of gangliosides, many of which have been implicated in a number of cellular functions, including maintenance of lipid rafts (148). For a complete analysis of the effects of knocking out GBA or UGCG on influenza infection these long chain gangliosides must be considered as well as the numerous sphingolipids listed throughout this thesis. However, currently our laboratory is unable to measure or quantitate these lipids, and as such they remain an avenue for future research.

5.3 Implications for Cellular Endocytosis

5.3.1 Membranes and Vesicles

The plasma membrane is made up a variety of phospholipids, including the glycerophospholipids phosphatidylcholine (PC), phosphatidylethanolamine (PE), phosphatidylserine (PS), phosphatidylinositol (PI) and phosphatidic acid (PA). Sphingolipids play an important role in membrane organization and membrane mobility, as their fatty acid chains allow for more ordered packing and therefore

represent a ‘solid gel’ phase of membranes (149). The most abundant sphingolipid in the plasma membrane is sphingomyelin, though ceramide, GlcCer, and higher order gangliosides are all found as well. In conjunction with cholesterol, sphingolipids in plasma membranes are thought to form ‘lipid rafts’ – ordered lipid micro-domains selectively enriched in particular protein and lipid groups.

The formation of endosomes and the start of the endocytic pathway begin with the creation of a vesicle that is pinched off from the plasma membrane. These vesicles contain a lipid bilayer comprised of the portion of plasma membrane from which they originated. Thus, alterations in the plasma membrane content would result in alterations in the composition of the membranes of these intracellular vesicles. The lipid composition of cellular vesicles is crucial to vesicle form, function, and localization (150). Lipids are responsible for a variety of vesicle characteristics, including their ability to recruit and bind cellular proteins involved in vesicle trafficking (151). By altering the endogenous sphingolipid ratios within UGCG and GBA KO cells, we hypothesize that cellular vesicles (including endosomes) will contain altered lipid membrane compositions, and therefore, altered characteristics.

Experiment 5.3.1.a – *Characterization of lipids in the early endosome, late endosome, and lysosome.* We hypothesize that KO cells contain endosomes with altered sphingolipid compositions, and that these alterations may cause the delayed endosome trafficking we observed in Chapter 3. Study of the lipid compositions of cellular vesicles is fraught with challenges, as there currently

exists no perfect method of isolating specific endosomes. As such, contamination from other sources such as the plasma membrane often yields misleading or inconsistent data. Nevertheless, by performing fractionation following osmotic shock, freeze/thaw cycles, or cell cracking and then running a resulting post nuclear supernatant fraction through a sucrose gradient at ultra-centrifugation speeds it is theoretically possible to isolate endosomes from the rest of the cell (152). The isolated endosomes may then be analyzed by mass spectrometry for lipid content and the endosomes of GBA and UGCG KO cells may be compared to those of WT cells. We caution that great care must be taken to perform thorough quality control on the resultant fractions, including analysis of each fraction for markers of endosomes and markers of other cellular organelles (including the plasma membrane). See **Table 5.2** for a selection of specific markers that may be used. In addition, it is extremely challenging to separate out each stage of endocytosis, as endosomes do not undergo a stratified linear progression but more of a fluid metamorphosis as they mature and acidify.

5.3.2 Trafficking

As evidenced in Chapter 3, GBA maintains viral entry through regulation of endocytosis. However, the exact endocytic defect in GBA KO cells is not yet fully understood. Because both influenza and EGF are impaired in trafficking to endolysosomes (marked by Lamp1), we hypothesize that one of the earlier stages of endosome maturation or trafficking is also affected by knocking out GBA. Binding of influenza and EGF to their respective cell surface receptors remained unaffected (in the case of influenza) or increased slightly (in the case of EGF),

Organelle	Marker(s)
Early Endosome	EEA1, Rab5 (153, 154)
Late Endosome	Rab7, LBPA (153, 154)
Lysosome	Lamp1, Lamp2, TPCN2 (153, 154)
Nucleus	NF-kB, Oct-1, AP1 (155)
Endoplasmic Reticulum	DPM1 (156)
Mitochondria	Tom22 (157)
Golgi	B4GALT1 (158)

Table 5.2 List of markers for a variety of cellular organelles

Proteins that localize to specific organelles serve as markers for those organelles. By analyzing purified organelle fractions for these specific markers it is possible to assess the purity of each fraction.

suggesting that whatever role GBA has on endocytosis, it does not affect the binding of influenza or EGF to the cell surface.

After binding to the cell surface, the next step of entry for any endocytosed virus is its internalization into a protective vesicle that becomes an early endosome. A 2018 study found that internalization of transferrin was retarded in cells treated with conduritol B epoxide, an inhibitor of GBA (159). Dysregulation of internalization may be the source of the delayed trafficking phenotype we observed in GBA KO cells, as any delay in the formation of the early endosome would translate to a delay in trafficking to Lamp1⁺ compartments. Alternatively, internalization may be unaffected by the ablation of GBA, but cargo movement or maturation from the early endosome to the late endosome or lysosome could be affected.

Experiment 5.3.2.a – *Internalization Assay for Influenza and EGF*. By first binding influenza to the cell surface at 4°C, successful viral-host binding can occur while subsequent steps of viral entry are halted. Thoroughly washing the cells after binding and then allowing the cells to incubate at 37°C enables viral particles to be internalized and therefore protected from subsequent proteinase K treatment. Finally, by repeating the experiment with different lengths of incubation at 37°C and then measuring the amount of virus in each sample via western blot it is possible to determine the extent to which viruses are able to be internalized. The same principle can be applied to EGF internalization, though in that case the labeling of cell surface EGFR is first done using biotin. Excess biotin is washed off and upon addition of EGF the EGF-EGFR-biotin complex is

internalized. By first pulling down all biotinylated proteins and then probing for EGFR it is possible to examine only the internalized EGFR instead of total EGFR.

Experiment 5.3.2.b – *Early endosome and late endosome colocalization to determine precise stage of disrupted endosome trafficking in GBA KO cells.* Early endosomes are marked by the expression of early endosome antigen 1 (EEA1), and Rab 5 while late endosomes express Rab7 and, for example, Lamp 1. Staining for EEA1 and Rab7 and performing time course experiments to examine colocalization of EEA1, Rab7, and influenza (or EGF) will determine whether viral particles and EGF are retarded in trafficking to early endosomes or whether the defect in GBA KO cells occurs at the stage of transport from early to late endosomes. Finally, colocalization of viral particles or EGF with endosomes expressing both Lamp1 and Rab7 will provide a more precise picture of late endosome trafficking.

In addition to determining the trafficking capabilities of endosomal cargos, trafficking of lipids throughout the cell must be analyzed in order to more accurately assess the effect of deleting GBA on endocytosis. Previous studies demonstrated that glycosylated sphingolipids such as GlcCer and lactosylceramide are targeted to the Golgi in certain cell types, but in sphingolipid storage disorders or upon addition of inhibitors of GBA or UGCG they are instead trafficked to lysosomes (76, 160, 161). These data suggest that GlcCer metabolism may maintain endocytic trafficking through regulation of lipid trafficking.

Experiment 5.3.2.c – *Subcellular localization of sphingolipids to early endosomes, late endosomes, and the Golgi.* Incubating cells with fluorescent

analogues of ceramide, sphingosine, sphingomyelin, and GlcCer (all commercially available) will determine the localization of these sphingolipids in WT vs. KO cells. By co-staining the cells with markers for endosomes and/or the Golgi, any mislocalization of sphingolipids from the Golgi to the endocytic pathway may be observed.

5.3.3 Endo-lysosome biogenesis

If trafficking of endocytic cargos to the late endosome or lysosome is impaired in GBA KO cells (**Chapter 3**), then any cellular functions that utilize the same trafficking mechanisms may be impaired as well. Many proteases that reside in the lysosome traffic there by entering the endocytic pathway via mannose-6-phosphate at sites of late endosomes (sometimes termed pre-lysosomal compartments) and are carried into the lysosome as the endosomes mature (162). Our data determined that GBA knockout cells displayed increased levels of one lysosomal protease, Cathepsin B (**Figure 3.11**). In addition, we determined that Cathepsin B activity levels were increased in our KO cells as compared to WT (~1.4 fold higher), and upon lysis of the cell, Cathepsin B activity *in vitro* was ~3.5 fold higher in GBA KO cells as compared to WT. These results are in agreement with previous studies that found cells from patients with Gaucher's disease display increased activity of Cathepsin B (though no data was provided on Cathepsin L) (163, 164).

We hypothesize that all three pieces of data may be explained by a trafficking defect of Cathepsin B. Should Cathepsin B be unable to localize to the lysosomes,

we hypothesize that it would remain in the endosomal compartments. In response, the cell would seek to up-regulate Cathepsin B production in an attempt to increase lysosomal Cathepsin B. One caveat to this hypothesis are the activity assays of Cathepsin L that revealed no statistically significant change in activity of GBA KO Cathepsin L as compared to WT. Because Cathepsin L normally traffics via the same mechanism as Cathepsin B, these data do not reinforce our hypothesis. However, upon searching the literature we discovered that in several cancer models, including breast, colorectal, and prostate cancer, Cathepsin L is expressed in a splice variant that lacks the localization signal normally responsible for its trafficking to the lysosome (165–167). This isoform localizes instead to the nucleus and is responsible for pushing cells into the proliferation phase of the cell cycle.

As A549 cells are derived from a lung adenocarcinoma, we hypothesize that the reason Cathepsin L activity levels were not increased in GBA KO cells as compared to WT is that A549 cells expressed the nuclear isoform of Cathepsin L. To test this hypothesis we will examine the localization of Cathepsin L using immunofluorescence, as well as determining the approximate size of Cathepsin L via western blot. Should these results determine that A549 cells do not express the nuclear Cathepsin L isoform, we hypothesize that the differences we observe between Cathepsin B and Cathepsin L may be the result of differences in the respective proteases to function at different pHs. It is possible that both enzymes are accumulating in the late endosome, but if Cathepsin B may be functional at the higher pH of the endosome (~5.0-5.9) compared to the lysosome (pH ~4.5-

5.0), while Cathepsin L is not. In either case, further investigation into the discrepancy between Cathepsin L and Cathepsin B activity in GBA KO cells is warranted.

5.4 Implications for Viral Infections

5.4.1 Viral Entry

As evidenced in Chapter 3, we hypothesize that GBA maintains viral entry by regulating endocytosis. However, the precise mechanism behind the endocytic defect in GBA KO cells is not yet fully understood. Because both influenza and EGF are unable to traffic to late endosomes as efficiently in GBA KO cells as in WT cells, we hypothesize that trafficking defects are the main cause for the reduction in viral entry we observed. However, several other factors may influence our results and must be further explored in order to solidify the mechanism behind our findings.

Influenza fusion with host endosomes is triggered when the primed hemagglutinin (HA) glycoprotein of the virus undergoes a conformational change (168). This conformational change is driven by acidification of the endosome to a pH of ~5.0-5.5 (169), which leads to anchoring of HA fusion peptides within the endosome membrane (170). Next, a combination of several HA proteins directs the formation of a pore-like complex between the viral membrane and the endosomal membrane, leading to release of the viral genome into the cell (171, 172). This highly complex process involves mixing of lipids both from the viral membrane as well as the endosome itself, providing an intriguing possibility for

the involvement of sphingolipids such as GlcCer. Lack of any detectable defect in endosomal acidification in GBA KO cells suggested that the conformational changes in HA associated with influenza fusion are likely still functional, though further testing is necessary to confirm that assumption.

Experiment 5.4.1.a – *Examination of the ability of influenza HA to undergo conformational changes and induce viral fusion.* When influenza HA undergoes its conformational change in the presence of acidic conditions, previously protected portions of the protein are exposed. Highly specific antibodies against either the acidic or the neutral conformations of HA are available, and can be used to determine if HA is able to convert to its low pH form in the KO cells. The experiment is classically performed as an immunofluorescence assay, though if necessary it can be performed by flow cytometry.

5.4.2 Viral Exit

One intriguing finding of our work is the possibility that sphingolipids may play a role in the assembly and/or exit of influenza particles. Influenza entry is reduced in our GBA KO cells, but when the virus undergoes multiple cycles of replication, that phenotype is lost (**Fig. 3.4**). A 2012 study determined that the envelope of influenza is enriched in sphingolipids (6), and numerous studies indicate that influenza exits cells at sites of lipid microdomains, which are often enriched in sphingolipids (173). We hypothesize that the disruption of homeostasis of cellular sphingolipids resulting from knocking out GBA enhances influenza exit from host cells.

An enhanced exit phenotype could be due to either an increase in the number of viral particles budding from each host cell, an increase in the infectivity of each budding particle, or both. The enrichment of GlcCer in GBA KO cells may lead to formation of lipid microdomains conducive to future infections, and upon influenza envelopment in host membranes these microdomains increase the ability of the virus to infect new cells. Alternatively, these altered membrane compositions may result in increased HA or NA abundance, enhancing the ability of any budded particles to infect new cells. Finally, GBA may promote an increase in the number of viral particles that are generated by each infected cell, thereby increasing the rate at which new cells are infected. These hypotheses provide a tantalizing and rich area for further study that would both increase our scientific understanding of influenza biology as well as provide important clues for future combinatorial therapeutic interventions against the virus. However, a combination of experiments (outlined below) will be necessary to gain insight into this model.

Experiment 5.4.2.a – *Generation of VLPs from KO cells.* The first step to determining the effect of sphingolipids on viral assembly and/or exit is to generate VLPs from KO cells and compare their entry efficiency to VLPs generated from WT cells. If sphingolipids enhance viral exit, the VLPs produced from the KO cells might be more entry competent than those from WT cells. Results must be normalized to a transfection control in order to ensure that any differences observed are not due to varying transfection efficiencies in KO cells as compared to WT.

Experiment 5.4.2.b – *Direct count of VLP particles.* Electron microscopy and dynamic light scattering analysis of VLPs will allow for a direct count of the number of particles that successfully bud from transfected cells.

Experiment 5.4.2.c – *Analysis of VLP lipid composition.* VLPs generated from both WT and KO cells could be purified and analyzed by mass spectrometry for their sphingolipid composition. We hypothesize that the membranes of the VLPs will vary in their glucosylceramide content according to the cell type used to generate them, and that this difference partially account for the proposed increased viral assembly phenotype. Results must be normalized to the VLP particle count provided by electron microscopy to ensure any differences in lipid abundance are not simply due to more VLP particles.

Experiment 5.4.2.d – *Analysis of VLP protein abundance.* Western blots to examine the glycoproteins of influenza found on VLPs generated from KO cells as compared to VLPs generated from WT cells may provide rough estimation of the effect of sphingolipids on influenza HA, NA, M1, and M2 abundance. Comparing the ratios of HA, NA, M1, and M2 may provide a quantitative estimate of each protein involved in influenza capsid and membrane structure. Results must be normalized to the VLP particle count provided by electron microscopy and/or dynamic light scattering to ensure any differences in protein abundance are not simply due to more VLP particles.

Experiment 5.4.2.e – *Analysis of influenza glycoprotein localization.* Sphingomyelin is essential for intracellular transport of influenza glycoproteins (72), but the role of other sphingolipids such as GlcCer remains unexplored. Studying the transport of HA, NA, M1, and M2 to sites of viral assembly will

provide insight into our hypothesized influenza exit phenotype. Immunofluorescence staining against influenza glycoproteins in KO cells will determine their cellular localization as compared to WT cells, while immunoprecipitation of cell surface-biotinylated proteins followed by western blotting for the influenza glycoproteins will provide added insights into the potential for sphingolipids to enhance influenza assembly at the cell surface.

Alternatively, the data in **Figure 3.4** may not be due to an increase in viral exit, but rather an increase in viral replication GBA KO cells as compared to WT. We propose that this hypothesis is less likely than our favored interpretation of an enhanced exit phenotype because infection assays that incorporate a PR8 live influenza virus (**Figures 3.2 and 4.3**) or a pseudovirus system (**Figures 3.6 and 4.5**) incorporate the transcription of viral RNA and translation of viral proteins containing a GFP reporter as their primary readout. Any increases in viral replication that would result in the rescue we observed in **Figure 3.4** would therefore also affect the results in **Figures 3.2, 3.6, 4.3, and 4.5**, which we did not observe. In addition, the readout of **Figure 3.4** is mRNA production, which suggests that production of influenza RNA alone is not enough to result in the rescue observed in **Figure 3.4B**. Nevertheless we cannot rule out replication completely, as it's possible that sphingolipids play a role in viral replication that we cannot observe in our infection assays. To determine what effect our GBA and UGCG KOs have on viral replication it would be necessary to incorporate a reverse genetics system in combination with inhibitors of viral budding such as Oseltimivar (Tamiflu) (174). Reverse genetics systems are similar to our proposed

experiment utilizing VLP generation: cells of interest are transfected with plasmids containing genes necessary for the assembly of influenza virus. By measuring influenza protein production via western blot we may gain insight into the replication machinery of GBA and UGCG KO cells. The incorporation of neuraminidase inhibitors will ensure that any phenotype we observe is not confounded by release of new viral particles into the media.

5.4.3 Other Viruses

Though we examined the effects of knocking out UGCG and GBA on influenza, Ebola, VSV, and measles, more virus types remain to be tested. A 2017 paper published by the laboratory of Paul Bates suggested a role for GlcCer in infections by severe fever with thrombocytopenia syndrome virus (SFTSV), as well as several other bunyaviruses, through the use of both pharmacological inhibition as well as siRNA knockdown of UGCG (175). These findings must be replicated in the UGCG KO cells, in order to determine the extent to which our findings agree with that study. In addition, sphingolipids have been implicated in infections by HIV, caliciviruses, rhinovirus, and hepatitis C virus (60–63, 65, 68, 103, 176, 177), all of which may be good candidates to test in our generated cell lines.

Viruses that enter cells through the plasma membrane provide excellent candidates for future studies. Measles virus, which directly injects its genome into host cells via the plasma membrane (178), exhibited increased infectious capability in A549 UGCG KOs (**Fig. 4.5**), suggesting that the lipid composition of the plasma membrane may play a role in its pathogenicity. Indeed, a 2004 study

found that measles virus may enter cells at sites enriched in sphingolipids (134). Though this phenotype was not observed in HEK 293 UGCG KO cells, it does warrant further examination. We hypothesize that other plasma membrane entering viruses, such as simian virus 5 (a paramyxovirus), may also exhibit increased or decreased infection levels in GBA and UGCG KO cells as compared to WT. However, unlike our findings in Chapter 3, we do not hypothesize a shared phenotype amongst plasma membrane entering viruses, as each virus tested may require a different lipid conditions for successful infection.

Experiment 5.4.3.a – Infections by other viruses. Measurement of infectious rates of a variety of viruses in UGCG and GBA KO cells may provide insight into the sphingolipid requirements of each virus tested. A combination of live-virus assays and pseudovirus systems may be employed to examine as wide a range of viruses as possible. However, caution should be taken to ensure that in assays using live viruses with multiple cycles of infection differences in entry of viruses are not confounded by differences in exit.

5.4.4 Implications for Influenza Therapeutics

Our findings indicate a role for GlcCer in maintaining cellular endocytosis, with implications for a number of clinical fields. Viruses and other pathogens that enter host cells through endocytosis may be considered strong candidates for combinatorial therapies of sphingolipid inhibitors or analogues with current treatments. In addition, our work may enhance drug delivery strategies, as escape from the degradation proteases present in endo-lysosomes presents a challenge for successful drug entry into host cells. Understanding the role of GlcCer in

normal trafficking of endosomes may shed insight into better approaches to escape those proteases and increase the efficacy of drug delivery.

Influenza in particular presents an exciting opportunity for applications of our work in a translational setting. As we have shown, modulation of GlcCer levels by knocking out their metabolizing enzymes reduces influenza entry *in vitro*, suggesting a novel avenue for future influenza therapies. However, any therapeutic approach must be undertaken with great caution, as preliminary data suggests a potential role for these sphingolipids may play a role in enhancing influenza exit thereby countering the inhibitory effect of blocking entry. Should the translational aspect of this project be explored further, we recommend a combinatorial approach to target influenza; combining sphingolipid-based entry inhibition with known inhibitors of influenza particle release, such as the neuraminidase inhibitors Oseltamivir (Tamiflu), Laninamivir (Inavir), and Zanamivir (Relenza).

In conclusion, the work presented in this thesis reveals the critical need to further study sphingolipids in the context of viral infections. By gaining a better idea of how these lipids regulate cellular endocytosis, we now have a more complete understanding of the role of sphingolipids in viral-host interactions. Taken together, our work demonstrates a clear relationship between viruses and sphingolipids and has broad implications both for the fields of virology and cell biology.

Table 5.3 Proposed Future Experiments

Number	Name	Purpose
5.2.1.a	Serine labeling and tracking via mass spec to confirm activation of de novo synthesis in GBA KO cells	Confirm ceramide increases are due to de novo synthesis
5.2.1.b	Protein and mRNA expression of serine palmitoyltransferase	Determine if increased de novo synthesis is due to enzyme upregulation
5.2.1.c	Measurement of substrate abundance for de novo synthesis of ceramide	Determine if increased de novo synthesis of ceramide is due to substrate availability
5.2.1.d	Tracking glucosylsphingosine-d7 to determine possible glucosylsphingosine catabolic enzymes	Determine if GBA is the sole method of catabolism for glucosylsphingosine
5.2.2.a	Analysis of plasma membrane sphingolipid content	Determine the levels of sphingolipids in GBA and UGCG KO cells compared to WT
5.2.2.b	Tracking sphingosine-d7 and glucosylceramide-d5 to determine the lipid precursor to glucosylsphingosine	Determine the lipid origin of glucosylsphingosine
5.3.1.a	Characterization of lipids in the early endosome, late endosome, and lysosome	Determine if endocytic organelles of KO cells express different sphingolipids than those from WT cells
5.3.2.a	Internalization Assay for Influenza and EGF	Determine if internalization is delayed in KO cells
5.3.2.b	Early endosome and late endosome colocalization to determine precise stage of disrupted endosome trafficking	Determine if trafficking to or from the early endosome is delayed in KO cells
5.3.2.c	Subcellular localization of sphingolipids to early endosomes, late endosomes, and the Golgi	Determine if sphingolipids localize to different parts of the cell in KOs vs WT

5.4.1.a	Examination of the ability of influenza HA to undergo conformational changes and induce viral fusion.	Determine if fusion of influenza is impaired due to aberrant HA conformational changes (in addition to the delay in endosome trafficking)
5.4.2.a	Generation of VLPs from KO cells	Measure the infectivity of VLPs generated from WT and KO cells to determine if virus exit is affected in KO cells
5.4.2.b	Direct count of VLP particles	Assess the number of particles generated from WT vs KO cells with a variety of techniques
5.4.2.c	Analysis of VLP lipid composition	Determine the lipid composition of VLPs generated from WT vs KO cells
5.4.2.d	Analysis of VLP protein abundance	Determine the relative protein abundance of influenza glycoproteins on VLPs from WT and KO cells
5.4.2.e	Analysis of influenza glycoprotein localization	Determine what effect KOs of UGCG and GBA have on localization of influenza glycoproteins, especially as it relates to viral exit
5.4.3.a	Infections by other viruses	Determine the sphingolipid requirements for entry and infection other viruses

CHAPTER 6 – REFERENCES

1. Pappas G, Kiriaze IJ, Falagas ME. 2008. Insights into infectious disease in the era of Hippocrates. *Int J Infect Dis* 12:347–350.
2. Threats I of M (US) F on M, Knobler SL, Mack A, Mahmoud A, Lemon SM. 2005. *The Story of Influenza*. National Academies Press (US).
3. Taubenberger JK, Morens DM. 2006. 1918 Influenza: the Mother of All Pandemics. *Emerg Infect Dis* 12:15–22.
4. Frith J. 2012. The history of plague - part 1: The three great pandemics. *Journal of Military and Veterans Health* 20:11.
5. Einfeld AJ, Neumann G, Kawaoka Y. 2015. At the centre: influenza A virus ribonucleoproteins. *Nat Rev Microbiol* 13:28–41.
6. Gerl MJ, Sampaio JL, Urban S, Kalvodova L, Verbavatz J-M, Binnington B, Lindemann D, Lingwood CA, Shevchenko A, Schroeder C, Simons K. 2012. Quantitative analysis of the lipidomes of the influenza virus envelope and MDCK cell apical membrane. *J Cell Biol* 196:213–221.
7. Chen BJ, Leser GP, Jackson D, Lamb RA. 2008. The Influenza Virus M2 Protein Cytoplasmic Tail Interacts with the M1 Protein and Influences Virus Assembly at the Site of Virus Budding. *J Virol* 82:10059–10070.
8. Rossman JS, Jing X, Leser GP, Balannik V, Pinto LH, Lamb RA. 2010. Influenza Virus M2 Ion Channel Protein Is Necessary for Filamentous Virion Formation. *J Virol* 84:5078–5088.
9. Rossman JS, Lamb RA. 2011. Influenza Virus Assembly and Budding. *Virology* 411:229–236.
10. Barman S, Nayak DP. 2007. Lipid Raft Disruption by Cholesterol Depletion Enhances Influenza A Virus Budding from MDCK Cells. *J Virol* 81:12169–12178.
11. Nayak DP, Balogun RA, Yamada H, Zhou ZH, Barman S. 2009. Influenza virus morphogenesis and budding. *Virus Research* 143:147–161.
12. Nicholls JM, Chan RWY, Russell RJ, Air GM, Peiris JSM. 2008. Evolving complexities of influenza virus and its receptors. *Trends in Microbiology* 16:149–157.
13. Horimoto T, Kawaoka Y. 2005. Influenza: lessons from past pandemics, warnings from current incidents. *Nature Reviews Microbiology* 3:591–600.

14. Shi Y, Wu Y, Zhang W, Qi J, Gao GF. 2014. Enabling the “host jump”: structural determinants of receptor-binding specificity in influenza A viruses. *Nature Reviews Microbiology* 12:822–831.
15. Matlin KS, Reggio H, Helenius A, Simons K. 1981. Infectious entry pathway of influenza virus in a canine kidney cell line. *J Cell Biol* 91:601–613.
16. Galloway CJ, Dean GE, Marsh M, Rudnick G, Mellman I. 1983. Acidification of macrophage and fibroblast endocytic vesicles in vitro. *Proc Natl Acad Sci USA* 80:3334–3338.
17. Pérez L, Carrasco L. 1994. Involvement of the vacuolar H(+)-ATPase in animal virus entry. *J Gen Virol* 75 (Pt 10):2595–2606.
18. Chen J, Skehel JJ, Wiley DC. 1999. N- and C-terminal residues combine in the fusion-pH influenza hemagglutinin HA(2) subunit to form an N cap that terminates the triple-stranded coiled coil. *Proc Natl Acad Sci USA* 96:8967–8972.
19. Bullough PA, Hughson FM, Skehel JJ, Wiley DC. 1994. Structure of influenza haemagglutinin at the pH of membrane fusion. *Nature* 371:37.
20. Carr CM, Kim PS. 1993. A spring-loaded mechanism for the conformational change of influenza hemagglutinin. *Cell* 73:823–832.
21. O’Neill RE, Jaskunas R, Blobel G, Palese P, Moroianu J. 1995. Nuclear import of influenza virus RNA can be mediated by viral nucleoprotein and transport factors required for protein import. *J Biol Chem* 270:22701–22704.
22. Cros JF, Palese P. 2003. Trafficking of viral genomic RNA into and out of the nucleus: influenza, Thogoto and Borna disease viruses. *Virus Res* 95:3–12.
23. Fodor E. 2013. The RNA polymerase of influenza a virus: mechanisms of viral transcription and replication. *Acta Virol* 57:113–122.
24. De Vlucht C, Sikora D, Pelchat M. 2018. Insight into Influenza: A Virus Cap-Snatching. *Viruses* 10.
25. Dou D, Revol R, Östbye H, Wang H, Daniels R. 2018. Influenza A Virus Cell Entry, Replication, Virion Assembly and Movement. *Front Immunol* 9.
26. Chen BJ, Leser GP, Morita E, Lamb RA. 2007. Influenza Virus Hemagglutinin and Neuraminidase, but Not the Matrix Protein, Are Required for Assembly and Budding of Plasmid-Derived Virus-Like Particles. *Journal of Virology* 81:7111–7123.
27. Lai JCC, Chan WWL, Kien F, Nicholls JM, Peiris JSM, Garcia J-M. 2010. Formation of virus-like particles from human cell lines exclusively expressing influenza neuraminidase. *J Gen Virol* 91:2322–2330.

28. Yondola MA, Fernandes F, Belicha-Villanueva A, Uccellini M, Gao Q, Carter C, Palese P. 2011. Budding Capability of the Influenza Virus Neuraminidase Can Be Modulated by Tetherin. *J Virol* 85:2480–2491.
29. Chlanda P, Schraidt O, Kummer S, Riches J, Oberwinkler H, Prinz S, Kräusslich H-G, Briggs JAG. 2015. Structural analysis of the roles of influenza A virus membrane-associated proteins in assembly and morphology. *J Virol* JVI.00592-15.
30. Gottschalk A. 1957. Neuraminidase: the specific enzyme of influenza virus and *Vibrio cholerae*. *Biochimica et Biophysica Acta* 23:645–646.
31. Thompson WW, Weintraub E, Dhankhar P, Cheng P-Y, Brammer L, Meltzer MI, Bresee JS, Shay DK. 2009. Estimates of US influenza-associated deaths made using four different methods. *Influenza Other Respir Viruses* 3:37–49.
32. Nair H, Brooks WA, Katz M, Roca A, Berkley JA, Madhi SA, Simmerman JM, Gordon A, Sato M, Howie S, Krishnan A, Ope M, Lindblade KA, Carosone-Link P, Lucero M, Ochieng W, Kamimoto L, Dueger E, Bhat N, Vong S, Theodoratou E, Chittaganpitch M, Chimah O, Balmaseda A, Buchy P, Harris E, Evans V, Katayose M, Gaur B, O’Callaghan-Gordo C, Goswami D, Arvelo W, Venter M, Briese T, Tokarz R, Widdowson M-A, Mounts AW, Breiman RF, Feikin DR, Klugman KP, Olsen SJ, Gessner BD, Wright PF, Rudan I, Broor S, Simões EAF, Campbell H. 2011. Global burden of respiratory infections due to seasonal influenza in young children: a systematic review and meta-analysis. *Lancet* 378:1917–1930.
33. 2017. How the Flu Virus Can Change: “Drift” and “Shift” | CDC.
34. CDC. 2018. Key Facts About Seasonal Flu Vaccine. Centers for Disease Control and Prevention.
35. CDC Novel H1N1 Flu | The 2009 H1N1 Pandemic: Summary Highlights, April 2009-April 2010.
36. CDC Novel H1N1 Flu | CDC Estimates of 2009 H1N1 Influenza Cases, Hospitalizations and Deaths in the United States, April 2009 – January 16, 2010.
37. Shin W-J, Seong BL. 2018. Novel antiviral drug discovery strategies to tackle drug-resistant mutants of influenza virus strains. *Expert Opinion on Drug Discovery* 0:1–16.
38. Heo Y-A. 2018. Baloxavir: First Global Approval. *Drugs* 78:693–697.
39. Maxwell SRJ. 2007. Tamiflu and neuropsychiatric disturbance in adolescents. *BMJ* 334:1232–1233.

40. Elkin SR, Lakoduk AM, Schmid SL. 2016. Endocytic Pathways and Endosomal Trafficking: A Primer. *Wien Med Wochenschr* 166:196–204.
41. Preston JE, Joan Abbott N, Begley DJ. 2014. Transcytosis of macromolecules at the blood-brain barrier. *Adv Pharmacol* 71:147–163.
42. Salzman NH, Maxfield FR. 1988. Intracellular fusion of sequentially formed endocytic compartments. *J Cell Biol* 106:1083–1091.
43. Mellman I, Fuchs R, Helenius A. 1986. Acidification of the endocytic and exocytic pathways. *Annu Rev Biochem* 55:663–700.
44. Huotari J, Helenius A. 2011. Endosome maturation. *EMBO J* 30:3481–3500.
45. Lim C-Y, Zoncu R. 2016. The lysosome as a command-and-control center for cellular metabolism. *J Cell Biol* 214:653–664.
46. Kaksonen M, Roux A. 2018. Mechanisms of clathrin-mediated endocytosis. *Nature Reviews Molecular Cell Biology* 19:313–326.
47. White JM, Whittaker GR. 2016. Fusion of Enveloped Viruses in Endosomes. *Traffic* 17:593–614.
48. Haimovitz-Friedman A, Kolesnick RN, Fuks Z. 1997. Ceramide signaling in apoptosis. *Br Med Bull* 53:539–553.
49. Shaw J, Costa-Pinheiro P, Patterson L, Drews K, Spiegel S, Kester M. 2018. Novel Sphingolipid-Based Cancer Therapeutics in the Personalized Medicine Era, p. 327–366. *In* Chalfant, CE, Fisher, PB (eds.), *Advances in Cancer Research*. Academic Press.
50. Hannun YA, Obeid LM. 2008. Principles of bioactive lipid signalling: lessons from sphingolipids. *Nat Rev Mol Cell Biol* 9:139–150.
51. Hannun YA, Obeid LM. 2018. Sphingolipids and their metabolism in physiology and disease. *Nat Rev Mol Cell Biol* 19:175–191.
52. Hannun YA, Luberto C, Mao C, Obeid LM. 2015. *Bioactive Sphingolipids in Cancer Biology and Therapy*. Springer.
53. Gault C, Obeid L, Hannun Y. 2010. An overview of sphingolipid metabolism: from synthesis to breakdown. *Adv Exp Med Biol* 688:1–23.
54. Bartke N, Hannun YA. 2009. Bioactive sphingolipids: metabolism and function. *Journal of lipid research* 50:S91–S96.
55. Truman J-P, García-Barros M, Obeid LM, Hannun YA. 2014. Evolving concepts in cancer therapy through targeting sphingolipid metabolism.

Biochimica et Biophysica Acta (BBA) - Molecular and Cell Biology of Lipids 1841:1174–1188.

56. Stirnemann J, Belmatoug N, Camou F, Serratrice C, Froissart R, Caillaud C, Levade T, Astudillo L, Serratrice J, Brassier A, Rose C, Billette de Villemeur T, Berger MG. 2017. A Review of Gaucher Disease Pathophysiology, Clinical Presentation and Treatments. *Int J Mol Sci* 18.
57. 2018. Gaucher Disease Treatment & Management: Medical Care, Surgical Care, Consultations.
58. Bae E-J, Yang NY, Lee C, Lee H-J, Kim S, Sardi SP, Lee S-J. 2015. Loss of glucocerebrosidase 1 activity causes lysosomal dysfunction and α -synuclein aggregation. *Exp Mol Med* 47:e153.
59. Schneider-Schaulies J, Schneider-Schaulies S. 2015. Sphingolipids in viral infection. *Biological Chemistry* 396:585–595.
60. Grassmé H, Riehle A, Wilker B, Gulbins E. 2005. Rhinoviruses Infect Human Epithelial Cells via Ceramide-enriched Membrane Platforms. *J Biol Chem* 280:26256–26262.
61. Dreschers S, Franz P, Dumitru C, Wilker B, Jahnke K, Gulbins E. 2007. Infections with human rhinovirus induce the formation of distinct functional membrane domains. *Cell Physiol Biochem* 20:241–254.
62. Puri A, Rawat SS, Lin H-MJ, Finnegan CM, Mikovits J, Ruscetti FW, Blumenthal R. 2004. An inhibitor of glycosphingolipid metabolism blocks HIV-1 infection of primary T-cells. *AIDS* 18:849.
63. Rawat SS, Gallo SA, Eaton J, Martin TD, Ablan S, KewalRamani VN, Wang JM, Blumenthal R, Puri A. 2004. Elevated Expression of GM3 in Receptor-Bearing Targets Confers Resistance to Human Immunodeficiency Virus Type 1 Fusion. *J Virol* 78:7360–7368.
64. Miller ME, Adhikary S, Kolokoltsov AA, Davey RA. 2012. Ebola virus Requires Acid Sphingomyelinase Activity and Plasma Membrane Sphingomyelin for Infection. *Journal of Virology* 86:7473–7483.
65. Shivanna V, Kim Y, Chang K-O. 2015. Ceramide formation mediated by acid sphingomyelinase facilitates endosomal escape of caliciviruses. *Virology* 483:218–228.
66. Drake MJ, Brennan B, Jr KB, Bart SM, Sherman E, Szemiel AM, Minutillo M, Bushman FD, Bates P. 2017. A role for glycolipid biosynthesis in severe fever with thrombocytopenia syndrome virus entry. *PLOS Pathogens* 13:e1006316.

67. Konan KV, Sanchez-Felipe L. 2014. Lipids and RNA virus replication. *Curr Opin Virol* 9:45–52.
68. Weng L, Hirata Y, Arai M, Kohara M, Wakita T, Watashi K, Shimotohno K, He Y, Zhong J, Toyoda T. 2010. Sphingomyelin Activates Hepatitis C Virus RNA Polymerase in a Genotype-Specific Manner. *J Virol* 84:11761–11770.
69. Kanj SS, Dandashi N, El-Hed A, Harik H, Maalouf M, Kozhaya L, Mousallem T, Tollefson AE, Wold WS, Chalfant CE, Dbaibo GS. 2006. Ceramide regulates SR protein phosphorylation during adenoviral infection. *Virology* 345:280–289.
70. Seo Y-J, Blake C, Alexander S, Hahm B. 2010. Sphingosine 1-Phosphate-Metabolizing Enzymes Control Influenza Virus Propagation and Viral Cytopathogenicity. *J Virol* 84:8124–8131.
71. Seo Y-J, Pritzl CJ, Vijayan M, Bomb K, McClain ME, Alexander S, Hahm B. 2013. Sphingosine Kinase 1 Serves as a Pro-Viral Factor by Regulating Viral RNA Synthesis and Nuclear Export of Viral Ribonucleoprotein Complex upon Influenza Virus Infection. *PLoS One* 8.
72. Tafesse FG, Sanyal S, Ashour J, Guimaraes CP, Hermansson M, Somerharju P, Ploegh HL. 2013. Intact sphingomyelin biosynthetic pathway is essential for intracellular transport of influenza virus glycoproteins. *Proc Natl Acad Sci USA* 110:6406–6411.
73. Ishibashi Y, Kohyama-Koganeya A, Hirabayashi Y. 2013. New insights on glucosylated lipids: Metabolism and functions. *Biochimica et Biophysica Acta (BBA) - Molecular and Cell Biology of Lipids* 1831:1475–1485.
74. Schulze H, Kolter T, Sandhoff K. 2009. Principles of lysosomal membrane degradation: Cellular topology and biochemistry of lysosomal lipid degradation. *Biochimica et Biophysica Acta (BBA) - Molecular Cell Research* 1793:674–683.
75. Rosenbloom BE, Weinreb NJ. 2013. Gaucher Disease: A Comprehensive Review. *CRO* 18.
76. Sillence DJ. 2002. Glucosylceramide modulates membrane traffic along the endocytic pathway. *The Journal of Lipid Research* 43:1837–1845.
77. Hufford MM, Richardson G, Zhou H, Manicassamy B, García-Sastre A, Enelow RI, Braciale TJ. 2012. Influenza-Infected Neutrophils within the Infected Lungs Act as Antigen Presenting Cells for Anti-Viral CD8+ T Cells. *PLoS One* 7.

78. Gotoh B, Yamauchi F, Ogasawara T, Nagai Y. 1992. Isolation of factor Xa from chick embryo as the amniotic endoprotease responsible for paramyxovirus activation. *FEBS Letters* 296:274–278.
79. Gotoh B, Ogasawara T, Toyoda T, Inocencio NM, Hamaguchi M, Nagai Y. 1990. An endoprotease homologous to the blood clotting factor X as a determinant of viral tropism in chick embryo. *EMBO J* 9:4189–4195.
80. Tatsuo H, Okuma K, Tanaka K, Ono N, Minagawa H, Takade A, Matsuura Y, Yanagi Y. 2000. Virus Entry Is a Major Determinant of Cell Tropism of Edmonston and Wild-Type Strains of Measles Virus as Revealed by Vesicular Stomatitis Virus Pseudotypes Bearing Their Envelope Proteins. *Journal of Virology* 74:4139–4145.
81. Whitt MA. 2010. Generation of VSV Pseudotypes Using Recombinant Δ G-VSV for Studies on Virus Entry, Identification of Entry Inhibitors, and Immune Responses to Vaccines. *J Virol Methods* 169:365–374.
82. Sun X, Tse LV, Ferguson AD, Whittaker GR. 2010. Modifications to the Hemagglutinin Cleavage Site Control the Virulence of a Neurotropic H1N1 Influenza Virus. *J Virol* 84:8683–8690.
83. Tscherne DM, Manicassamy B, García-Sastre A. 2010. An enzymatic virus-like particle assay for sensitive detection of virus entry. *Journal of Virological Methods* 163:336–343.
84. Nelson EA, Barnes AB, Wiehle RD, Fontenot GK, Hoenen T, White JM. 2016. Clomiphene and Its Isomers Block Ebola Virus Particle Entry and Infection with Similar Potency: Potential Therapeutic Implications. *Viruses* 8.
85. Hankins JL, Fox TE, Barth BM, Unrath KA, Kester M. 2011. Exogenous Ceramide-1-phosphate Reduces Lipopolysaccharide (LPS)-mediated Cytokine Expression. *J Biol Chem* 286:44357–44366.
86. Johansen LM, Brannan JM, Delos SE, Shoemaker CJ, Stossel A, Lear C, Hoffstrom BG, DeWald LE, Schornberg KL, Scully C, Lehár J, Hensley LE, White JM, Olinger GG. 2013. FDA-Approved Selective Estrogen Receptor Modulators Inhibit Ebola Virus Infection. *Science Translational Medicine* 5:190ra79-190ra79.
87. Ebert DH, Deussing J, Peters C, Dermody TS. 2002. Cathepsin L and Cathepsin B Mediate Reovirus Disassembly in Murine Fibroblast Cells. *J Biol Chem* 277:24609–24617.
88. Sakai T, Ohuchi M, Imai M, Mizuno T, Kawasaki K, Kuroda K, Yamashina S. 2006. Dual Wavelength Imaging Allows Analysis of Membrane Fusion of Influenza Virus inside Cells. *J Virol* 80:2013–2018.

89. Banerjee I, Yamauchi Y, Helenius A, Horvath P. 2013. High-Content Analysis of Sequential Events during the Early Phase of Influenza A Virus Infection. *PLoS ONE* 8:e68450.
90. Sakai T, Nishimura SI, Naito T, Saito M. 2017. Influenza A virus hemagglutinin and neuraminidase act as novel motile machinery. *Scientific Reports* 7:45043.
91. Eriksson I, Öllinger K, Appelqvist H. 2017. Analysis of Lysosomal pH by Flow Cytometry Using FITC-Dextran Loaded Cells, p. 179–189. *In* Öllinger, K, Appelqvist, H (eds.), *Lysosomes: Methods and Protocols*. Springer New York, New York, NY.
92. Dawood FS, Iuliano AD, Reed C, Meltzer MI, Shay DK, Cheng P-Y, Bandaranayake D, Breiman RF, Brooks WA, Buchy P, Feikin DR, Fowler KB, Gordon A, Hien NT, Horby P, Huang QS, Katz MA, Krishnan A, Lal R, Montgomery JM, Mølbak K, Pebody R, Presanis AM, Razuri H, Steens A, Tinoco YO, Wallinga J, Yu H, Vong S, Bresee J, Widdowson M-A. 2012. Estimated global mortality associated with the first 12 months of 2009 pandemic influenza A H1N1 virus circulation: a modelling study. *The Lancet Infectious Diseases* 12:687–695.
93. Imai M, Kawaoka Y. 2012. The role of receptor binding specificity in interspecies transmission of influenza viruses. *Current Opinion in Virology* 2:160–167.
94. White JM, Delos SE, Brecher M, Schornberg K. 2008. Structures and Mechanisms of Viral Membrane Fusion Proteins. *Crit Rev Biochem Mol Biol* 43:189–219.
95. Sieczkarski SB, Whittaker GR. 2003. Differential Requirements of Rab5 and Rab7 for Endocytosis of Influenza and Other Enveloped Viruses. *Traffic* 4:333–343.
96. Batishchev OV, Shilova LA, Kachala MV, Tashkin VY, Sokolov VS, Fedorova NV, Baratova LA, Knyazev DG, Zimmerberg J, Chizmadzhev YA. 2016. pH-Dependent Formation and Disintegration of the Influenza A Virus Protein Scaffold To Provide Tension for Membrane Fusion. *J Virol* 90:575–585.
97. Li S, Sieben C, Ludwig K, Höfer CT, Chiantia S, Herrmann A, Eghiaian F, Schaap IAT. 2014. pH-Controlled Two-Step Uncoating of Influenza Virus. *Biophys J* 106:1447–1456.
98. Gillespie EJ, Ho C-LC, Balaji K, Clemens DL, Deng G, Wang YE, Elsaesser HJ, Tamilselvam B, Gargi A, Dixon SD, France B, Chamberlain BT, Blanke SR, Cheng G, Torre JC de la, Brooks DG, Jung ME, Colicelli J, Damoiseaux R,

- Bradley KA. 2013. Selective inhibitor of endosomal trafficking pathways exploited by multiple toxins and viruses. *PNAS* 110:E4904–E4912.
99. Yeganeh B, Ghavami S, Kroeker AL, Mahood TH, Stelmack GL, Klonisch T, Coombs KM, Halayko AJ. 2015. Suppression of influenza A virus replication in human lung epithelial cells by noncytotoxic concentrations bafilomycin A1. *Am J Physiol Lung Cell Mol Physiol* 308:L270–L286.
100. Ochiai H, Sakai S, Hirabayashi T, Shimizu Y, Terasawa K. 1995. Inhibitory effect of bafilomycin A1, a specific inhibitor of vacuolar-type proton pump, on the growth of influenza A and B viruses in MDCK cells. *Antiviral Research* 27:425–430.
101. Tani H, Shiokawa M, Kaname Y, Kambara H, Mori Y, Abe T, Moriishi K, Matsuura Y. 2010. Involvement of Ceramide in the Propagation of Japanese Encephalitis Virus. *J Virol* 84:2798–2807.
102. Jan JT, Chatterjee S, Griffin DE. 2000. Sindbis virus entry into cells triggers apoptosis by activating sphingomyelinase, leading to the release of ceramide. *J Virol* 74:6425–6432.
103. Finnegan CM, Rawat SS, Cho EH, Guiffre DL, Lockett S, Merrill AH, Blumenthal R. 2007. Sphingomyelinase Restricts the Lateral Diffusion of CD4 and Inhibits Human Immunodeficiency Virus Fusion. *J Virol* 81:5294–5304.
104. Tafesse FG, Sanyal S, Ashour J, Guimaraes CP, Hermansson M, Somerharju P, Ploegh HL. 2013. Intact sphingomyelin biosynthetic pathway is essential for intracellular transport of influenza virus glycoproteins. *Proc Natl Acad Sci U S A* 110:6406–6411.
105. Libersou S, Albertini AAV, Ouldali M, Maury V, Maheu C, Raux H, Haas F de, Roche S, Gaudin Y, Lepault J. 2010. Distinct structural rearrangements of the VSV glycoprotein drive membrane fusion. *The Journal of Cell Biology* 191:199–210.
106. Bär S, Takada A, Kawaoka Y, Alizon M. 2006. Detection of Cell-Cell Fusion Mediated by Ebola Virus Glycoproteins. *Journal of Virology* 80:2815–2822.
107. Levy M, Futerman AH. 2010. Mammalian Ceramide Synthases. *IUBMB Life* 62:347–356.
108. Hoenen T, Watt A, Mora A, Feldmann H. 2014. Modeling The Lifecycle Of Ebola Virus Under Biosafety Level 2 Conditions With Virus-like Particles Containing Tetracistronic Minigenomes. *J Vis Exp*.
109. White J, Kartenbeck J, Helenius A. 1982. Membrane fusion activity of influenza virus. *EMBO J* 1:217–222.

110. Opresko LK, Chang C-P, Will BH, Burke PM, Gill GN, Wiley HS. 1995. Endocytosis and Lysosomal Targeting of Epidermal Growth Factor Receptors Are Mediated by Distinct Sequences Independent of the Tyrosine Kinase Domain. *J Biol Chem* 270:4325–4333.
111. Duncan JA, Gao X, Huang M, O'Connor BP, Thomas CE, Willingham SB, Bergstralh DT, Jarvis GA, Sparling PF, Ting JP-Y. 2009. *Neisseria gonorrhoeae* activates the proteinase Cathepsin B to mediate the signaling activities of the NLRP3 and ASC - containing inflammasome. *J Immunol* 182:6460–6469.
112. Yamauchi Y, Helenius A. 2013. Virus entry at a glance. *J Cell Sci* 126:1289–1295.
113. Lozach P-Y, Huotari J, Helenius A. 2011. Late-penetrating viruses. *Current Opinion in Virology* 1:35–43.
114. Grove J, Marsh M. 2011. The cell biology of receptor-mediated virus entry. *J Cell Biol* 195:1071–1082.
115. Marsh M, Helenius A. 2006. Virus Entry: Open Sesame. *Cell* 124:729–740.
116. Pewzner-Jung Y, Brenner O, Braun S, Laviad EL, Ben-Dor S, Feldmesser E, Horn-Saban S, Amann-Zalcenstein D, Raanan C, Berkutzki T, Erez-Roman R, Ben-David O, Levy M, Holzman D, Park H, Nyska A, Merrill AH, Futerman AH. 2010. A Critical Role for Ceramide Synthase 2 in Liver Homeostasis. *J Biol Chem* 285:10911–10923.
117. Murugesan V, Chuang W-L, Liu J, Lischuk A, Kacena K, Lin H, Pastores GM, Yang R, Keutzer J, Zhang K, Mistry PK. 2016. Glucosylsphingosine is a key biomarker of Gaucher disease. *Am J Hematol* 91:1082–1089.
118. Rolfs A, Giese A-K, Grittner U, Mascher D, Elstein D, Zimran A, Böttcher T, Lukas J, Hübner R, Gölnitz U, Röhle A, Dudesek A, Meyer W, Wittstock M, Mascher H. 2013. Glucosylsphingosine Is a Highly Sensitive and Specific Biomarker for Primary Diagnostic and Follow-Up Monitoring in Gaucher Disease in a Non-Jewish, Caucasian Cohort of Gaucher Disease Patients. *PLOS ONE* 8:e79732.
119. Dekker N, Dussen L van, Hollak CEM, Overkleeft H, Scheij S, Ghauharali K, Breemen MJ van, Ferraz MJ, Groener JEM, Maas M, Wijburg FA, Speijer D, Tylki-Szymanska A, Mistry PK, Boot RG, Aerts JM. 2011. Elevated plasma glucosylsphingosine in Gaucher disease: relation to phenotype, storage cell markers, and therapeutic response. *Blood* 118:e118–e127.
120. Laude AJ, Prior IA. 2004. Plasma membrane microdomains: organisation, function and trafficking. *Mol Membr Biol* 21:193–205.

121. Helms JB, Zurzolo C. 2004. Lipids as targeting signals: lipid rafts and intracellular trafficking. *Traffic* 5:247–254.
122. Urade R, Hayashi Y, Kito M. 1988. Endosomes differ from plasma membranes in the phospholipid molecular species composition. *Biochim Biophys Acta* 946:151–163.
123. Lima S, Milstien S, Spiegel S. 2017. Sphingosine and Sphingosine Kinase 1 Involvement in Endocytic Membrane Trafficking. *J Biol Chem* jbc.M116.762377.
124. Pepperl J, Reim G, Lüthi U, Kaech A, Hausmann G, Basler K. 2013. Sphingolipid depletion impairs endocytic traffic and inhibits Wingless signaling. *Mechanisms of Development* 130:493–505.
125. Yonamine I, Bamba T, Nirala NK, Jesmin N, Kosakowska-Cholody T, Nagashima K, Fukusaki E, Acharya JK, Acharya U. 2011. Sphingosine kinases and their metabolites modulate endolysosomal trafficking in photoreceptors. *The Journal of Cell Biology* 192:557–567.
126. Lloyd-Evans E, Morgan AJ, He X, Smith DA, Elliot-Smith E, Sillence DJ, Churchill GC, Schuchman EH, Galione A, Platt FM. 2008. Niemann-Pick disease type C1 is a sphingosine storage disease that causes deregulation of lysosomal calcium. *Nature Medicine* 14:1247–1255.
127. de Almeida RFM, Fedorov A, Prieto M. 2003. Sphingomyelin/Phosphatidylcholine/Cholesterol Phase Diagram: Boundaries and Composition of Lipid Rafts. *Biophys J* 85:2406–2416.
128. Varela ARP, Ventura AE, Carreira AC, Fedorov A, Futerman AH, Prieto M, Silva LC. 2016. Pathological levels of glucosylceramide change the biophysical properties of artificial and cell membranes. *Phys Chem Chem Phys* 19:340–346.
129. Batta G, Soltész L, Kovács T, Bozó T, Mészár Z, Kellermayer M, Szöllösi J, Nagy P. 2018. Alterations in the properties of the cell membrane due to glycosphingolipid accumulation in a model of Gaucher disease. *Scientific Reports* 8:157.
130. Drews K, Calgi MP, Harrison WC, Drews CM, Costa-Pinheiro P, Shaw JJP, Jobe KA, Nelson EA, Han JD, Fox T, White JM, Kester M. 2019. Glucosylceramidase Maintains Influenza Infection By Regulating Endocytosis. *Journal of Virology* JVI.00017-19.
131. Soudani N, Hage-Sleiman R, Karam W, Dbaibo G, Zaraket H. 2019. Ceramide Suppresses Influenza A Virus Replication In Vitro. *Journal of Virology* 93:e00053-19.

132. Ichikawa S, Hirabayashi Y. 1998. Glucosylceramide synthase and glycosphingolipid synthesis. *Trends in Cell Biology* 8:198–202.
133. Marvin SA, Russier M, Huerta CT, Russell CJ, Schultz-Cherry S. 2017. Influenza Virus Overcomes Cellular Blocks To Productively Replicate, Impacting Macrophage Function. *J Virol* 91.
134. Avota E, Müller N, Klett M, Schneider-Schaulies S. 2004. Measles Virus Interacts with and Alters Signal Transduction in T-Cell Lipid Rafts. *Journal of Virology* 78:9552–9559.
135. Taniguchi M, Okazaki T. 2014. The role of sphingomyelin and sphingomyelin synthases in cell death, proliferation and migration—from cell and animal models to human disorders. *Biochimica et Biophysica Acta (BBA) - Molecular and Cell Biology of Lipids* 1841:692–703.
136. Rasbach A, Abel T, Münch RC, Boller K, Schneider-Schaulies J, Buchholz CJ. 2013. The Receptor Attachment Function of Measles Virus Hemagglutinin Can Be Replaced with an Autonomous Protein That Binds Her2/neu While Maintaining Its Fusion-Helper Function. *J Virol* 87:6246–6256.
137. Wheeler S, Haberkant P, Bhardwaj M, Tongue P, Ferraz MJ, Halter D, Sprong H, Schmid R, Aerts JMFG, Sullo N, Sillence DJ. 2019. Cytosolic glucosylceramide regulates endolysosomal function in Niemann-Pick type C disease. *Neurobiology of Disease* 127:242–252.
138. Lowther J, Naismith JH, Dunn TM, Campopiano DJ. 2012. Structural, mechanistic and regulatory studies of serine palmitoyltransferase. *Biochemical Society Transactions* 40:547–554.
139. Tanner LB, Chng C, Guan XL, Lei Z, Rozen SG, Wenk MR. 2014. Lipidomics identifies a requirement for peroxisomal function during influenza virus replication. *J Lipid Res* 55:1357–1365.
140. Murugesan V, Chuang W-L, Liu J, Lischuk A, Kacena K, Lin H, Pastores GM, Yang R, Keutzer J, Zhang K, Mistry PK. 2016. Glucosylsphingosine is a key biomarker of Gaucher disease. *Am J Hematol* 91:1082–1089.
141. Slotte JP, Ramstedt B. 2007. The functional role of sphingomyelin in cell membranes. *European Journal of Lipid Science and Technology* 109:977–981.
142. Pankov R, Markovska T, Hazarosova R, Antonov P, Ivanova L, Momchilova A. 2005. Cholesterol distribution in plasma membranes of β 1 integrin-expressing and β 1 integrin-deficient fibroblasts. *Archives of Biochemistry and Biophysics* 442:160–168.
143. Atkinson PH, Summers DF. 1971. Purification and Properties of HeLa Cell Plasma Membranes. *J Biol Chem* 246:5162–5175.

144. Grison MS, Brocard L, Fouillen L, Nicolas W, Wewer V, Dörmann P, Nacir H, Benitez-Alfonso Y, Claverol S, Germain V, Boutté Y, Mongrand S, Bayer EM. 2015. Specific Membrane Lipid Composition Is Important for Plasmodesmata Function in Arabidopsis. *The Plant Cell* 27:1228–1250.
145. Yamaguchi Y, Sasagasako N, Goto I, Kobayashi T. 1994. The Synthetic Pathway for Glucosylsphingosine in Cultured Fibroblasts. *J Biochem (Tokyo)* 116:704–710.
146. Wang P, Zhou Z, Hu A, Ponte de Albuquerque C, Zhou Y, Hong L, Siernecki E, Ajiro M, Kruhlak M, Harris C, Guan K-L, Zheng Z-M, Newton AC, Sun P, Zhou H, Fu X-D. 2014. Both Decreased and Increased SRPK1 Levels Promote Cancer by Interfering with PHLPP-Mediated Dephosphorylation of Akt. *Molecular Cell* 54:378–391.
147. Braune E-B, Lendahl U. 2016. Notch — a Goldilocks Signaling Pathway in Disease and Cancer Therapy. *Discovery Medicine* 21:189–196.
148. Yu RK, Tsai Y-T, Ariga T, Yanagisawa M. 2011. Structures, biosynthesis, and functions of gangliosides—An overview. *J Oleo Sci* 60:537–544.
149. van Meer G, Voelker DR, Feigenson GW. 2008. Membrane lipids: where they are and how they behave. *Nat Rev Mol Cell Biol* 9:112–124.
150. Gruenberg J. 2003. Lipids in endocytic membrane transport and sorting. *Current Opinion in Cell Biology* 15:382–388.
151. Simonsen A, Wurmser AE, Emr SD, Stenmark H. 2001. The role of phosphoinositides in membrane transport. *Current Opinion in Cell Biology* 13:485–492.
152. Kobayashi T, Beuchat M-H, Chevallier J, Makino A, Mayran N, Escola J-M, Lebrand C, Cosson P, Kobayashi T, Gruenberg J. 2002. Separation and Characterization of Late Endosomal Membrane Domains. *J Biol Chem* 277:32157–32164.
153. Schieder M, Rötzer K, Brüggemann A, Biel M, Wahl-Schott CA. 2010. Characterization of Two-pore Channel 2 (TPCN2)-mediated Ca²⁺ Currents in Isolated Lysosomes. *J Biol Chem* 285:21219–21222.
154. Naslavsky N, Caplan S. 2018. The enigmatic endosome – sorting the ins and outs of endocytic trafficking. *J Cell Sci* 131:jcs216499.
155. Cell Fractionation and Organelle Isolation - US.
156. Williamson CD, Wong DS, Bozidis P, Zhang A, Colberg-Poley AM. 2015. Isolation of Endoplasmic Reticulum, Mitochondria, and Mitochondria-Associated Membrane and Detergent Resistant Membrane Fractions from

- Transfected Cells and from Human Cytomegalovirus-Infected Primary Fibroblasts. *Curr Protoc Cell Biol* 68:3.27.1-3.27.33.
157. Franko A, Baris OR, Bergschneider E, von Toerne C, Hauck SM, Aichler M, Walch AK, Wurst W, Wiesner RJ, Johnston ICD, de Angelis MH. 2013. Efficient Isolation of Pure and Functional Mitochondria from Mouse Tissues Using Automated Tissue Disruption and Enrichment with Anti-TOM22 Magnetic Beads. *PLoS One* 8.
 158. Tang D, Wang Y. 2015. Golgi Isolation. *Cold Spring Harb Protoc* 2015:pdb.prot075911.
 159. Batta G, Soltész L, Kovács T, Bozó T, Mészár Z, Kellermayer M, Szöllösi J, Nagy P. 2018. Alterations in the properties of the cell membrane due to glycosphingolipid accumulation in a model of Gaucher disease. *Scientific Reports* 8:157.
 160. Halter D, Neumann S, van Dijk SM, Wolthoorn J, de Mazière AM, Vieira OV, Mattjus P, Klumperman J, van Meer G, Sprong H. 2007. Pre- and post-Golgi translocation of glucosylceramide in glycosphingolipid synthesis. *J Cell Biol* 179:101–115.
 161. Pagano RE. 2003. Endocytic trafficking of glycosphingolipids in sphingolipid storage diseases. *Philos Trans R Soc Lond B Biol Sci* 358:885–891.
 162. Staudt C, Puissant E, Boonen M. 2016. Subcellular Trafficking of Mammalian Lysosomal Proteins: An Extended View. *Int J Mol Sci* 18.
 163. Vitner EB, Dekel H, Zigdon H, Shachar T, Farfel-Becker T, Eilam R, Karlsson S, Futerman AH. 2010. Altered expression and distribution of cathepsins in neuronopathic forms of Gaucher disease and in other sphingolipidoses. *Hum Mol Genet* 19:3583–3590.
 164. Moran MT, Schofield JP, Hayman AR, Shi GP, Young E, Cox TM. 2000. Pathologic gene expression in Gaucher disease: up-regulation of cysteine proteinases including osteoclastic cathepsin K. *Blood* 96:1969–1978.
 165. Tamhane T, Illukkumbura R, Lu S, Maelandsmo GM, Haugen MH, Brix K. 2016. Nuclear cathepsin L activity is required for cell cycle progression of colorectal carcinoma cells. *Biochimie* 122:208–218.
 166. Burton LJ, Henderson V, Liburd L, Odero-Marah VA. 2017. Snail transcription factor NLS and importin β 1 regulate the subcellular localization of Cathepsin L and Cux1. *Biochem Biophys Res Commun* 491:59–64.
 167. Sullivan S, Tosetto M, Kevans D, Coss A, Wang L, O'Donoghue D, Hyland J, Sheahan K, Mulcahy H, O'Sullivan J. 2009. Localization of nuclear

- cathepsin L and its association with disease progression and poor outcome in colorectal cancer. *Int J Cancer* 125:54–61.
168. Ramalho-Santos J, Pedroso de Lima MC. 1998. The influenza virus hemagglutinin: a model protein in the study of membrane fusion. *Biochimica et Biophysica Acta (BBA) - Reviews on Biomembranes* 1376:147–154.
169. White JM, Wilson IA. 1987. Anti-peptide antibodies detect steps in a protein conformational change: low-pH activation of the influenza virus hemagglutinin. *The Journal of Cell Biology* 105:2887–2896.
170. Han X, Bushweller JH, Cafiso DS, Tamm LK. 2001. Membrane structure and fusion-triggering conformational change of the fusion domain from influenza hemagglutinin. *Nat Struct Biol* 8:715–720.
171. Stegmann T, White JM, Helenius A. 1990. Intermediates in influenza induced membrane fusion. *EMBO J* 9:4231–4241.
172. Chernomordik LV, Kozlov MM. 2005. Membrane hemifusion: crossing a chasm in two leaps. *Cell* 123:375–382.
173. Mitsutake S, Igarashi Y. 2013. Chapter Twelve - Sphingolipids in Lipid Microdomains and Obesity, p. 271–284. *In* Litwack, G (ed.), *Vitamins & Hormones*. Academic Press.
174. Lee C-W. 2014. Reverse genetics of influenza virus. *Methods Mol Biol* 1161:37–50.
175. Drake MJ, Brennan B, Jr KB, Bart SM, Sherman E, Szemiel AM, Minutillo M, Bushman FD, Bates P. 2017. A role for glycolipid biosynthesis in severe fever with thrombocytopenia syndrome virus entry. *PLOS Pathogens* 13:e1006316.
176. Blumenthal R, Durell S, Viard M. 2012. HIV Entry and Envelope Glycoprotein-mediated Fusion. *Journal of Biological Chemistry* 287:40841–40849.
177. Finnegan CM, Rawat SS, Puri A, Wang JM, Ruscetti FW, Blumenthal R. 2004. Ceramide, a target for antiretroviral therapy. *PNAS* 101:15452–15457.
178. 2010. 684. Insights on the Mechanisms of Measles Virus Entry into Cells. *Molecular Therapy* 18:S267.

VITA

Kelly Christopher Drews was born in Falls Church, Virginia to Michael and Simone Drews. He earned three Bachelors degrees from Virginia Tech in 2014: one in History, one in Biology, and one in Biochemistry. While at Virginia Tech Kelly worked in the lab of Dr. Shiv Kale studying the interactions of effector proteins of the fungus *Aspergillus fumigatus* with host lipid receptors. Upon his graduation, Kelly enrolled in the University of Virginia to pursue his doctorate degree in the Molecular and Cellular Basis of Human Disease. Fascinated by viruses, Kelly formed a collaboration between the labs of Drs. Judith White and Mark Kester to study the relationship between human influenza virus and host sphingolipids. Kelly currently resides in Durham, NC with his wife Camille and their two dogs – River and D’Artagnan – and two cats – Willow and Kinase.